Aalto University
School of Chemical
Engineering

Janne-Joonas Tiitinen

Gold catalyst supported on titania for 1-butanol partial oxidation in a microreactor

Master´s Programme in Chemical, Biochemical and Materials Engineering

Major in Chemistry

Master's thesis for the degree of Master of Science in Technology submitted for inspection, Espoo, 09.01.2019.

Supervisor Professor Riikka Puurunen

Instructors M.Sc. Yaseen Khan, D.Sc. Tiia Viinikainen

Aalto University
School of Chemical
Engineering

Aalto University, P.O. BOX 11000, 00076 AALTO
www.aalto.fi

Abstract of master's thesis

Author Janne-Joonas Tiitinen

Title of thesis Gold catalyst supported on titania for 1-butanol partial oxidation in a microreactor

Degree Programme Master's programme in Chemical, Biochemical and Materials Engineering

Major Chemistry

Thesis supervisor Professor Riikka Puurunen

Thesis advisor(s) / Thesis examiner(s) M.Sc. Yaseen Khan, D.Sc. Tiia Viinikainen

Date 09.01.2019 **Number of pages** 91(28) **Language** English

Abstract

Theoretical background of the catalytical activity of gold nanoparticles, TiO_2 as support, sol-immobilization method and oxidation of alcohols in microreactor are explained briefly in the literature part.

In the experimental part, five gold on titania (TiO_2) support catalysts were made with sol-immobilization method. Catalyst were made to observe the effect of catalyst preparation parameters to the size of gold particles, size distribution of the gold particles and the activity of the catalyst. Preparation parameters were the amount of gold in the solution, the pH adjustment timing and the pH level of the catalyst preparation solution. As catalytic activity test reaction 1-butanol was partial oxidized to butyraldehyde.

The catalysts were prepared with target loading of 0.3, 0.6 and 1.0 wt.% Au/TiO_2. The effect of adding H_2SO_4 at different stages of catalyst preparation was tested by acidifying the gold nanoparticle solution before addition of the support instead of acidifying after addition of the support. The wanted target acidity of the solution varied from pH 1 to 3. Catalysts were characterized by transmission electron microscopy (TEM), energy dispersive spectroscopy, x-ray fluorescence, thermogravimetric analysis, x-ray photoelectron spectroscopy and rheology, and tested in a microreactor for 1-butanol partial oxidation in the gas phase. All the catalysts were tested at temperature range of 130 to 400 °C and partial pressure of 13.5 kPa. One catalyst was tested also at 1-butanol partial pressure of 18.0 kPa.

The TEM analysis showed that the 1.0 wt.% Au/TiO_2 sample gave 3.9 nm average size of Au particles and 0.3 wt.% sample 2.0 nm average size of particles. Acidifying the catalyst preparation solution before adding TiO_2 affected size of the particles by reducing their average size from 3.9 to 3.2 nm. Acidifying the catalyst preparation solution to pH 3 instead of 1, increased the average size of the particles from 2.7 to 3.8 nm with 0.6 wt.% Au/TiO_2 sample.

All catalysts yielded 20% - 55% of butyraldehyde at 400 °C. Yields of other products such as carbon monoxide (3% - 10%), carbon dioxide (5% - 25%), trans-2-butene (1% - 10%), 1-butene (1% - 5%) and propene (0% - 5%) at 400 °C were observed. By decreasing the residence time and increasing the partial pressure of 1-butanol it was possible to have more selective reactor conditions to butyraldehyde.

Keywords Gold catalyst, nanoparticles, partial oxidation, microreactor, gas phase, heterogeneous catalysis, 1-butanol, butyraldehyde, sol-immobilization, PVA, NaBH4

Aalto-yliopisto
Kemian tekniikan korkeakoulu

Aalto-yliopisto, PL 11000, 00076 AALTO
www.aalto.fi

Diplomityön tiivistelmä

Tekijä Janne-Joonas Tiitinen

Työn nimi 1-Butanolin osittaishapetus mikroreaktorissa kultakatalyytillä titaanidioksidikantajalla

Koulutusohjelma Master's programme in Chemical, Biochemical and Materials Engineering

Pääaine Chemistry

Työn valvoja Professori Riikka Puurunen

Työn ohjaaja(t)/Työn tarkastaja(t) M.Sc. Yaseen Khan, D.Sc. Tiia Viinikainen

Päivämäärä 09.01.2019 **Sivumäärä** 91(28) **Kieli** englanti

Tiivistelmä

Kirjallisuusosassa käydään lyhyesti läpi teoreettista taustaa kultananopartikkeleiden katalyyttiselle aktiviisisuudelle, titaanidioksidi kantajana, sooli-immolibilisaatio ja alkoholin hapetus mikroreaktorissa.

Kokeellisessa osassa tehtiin viisi erilaista kultakatalyyttiä titaanidioksidikantajalla sooli-immobilisaatiomenetelmällä. Katalyytinvalmistusparametrien vaikutusta tarkkailtiin katalyyttien aktiivisuuteen ja ominaisuuksiin, jotka olivat kultahiukkasten koko ja niiden kokojakautuminen. Katalyytin valmistusliuoksen parametrit olivat kullan määrä, pH:n säätämisen vaihe ja pH-arvo. katalyyttien aktiivisuutta testattiin osittain hapettamalla 1-butanolia butanaaliksi.

Katalyytit tähdättiin sisältämään 0,3; 0,6 ja 1,0 painoprosenttia kultaa. H_2SO_4:n lisäämisen vaikutusta katalyytin valmistuksen eri vaiheissa testattiin happamoittamalla kullan nanopartikkeliliuos ennen titaanioksidi kantajan lisäämistä sen sijaan, että se oli happamoitettu kantajan lisäämisen jälkeen. Liuoksen haluttu pH vaihteli 1 ja 3 välillä. Katalyytit karakterisoitiin transmissioelektronimikroskopialla (TEM), termogravimetrisella analyysillä, röntgenfluoresenssilla energiadispersiivispektroskopialla, röntgenfotoelektronispektroskopialla ja reologisesti. Katalyytit testattiin mikroreaktorissa kaasufaasissa olevalla 1-butanolilla lämpötila-alueella 130 – 400 °C. Yksi katalyytti testattiin myös 18,0 kPa:n 1-butanolin osapaineella normaalin 13,5 kPa: n sijaan.

TEM analyysin mukaan kullan 1,0% määrä katalyytissä antoi keskimäärin 3,9 nm:n partikkelikoon ja kullan 0,3% määrä antoi keskimäärin 2,0 nm partikkelikoon. Happamoittamalla katalyytinvalmisteliuos ennen TiO_2:n lisäämistä vaikutti kultahiukkasiin pienentämällä niiden kokoa 3,9 nm:sta 3,2 nm:iin. Happamoittamalla katalyyttiliuos pH-arvoon 3 vaikutti hiukkasten kokoon kasvattamalla niiden keskimääräistäkokoa 2,7 nm:sta 3,8 nm:iin kultaa 0,6% sisältävällä katalyytillä.

Katalyyttien butanaalin saanto vaihteli 20% - 55% välillä 400 °C asteessa. Muitakin tuotteita havainnointiin ja niiden saanto vaihteli 400 °C asteessa, esimerkiksi häkää (3% - 10%), hiilidioksidia (5% - 25%), trans-2-buteenia (1% - 10%), 1-buteenia (1% - 5%) ja propeenia (0% - 5%). Viipymisaikaa pienentämällä ja 1-butanolin osittaispainetta lisäämällä oli mahdollista saada selektiivisemmät reaktoriolosuhteet butanaalin tuottamiseksi.

Avainsanat Kultakatalyytti, nanopartikkelit, osittaishapetus, mikroreaktori, kaasufaasi, heterogeenin katalyysi, 1-butanoli, butanaali, sooli-immobilisaatio, PVA, NaBH4

Preface

Thesis was done during 13.12. – 31.1.2017 and 12.2. - 31.8.2018 in Catalysis research group at Aalto University School of Chemical engineering. Thesis was submitted on 09.01.2019. Process contained a few limiting factors. Thesis was partly funded by The Academy of Finland MICATOX-project (1.1.2014 -31.12.2017).

Thanks to Professor Riikka Puurunen for the opportunity of writing the thesis from this very interesting topic. Special thanks to M.Sc Yaseen Khan for teaching me operation of the microreactor, teaching catalyst preparation, information and knowledge about the topic and Catalyst O as reference catalyst. Thanks to D.Sc Tiia Viinikainen for help in finalizing the work. Thanks to Eero Korhonen for helping with microreactor experiments. Thanks to E417 coffee room and people there for giving me energy to working days and nights. Thanks for Steven Spoljaric (Rheology) and Phan Huy Nguyen (TGA) helping with equipments. Thanks for the characterization to Jiang Hua (TEM/EDS), Giovanni Marin (XRF) and Dr. Jouko Lahtinen (XPS).

Thanks to Aleksi Matikainen for the peer support and commenting the thesis. Thanks to people in Kotka for the remote support. Last, but not least, thanks to Jasmin Hertzberg for the special support and encouragement during the thesis.

Reading experience may vary between electronic and printed version.

In Espoo, Otaniemi, cradle of technology, 09.01.2019

Janne-Joonas “J-J” Tiitinen

Table of Contents

Symbols and Abbreviations

CTMR	Catalyst testing microreactor
EDS	Energy dispersive spectroscopy
FTIR	Fourier-transform infrared spectrometer
IEP	Isoelectric point
M_w	Weight average molecular weight (g/mol)
$\dot{n}$	Molar flow (mol/s)
PVA	Polyvinylalcohol
Rpm	Rounds per minute
S	Selectivity
TEM	Transmission electron microscope
TGA	Thermogravimetric analysis
X	Conversion
XPS	X-ray photoelectron spectroscopy
XRF	X-ray fluorescence
Y	Yield

1. Introduction

Gold was considered to be inert and poor catalyst in bulk size.[1] However, it was known that gold becomes active when the particle size is smaller than 10 nm and deposited on oxides.[1] Since then gold has been studied in many reactions as a catalyst: one example is using in low temperature CO oxidation.[2]

From environmentally sustainable bio-resources it is possible to obtain value-added chemicals. Acetone-butanol-ethanol (ABE) fermentation process is example to produce biobased chemicals.[3] 1-Butanol produce from ABE fermentation can be selectively oxidized to produce n-butyraldehyde. Butyraldehyde is currently produced by hydroformylation of propene with homogeneous catalyst.[4] Many important chemical and fuel components, such as, 2-ethylhexanol and acetal are made from butyraldehyde.[5] Using biobased 1-butanol provides prospects to an alternate industrial route to produce butyraldehyde.

Microreactors are miniaturized reactors with scale of at least one dimension below millimeter.[6] Benefits of microreactors are advanced heat and mass transfer.[6] It is possible to operate in isothermal conditions with highly exothermic and endothermic reactions using the characteristic mass and heat transfer advantages. The characteristic mass transfer advantages can be achieved if the layer of catalyst is less than 50 μm thin.[6] In continuous microreactor the needed amount of feeded chemicals are typically in scale ml/min or under.[7]

The main aim of the thesis was to obtain information about gold catalysts supported on titania to be applied in partial oxidation of 1-butanol in microreactor. The effect of different parameters, such as, pH, acidifying step and amount of gold were aimed to test on the final nanoparticle size and catalyst activity.To test this, five different catalysts were made with sol-immobilization method with different parameters to compare them to the original catalyst One catalyst was also tested in different residence time and partial pressure of 1-butanol to test the effect of reactor conditions.

2. Literature review

This chapter explains briefly theoretical background of gold as catalyst, sol-immobilization and oxidation of alcohol with gold catalyst.

2.1 Gold nanoparticles as a catalyst

2.1.1 General information

Gold is known to be catalytically active in nanoparticle size of approximately 3-5 nm and active sites are suggested to be the corners and edges of the nanoparticles.[2] Gold can be used for example in existing processes with significantly lower reaction temperatures for energy efficient processes.[2] There are several proposed explanations for activity of the gold nanoparticles: oxidation state of gold atoms, the role of low coordinated gold atoms in nanoparticles, quantum size effects, oxygen spill-over to and from the support, charge transfer to and from the support and support-inducted strain.[2] Understanding several effects that may occur simultaneously on gold and interaction between gold nanoparticles and support material is very important.[2] The compared catalytical activity of gold for CO oxidation reaction on different supports is shown in Figure 1.

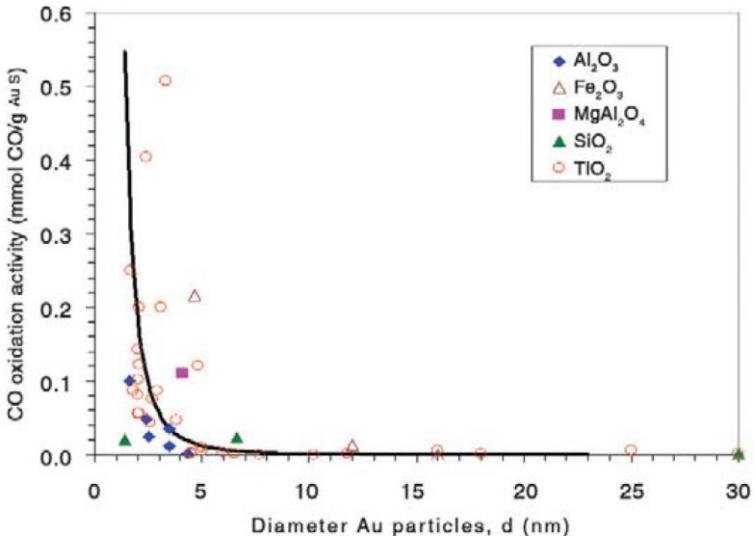

Figure 1. Reported catalytic activities for CO oxidation at 273 K as a function of Au particle size for different support materials. The supports are indicated by the symbol shape: open symbols correspond to reducible supports, closed symbols to non-reducible supports. The solid curve shows the calculated fraction of atoms located at the corners of nanoparticles as a function of particle diameter for uniform particles shaped as the top half of a regular cuboctahedron. [2]

2.1.2 TiO_2 support effect for gold

According to Hvolbæk et al.[2] understanding the interaction between Au particles and their support material is a key issue. Structure of the material affects to its properties. The crystal structure of TiO_2, anatase, is shown in Figure 2.

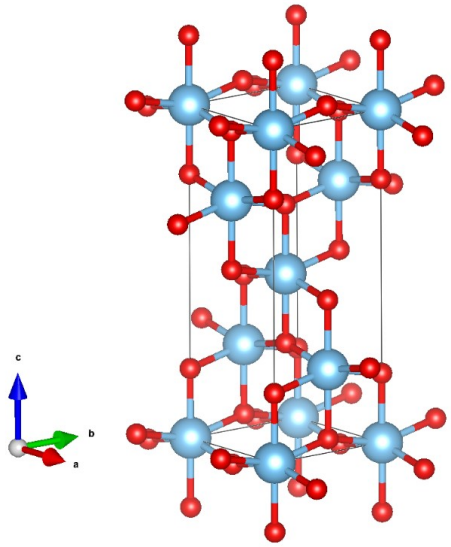

Figure 2. The crystal structure of TiO_2, anatase.[8]

Catalytic test and characterization methods confirmed the effect of the support on catalytic activity by Comotti et al.[9] TiO_2 is an active semiconductor material.[9] Active semiconductor materials can store and release oxygen.[10] It has oxygen vacancies and gold interface where oxygen adsorption is believed to occur by Schottky junction (metal-semiconductor junction). Supports having similar gold nanoparticles can be put on order by their activity of regeneration as, Au/TiO_2 > Au/ZrO_2 > Au/ZnO > Au/Al_2O_3.[10] Comotti et al. suggested that support interacts with metal cluster and changes the shape of the particles, leading to faceting and possibly creating defect sites, which effect to activity.[9] Gold particle size should not be effected by the gold loading between 0.5 wt.% and 7 wt.% on TiO_2 according to Sobolev et al.[11] There might be enough exposed adsorption centers to maintain high gold particle dispersion.[11] Haruta proposed that the interface between the gold nanoparticles and the support is the active site in CO oxidation reaction, where gold and the support adsorb and activate CO and O_2. [1]

Specific step for the activation of CO at the interfaces between gold and the support has been less reported, usually it is thought to be adsorbed and activated on gold nanoparticles.[10] In Figure 3 catalytic mechanisms on titania supported gold catalysts are shown.

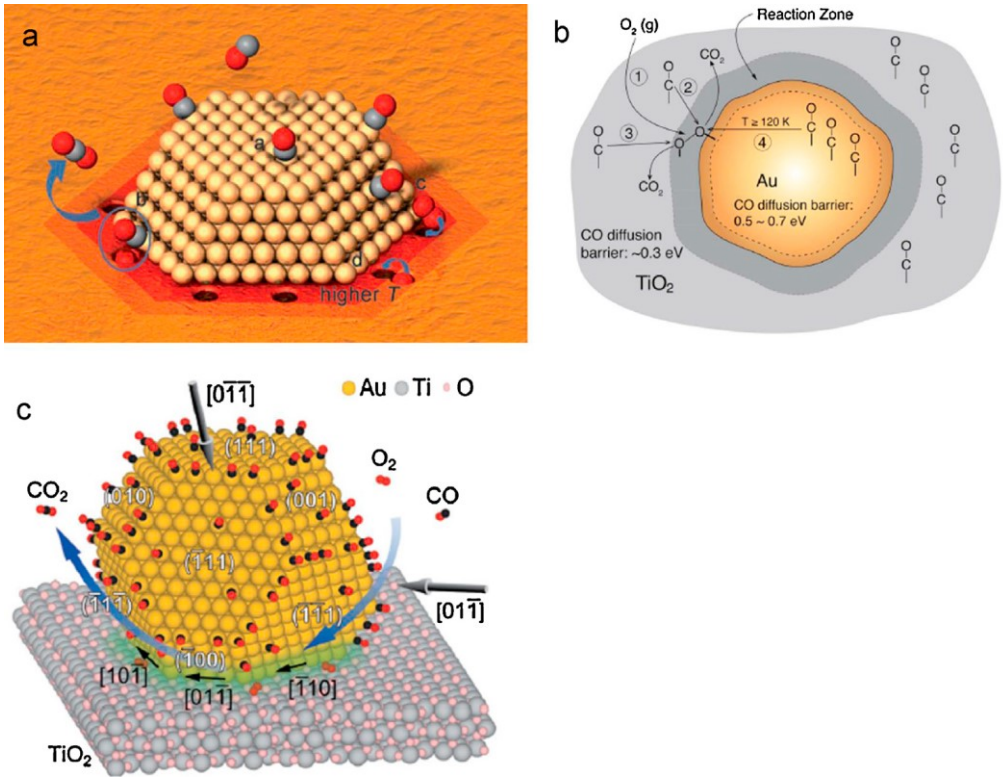

Figure 3. Catalytic mechanisms on supported gold catalysts. A) Au/TiO_2, activation of O_2 at different temperatures. B) Activation of CO over Au/TiO_2. C) Active sites on Au/TiO_2 for CO oxidation. Reproduced from Liu et al.[10]

Sobolev reported that significant acidity of the titania support itself inducts more acidic-catalyzed reactions for example ethylene and diethyl ether rather than acetalaldehyde from ethanol.[11] They proposed that key factor for low temperature oxidation oxygen species was the thermostability generated by the TiO_2 matrix.[11]

2.1.3 Binding of gold particles

Gold has high standard electrode potential and an unique electronic state.[12] Gold has endothermic chemisorption energy, which means that it does not bind to oxygen and this leads to gold being inert in atmosphere. Focusing on chemical bonding of the oxygen, which forms from coupling of the oxygen valence states and metal d-orbital in the d-band model, the energy of the gold d-orbital is not high enough, that interaction with oxygen 2p-orbital is net repulsive. Gold (calculated chemisorption energy +0.54) is more effective catalyst compared to platinum (or other transition metals), even at room temperature. For example platinum (calculated chemisorption energy -2.17) is used in oxidation of CO in automotive exhaust systems in high temperatures.[2] Calculated chemisorption values for transition metals are shown in Figure 4. Correlation of binding energy and coordination number is shown in Figure 5.

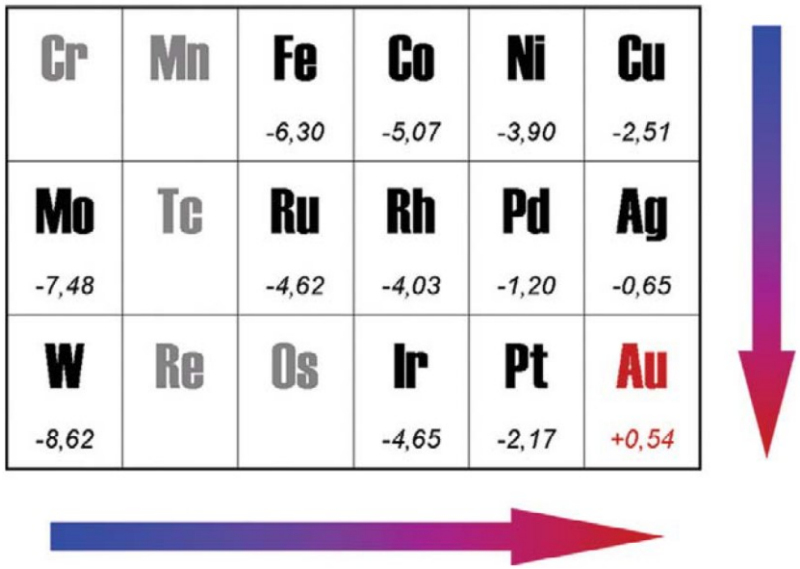

Figure 4. Chemisorption energies for oxygen on transition metal surfaces calculated with density functional theory (DFT).[2]

2.1.4 Coordination number of gold

Hvolbæk et al.[2] made a simplified simulation for surface properties of 10 gold atoms. Hvolbæk et al.[2] calculated oxidation of CO assuming two possible reaction routes: i) O_2 dissociates before reacting with CO to form CO_2 and reaction between molecular O_2 and CO. Molecular reaction is favored due the lower activation energy. [2] Ii) O_2 and CO (also O) bind to surface atoms of the gold cluster. Surface atoms (in simulated close-packed system) have 9 atoms and atoms at the step on the surface have coordination number 7, but 3 to 4 on the corners. The results from Hvolbæk et al.[2] simulations showed that binding energy decreases almost linearly with decreasing coordination number, shown in Figure 5. Small particles have relatively high number of low-coordinated gold atoms on edges and especially in corners, shown in Figure 6. This simulation supported the hypothesis that activity of the gold particles should be measured by the low-coordinated corners and not by surface area.[2] Icosahedral structures (polyhedron with 20 faces) of gold is found to be more active than cubic (polyhedron with 4 faces), indicating structure sensitive nature of the catalyst for gas phase.[12]

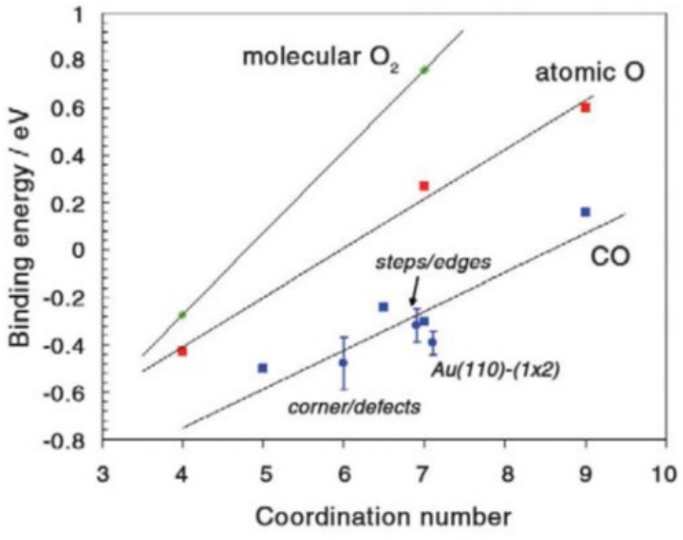

Figure 5. The correlation between the binding energies for O_2, O, and CO on Au. Binding energy decreases with lowering coordination number.[2]

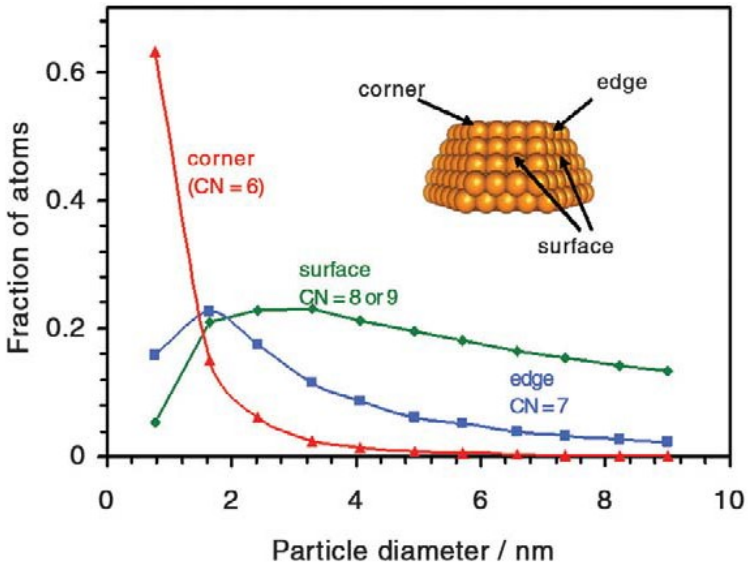

Figure 6. Calculated fractions of Au atoms at corners (red), edges (blue), and crystal faces (green) in uniform nanoparticles consisting of the top half of a truncated octahedron as a function of Au particle diameter. Fraction of corners in an atom decreases with increasing particle diameter.[2]

2.2 Sol-immobilization of gold nanoparticles

In the catalytic reactions, the interactions between the catalyst particles and the support have a key role for the activity and selectivity of the catalyst.[13] Sol-immobilization method allows the controlling of metal particle size and dispersion on different supports better than traditional catalyst synthesis methods (eg. incipient wetness impregnation).[14] Surface area and properties, IEP and morphology of the support have a significant effect on the deposition of the catalyst particles. Immobilizing the pre-formed metallic sol with a stabilizing agent has been shown to be a good method for prepare a catalyst.[14]

Effect of the support on the formation of the gold particles can be eliminated by formatting colloid gold metal particles before they are deposited on the support. This way identical gold particles can be created, which are not formed with deposition-precipitation or impregnation.[9]

2.2.1 PVA as a protecting agent for gold

Polyvinylalcohol (PVA) is a white (colorless) water soluble synthetic polymer, which is widely used in industries such as in textiles, papermaking.[15] In Figure 7 the structure of PVA in shown.

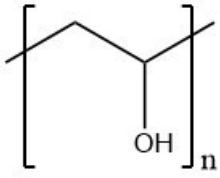

Figure 7. The structure of the PVA.

PVA is used as a protecting agent for gold, because of its ability to maintain gold particle size at the deposition step. Negative charges of PVA may shield the charges of the support (and gold clusters). In work of Comotti et al. typical gold particle size obtained with using PVA was 3.0 ± 1.3 nm. [9] After the experiment particle size and distribution was 3.8 ± 1.6 nm, which is not a significant change.[9]

2.2.2 $NaBH_4$ as a reducing agent

$NaBH_4$ is used as a reducer of soluble metal ions to insoluble elemental metal (2.1) in many waste water and products streams, where it is used to recover valuable and toxic heavy metals.[16] When $NaBH_4$ dissolved in a suitable solvent up to eight electrons per molecule are available for reduction (2.2).[16]

$$8Me^{+} + 8e^{-} \rightarrow 8Me^{0} \quad (2.1)$$

$$NaBH_4 + 2H_2O \rightarrow NaBH_2 + 8\,H^{+} + 8e^{-} \quad (2.2)$$

2.3 Oxidation of alcohol with gold catalyst on titania

Sobolev et al.[11] oxidized gas-phase ethanol with gold catalyst on titania with gold loadings between 0.5 - 7 wt.%, and the results are shown in the Figure 8. In the work, they noticed that ethanol conversion to acetaldehyde started to already occur at 125 °C, which was a significantly lower temperature compared to other similar catalysts in oxidation such as Au/SiO_2 or Au/Al_2O_3. Sobolev et al.[11] reported that for temperatures up to 300 °C, only complete oxidation occurred on every loading. With higher loadings of gold, the reaction was most active towards aldehyde at 125 °C. However complete oxidation occurred already after 250 °C and lower loadings of gold were active after 200 °C. The most efficient aldehyde producing catalyst at 125 °C contained 5% of gold by weight. The activity profile for all curves showed lower and upper peak, whose place depended on amount of the gold in the catalyst. Sobolev et al. suggest that at lower temperatures a reason for enhanced catalytic activity of Au/TiO_2 is direct participation of active oxygen, while it is not the case in higher temperatures. [11]

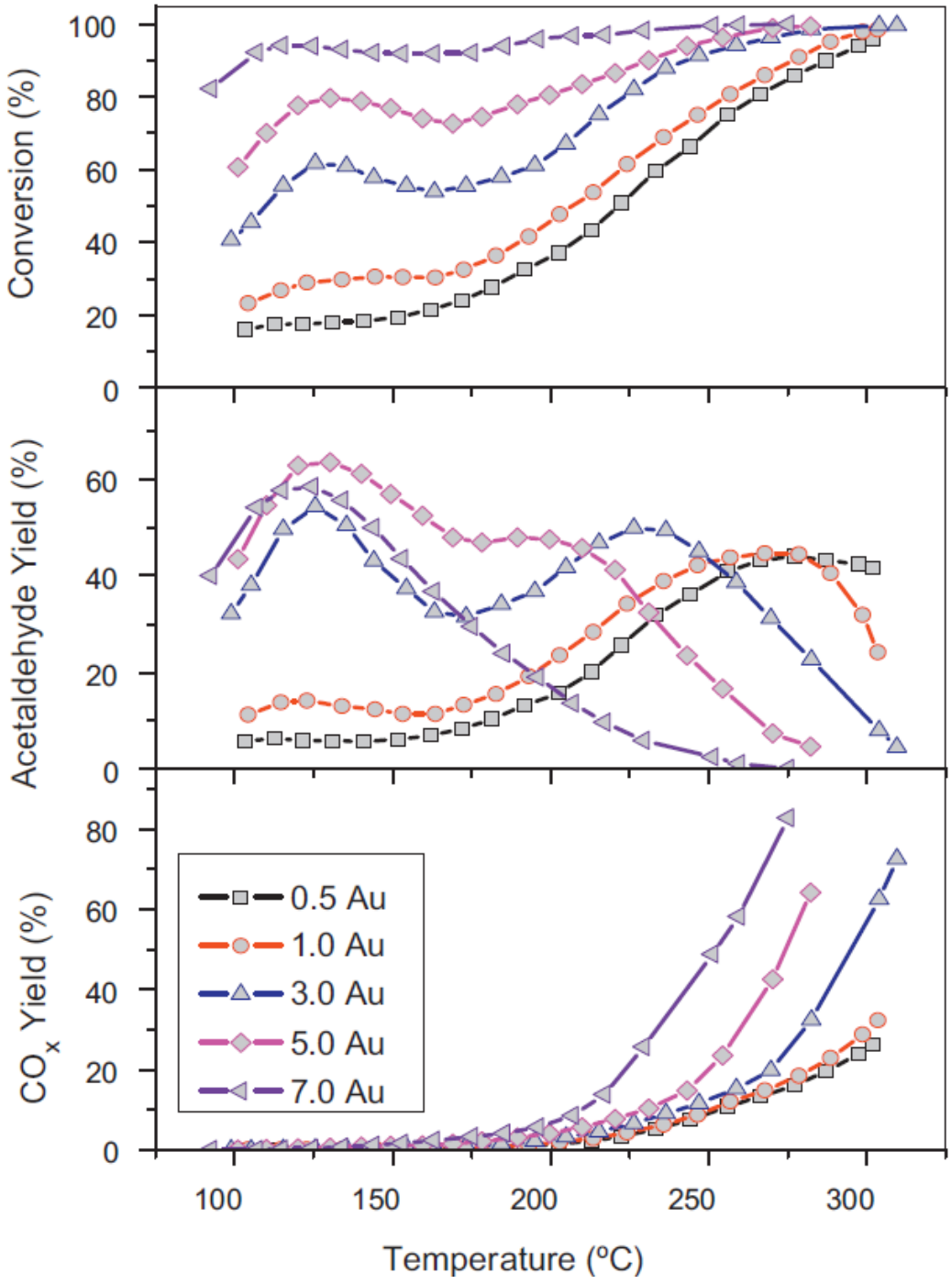

Figure 8. Performance of catalytic Au/TiO_2 with different weight percent of gold as a function of temperature: conversion of ethanol and yields of acetaldehyde and $CO+CO_2$.[11]

3. Experimental

This chapter describes preparation, activity tests with microreactor and characterization of the catalyst.

3.1 Preparation of the Au/TiO_2 catalysts

This section goes through the preparation steps of the catalyst. The overall scheme for the preparation process from the reagents to the suspension as reported Khan et al. is shown in Figure 9.[17] There are a few changes on the amounts of the reagents depending on the catalyst. After preparation of the suspension, the catalyst was coated on plate and placed in microreactor to activity tests.

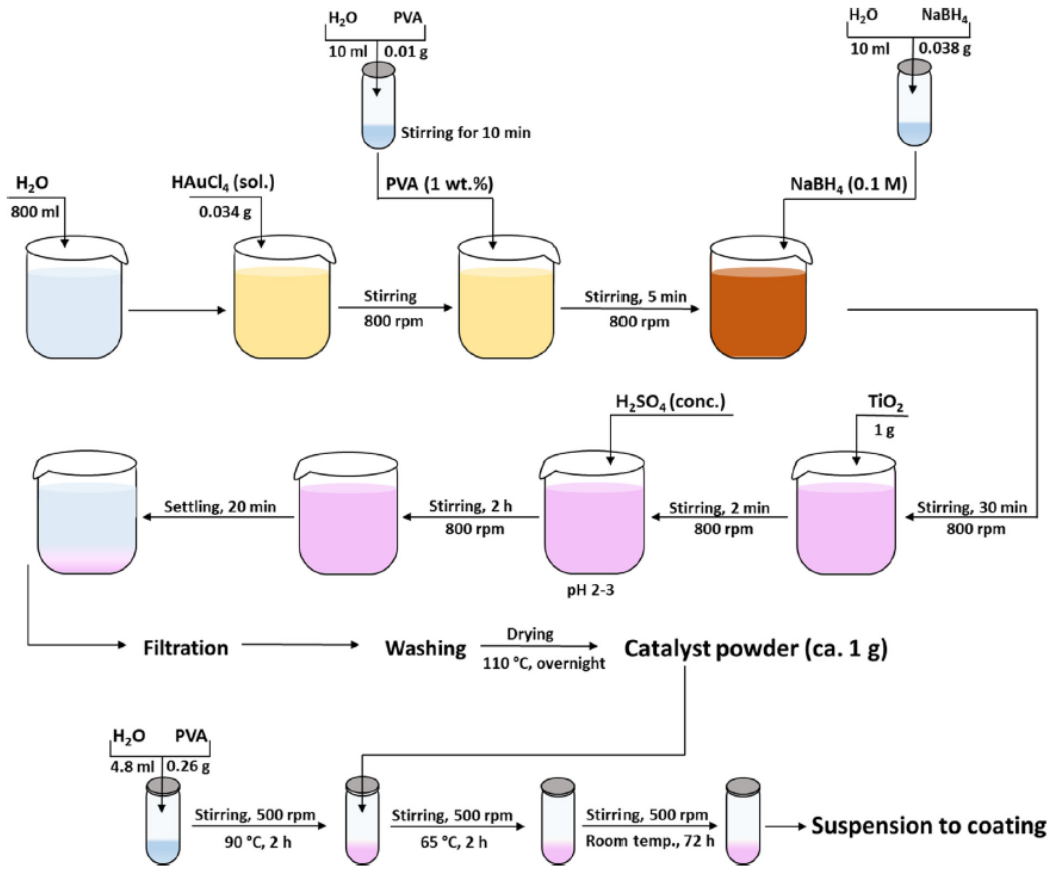

Figure 9. Overall schematic picture of the catalyst preparation.[17]

3.1.1 Preparation of the catalyst powder

Catalyst powders, referred to as A-E, were prepared following the recipe of Hutching et al.[18] and Khan et al.[17] The main steps in the recipe are as follows: protecting the Au nanoparticles in the solution from coalescence by adding PVA, reducing Au(III) to Au(0) by adding $NaBH_4$, promotion of metal deposition with decreasing pH and immobilisation of Au nanoparticles to TiO_2 by adding H2SO4 The main differences between catalysts A-E, are the amount of gold, amount of H_2SO_4 added and the adjusting step (pH adjustment) before or after TiO_2, as shown in Table 1. Catalysts A, C and E are comparable to each other because of the same pH and pH adjustment step, but different amount of gold: therefore it is possible compare the effect of the amount of gold to catalytic activity. Catalyst A and B have different pH adjustment time, Catalysts C and D have different pH as well for comparison.

Table 1. Summary of the catalysts made, targeted amount of gold, added H_2SO_4 and pH adjustment before or after TiO_2. Catalysts A-E were made by the author, Catalyst O was made by Yaseen Khan.

			PH adjustment	
Name	Amount of gold	Added H_2SO_4 (drops)	Before TiO_2	After TiO_2
Catalyst A	1.0% Au/TiO_2	15		1
Catalyst B	1.0% Au/TiO_2	15	**1**	
Catalyst C	0.6% Au/TiO_2	10		1
Catalyst D	0.6% Au/TiO_2	**3**		**3**
Catalyst E	0.3% Au/TiO_2	7		1
Catalyst O	0.6% Au/TiO_2	7-9		~1-2

Preparation of the gold solution

Preparation of the catalyst was started by preparing polyvinylalcohol (PVA) (80% hydrolyzed, weight averaged molecular weight M_w = 9000-10 000 g mol^{-1}, Aldrich) 1% by weight solution to ultrapure (“type 1”, distilled and ion-changed and 185 nm UV lamp purified) water and then stirring the solution at least for 10 minutes at 500 rpm in a vial. During the stirring, fresh sodium borohydride ($NaBH_4$, Sigma-Aldrich) 0.1 M solution was prepared to vial with ultrapure (type1) water.

Gold(III)chloride solution ($HAuCl_4$, Aldrich, Au composition 17% by weight diluted on 30% by weight HCl) was measured with scale (ENTRIS64I-1S) to vial and rinsed to 1 l beaker with 800 ml of ultrapure (type1) water. The formed clear (or yellowish) solution was stirred (800 rpm, with a magnetic stirrer) and its pH was measured with pH paper (Pehanon pH 1-12, 90401) by dipping the pH paper to the solution. The pH was 5-6 at this stage of the preparation.

PVA is used to protect the Au nanoparticles in the solution from coalescence. PVA was added with PVA/Au (weight ratio) = 1.2:1 (to solution via syringe) and pH was measured after 5 minutes. PH of the solution was around 5. The color of the solution stayed the same. Color of the solution after adding $HAuCl_4$ and PVA are shown in Figure 10. Specific amounts of $HAuCl_4$ and PVA reagents is shown in Table 2.

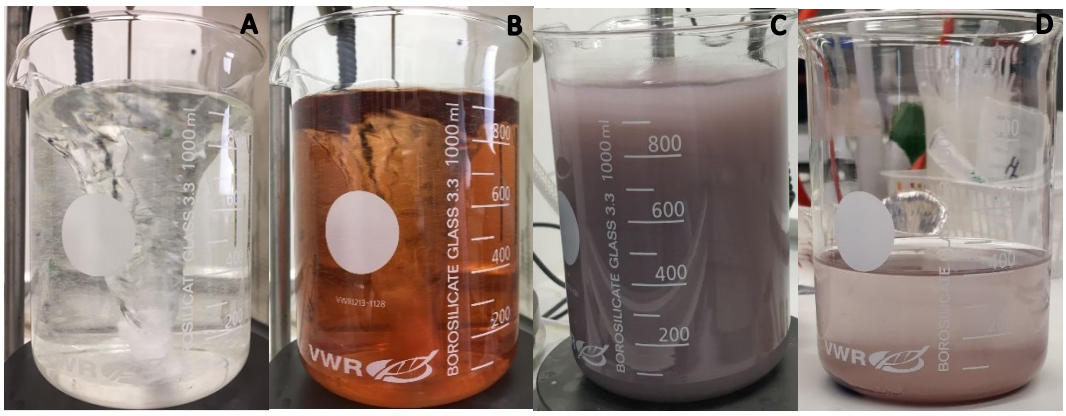

Figure 10. Catalyst preparation solutions in different stages. A) Solution after adding water, $HAuCl_4$ and PVA. Solution is clear. B) *S*olutions after adding NaBH4. Solution is orange and strength of the color depends on the amount of gold. C) *S*olution after adding TiO_2-support. Color of the solution is pinkish, which stronger color in more gold containing solutions. D) Solution after slurry had settled down. Part of the solution is already filtered.

Table 2. Summary of the preparation parameters of the gold nanoparticle solutions, amount of $HAuCl_4$, gold, PVA and water in grams.

Name	Target amount of gold	HAuCl4-sol. (g)	Au (g)	PVA (g)	Water (g)	Added PVA/water solution (ml)
Catalyst A	1.0% Au/TiO_2	0.0618	0.0105	0.101	10.0	1.30
Catalyst B	1.0% Au/TiO_2	0.0601	0.0102	0.100	10.0	1.25
Catalyst C	0.6% Au/TiO_2	0.0394	0.0067	0.100	9.99	0.75
Catalyst D	0.6% Au/TiO_2	0.0375	0.0064	0.100	9.99	0.75
Catalyst E	0.3% Au/TiO_2	0.0189	0.0032	0.100	10.0	0.37
Catalyst O	0.6% Au/TiO_2	0.0365	0.0062	0.113	11.3	1.2

Forming nanoparticles with $NaBH_4$ reduction

$NaBH_4$ was used for reducing Au(III) to Au(0) in the solution. $NaBH_4$ was added dropwise via syringe to obtain $NaBH_4$/Au (mol ratio) = 5:1. The color of the solution changed from clear to orange/brownish due to the reduction (Figure 10). Excess amount of $NaBH_4$ was added to ensure the reduction of all gold. Change of the color indicated formation of the gold sol. Acidity was around pH 5 at this point. After this solution was stirred for 30 min. Amounts of reagent $NaBH_4$ are shown in Table 3.

Sol-immobilisation of the gold to TiO_2

Support (titanium(IV) oxide, anatase, nanopowder, <25 nm particle size, 99.7% trace metals basis, Aldrich) was added to solution and the color of the solution turned pinkish. To promote metal deposition, pH was decreased to 1 with sulfuric acid (H_2SO_4, 99.99% Aldrich) after adding support (in Catalyst B acid was added first to see if there is any change compared to addition of acid before or after adding TiO_2). Color changes are shown after addition of TiO_2 in Figure 10. Amounts of added TiO_2 and calculated ratio of gold and TiO_2 by weight are shown in Table 3.

Table 3. Summary of the preparation parameters of TiO_2-immobilized Catalysts A-O, added amount of $NaBH_4$, water, TiO_2 and ratio of Au and TiO_2 by mass.

Name	Target amount of gold	$NaBH_4$ (mg)	Water (g)	Added $NaBH_4$/water solution (ml)	TiO_2 (g)	Obtained Au/TiO_2 wt.%
Catalyst A	1.0% Au/TiO_2	37.1	10.0	2.60	1.00	1.05
Catalyst B	1.0% Au/TiO_2	37.0	10.0	2.65	1.05	0.97
Catalyst C	0.6% Au/TiO_2	39.0	10.0	1.60	1.00	0.67
Catalyst D	0.6% Au/TiO_2	37.6	10.0	1.60	1.00	0.64
Catalyst E	0.3% Au/TiO_2	37.6	10.0	0.80	1.00	0.32
Catalyst O	0.6% Au/TiO_2	43.5	10	2.40	1.00	0.62

Filtering the nanoparticle powder from the solution

After stirring for 2 h, the solution was left to settle down for at least 20 min to be ready for filtering with water in order to remove dissolved species (for example SO_4^{-2}, Na^+, Cl^-). In the settled solution pinkish slurry was at the bottom. Settled catalyst powder solution is shown in Figure 10.

Polytetrafluoroethylene (PTFE) membrane filters (Whatman, pore size 0.45 µm, diameter 47 mm) were used for filtering the catalyst slurry with a vacuum pump (vacuum 4.3 Pa). For Catalyst A, water vacuum suction was used, but due to the long filtering period over 6 hours, water vacuum suction was changed to vacuum pump suction to speed up the filtering. First, slurry solution was carefully poured on the filter membrane and after that rinsed with 2 l of ultrapure ("type 1", distilled ion-exchanged and 185 nm UV lamp purified) water. For Catalyst A and B water was poured by hand, but for Catalysts C, D, and E a semi-automated water dropping system was built. The filtration system (Figure 11) consisted of a separating funnel attached on a stative to drip water over the suction flask to add water dropwise on the solid slurry. The water-dripping rate was set to the water-filtering rate. During the rinsing, water level was maintained such that the solid slurry did not dry. The color of the solid was purple.

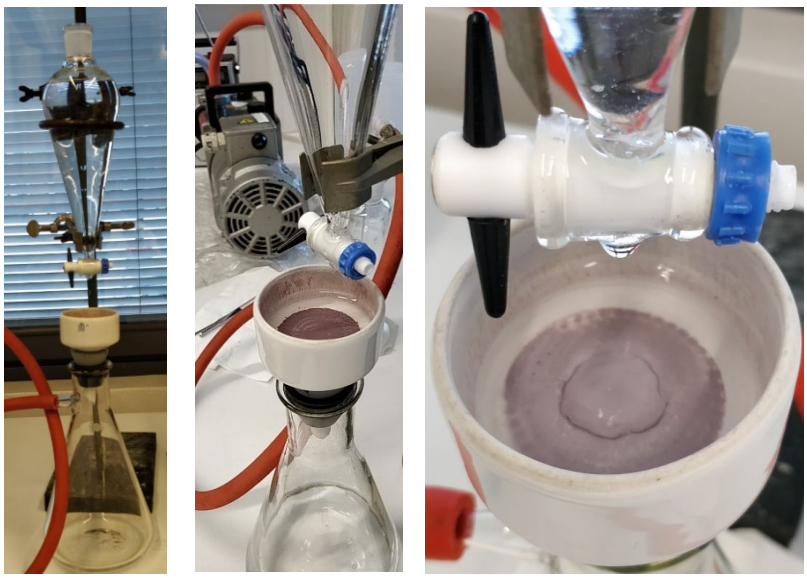

Figure 11. Filtering system. On the left picture, semi-automated water dropping set up with suction flask and Büchner funnel. In the middle, the pump used in the experiment and solid slurry on the membrane filter under water. On right, close-up picture from the filtration cake.

After the filtration process the filtrate water was clear, as the solid particles attached to the membrane. There were few occasions when the filtering membrane was not properly placed and some of the catalyst slurry got through the suction flask and the water was not clear. The color is a good indicator of the success of the filtration. A well and a poorly filtered catalyst solution is shown in Figure 12.

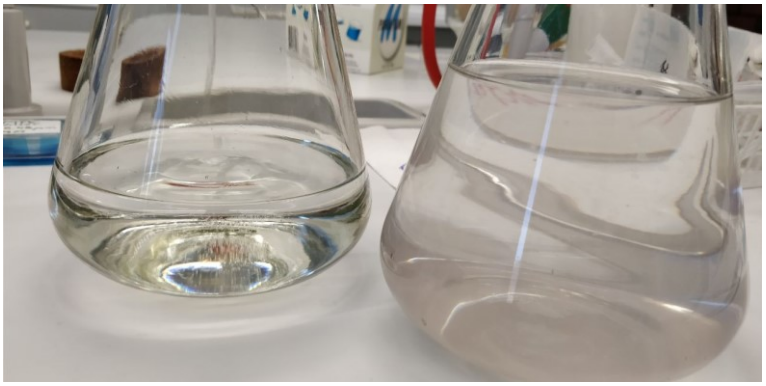

Figure 12. Well filtered water looks clear (left) and poorly filtered water looks dirty (right).

Drying the catalyst powder

After filtering, the slurry powder kept at 110 °C in an oven overnight to dry. After drying, the color of the solid catalyst had turned to more purple and it was stored in a vial. Powder was in form of brittle chips, which got broken down to powder. Magnetic stirrer was used as a pestle to crush powderish chips to evenly mixed powder. Catalyst preparation date and dry weight of the powder is shown in Table 4.

Table 4. Differences between the catalysts, catalyst preparation date and dry weight of the powder.

Name	Target amount of gold	Catalyst prep.(date)	Powder dry weight (g)
Catalyst A	1.0% Au/TiO_2	21.02.2018	0.97
Catalyst B	1.0% Au/TiO_2	22.02.2018	0.98
Catalyst C	0.6% Au/TiO_2	17.04.2018	0.96
Catalyst D	0.6% Au/TiO_2	18.04.2018	0.95
Catalyst E	0.3% Au/TiO_2	19.04.2018	0.98
Catalyst O	0.6% Au/TiO_2	16.11.2017	0.90

3.1.2 Suspension preparation for coating

The suspension was a mixture of PVA, deionized water and the catalyst. There were 3 different steps in the suspension preparation: mixing PVA with water at 90 °C, adding the catalyst, mixing at 65 °C and mixing 3 nights at room temperature. The ratio of PVA:water:catalyst was calculated to leave some unprocessed catalyst powder to analysis, but high enough to have good a suspension for coating microreactor plates and for coating blank plates. Around 4 ml of suspension was enough for this purpose. Calculated amounts and ratios for Catalyst A-E are shown in Table 5. Coated microreactor plates were used for an activity test and blank plates were calcined the same way as microreactor plates, by spreading the suspension the plate, but the calcined powder was used for characterization. Specific amounts of used reagents for suspension preparation are shown in Table 6.

Table 5. Calculated target amounts of PVA, water and catalyst powder to suspension for Catalysts A-E.

Parameter	PVA (195k g mol^{-1})	Water	Target amount of Au/TiO_2
Calculated mass (g)	0.22	4	0.774
Calculated %	4.4	80	15.6

Table 6. Suspension preparation. Specific amounts of reagents for suspension.

Name	Amount of gold	PVA (g)	Water (g)	Added Au/TiO_2 (g)
Catalyst A	1.0% Au/TiO_2	0.220	3.95	0.772
Catalyst B	1.0% Au/TiO_2	0.221	4.04	0.774
Catalyst C	0.6% Au/TiO_2	0.220	4.01	0.773
Catalyst D	0.6% Au/TiO_2	0.210	4.01	0.774
Catalyst E	0.3% Au/TiO_2	0.221	4.01	0.773
Catalyst O	0.6% Au/TiO_2	0.228	4.27	NA

PVA and water

Polyvinylalcohol (PVA) (weight averaged molecular weight M_w = 195 000 g mol^{-1}, Aldrich) was used to prepare the suspension for coating. PVA was weighted on a 30 ml vial and distilled water was added. A clear solution with white PVA particles was formed. After this, the vial was placed in 90 °C degree oil bath with magnetic stirring at 800 rpm with cap on (to prevent evaporation of the water, formed pressure was not high enough to pop off the cap). Solution was left to stir for at least 2 hours.

Adding catalyst powder

After stirring for 2 hours, the solution was clear and no PVA particles were visible. The weighted catalyst powder was added to a vial while stirring. The temperature of the oil was decreased to 65 °C and stirring speed to 500 rpm.

Mixing for three nights

After mixing for 2 h in 65 °C, heating was turned off and oil was let to cool down to room temperature. After that, the oil bath was removed and stirring decreased to 300 rpm and the suspension was left to stir for three nights. Mixing apparatus with oil bath is shown in Figure 13.

Figure 13. Suspension preparation. On the left side, mixing apparatus and oil bath. On the right side, close picture from suspension vial.

3.1.3 Pretreatment of the microreactor plates

The idea behind the pretreatment is to have as closely as possible the same surface condition to every plate. Every catalyst needs two plates to be coated to create channels covered with catalyst. All plates were cleaned and pretreated the same way except for both of the Catalyst A plates and one plate from Catalyst B, because they were unused. All plates used with Catalysts C-E and O were already used at least ones.

Cleaning the surface of the microreactor plate

For cleaning the surface, the plates were brushed under water and rinsed with ethanol. After the prewashing, the plates were placed in 1 l beaker which contained 0.4 l of water and 0.96 g of citric acid to have a 0.24% citric acid solution by weight, for an hour in a sonic bath.

Thermal treatment

After the sonic bath, plates were dried with hand paper. For the same thermal history and oxidation layer, plates were put on oven (Nabertherm, controller P 330) in an evaporating dish with synthetic air flow of 50 l/min. Heating program is showed in Figure 14.

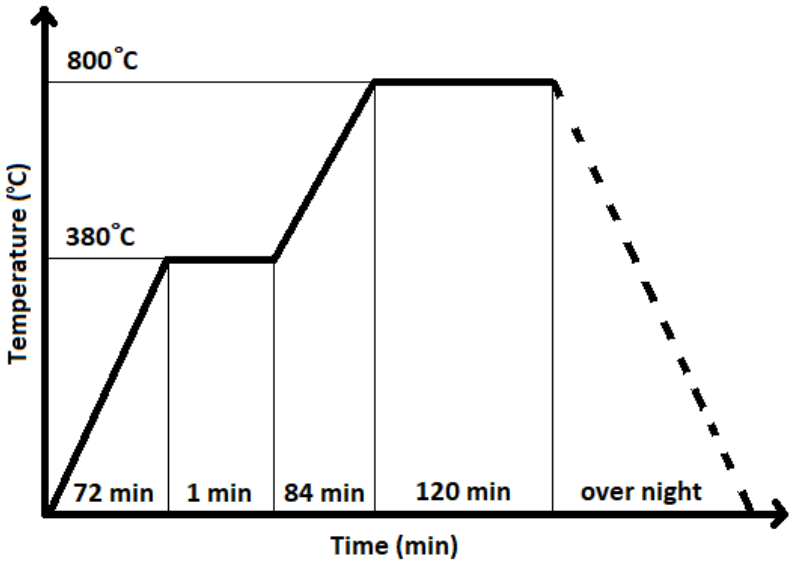

Figure 14. Heating program for the calcination of the microreactor plates (picture is not in scale).

When the plates were cooled down, they were weighed and stored for the coating. The color of the plates was darker than earlier because of the oxidation layer formed. The purpose of the oxidation layer is to help adhesion of the suspension. Plates for Catalyst A and B are shown in Figure 15.

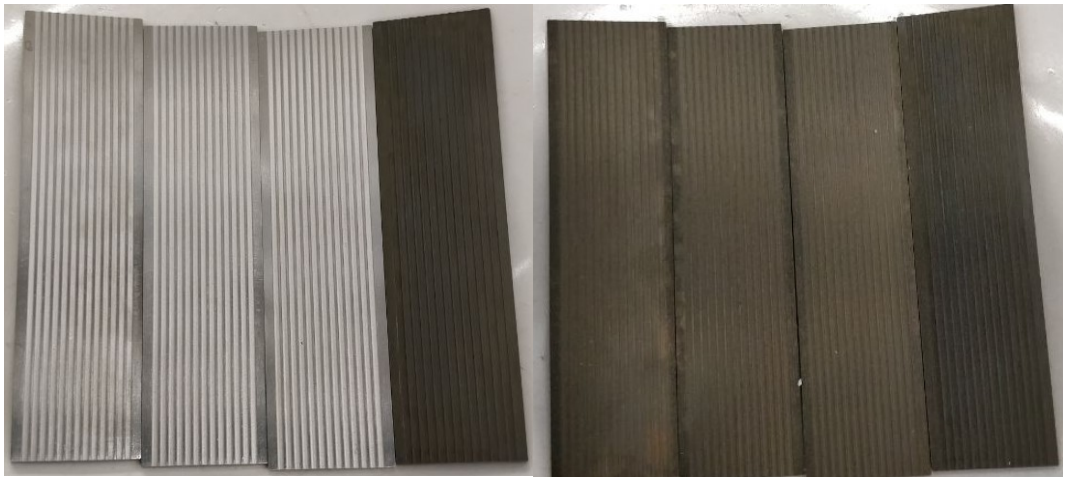

Figure 15. Microreactor plates before and after heat pretreatment for Catalysts A and B. The two from the left are unused plates for Catalyst A. The two on the right are one unused and one used plate for Catalyst B.

3.1.4 Coating and calcination of the microreactor plates

After the suspension and plate pretreatments are ready, coating and calcination can take place. Amount of the catalyst on calcined microreactor plates and the amount of the calcined powder for the analysis is shown the in Table 7.

Table 7. Coating of the plates. Amounts of the catalyst on microreactor plates and for the analysis.

Name	Amount of gold	Au/TiO_2 on plates (mg)	Calcined Au/TiO_2 powder (mg)	New plates
Catalyst A	1.0% Au/TiO_2	23.7 & 30.1	345	Yes & Yes
Catalyst B	1.0% Au/TiO_2	94 & 88 (dots)	401	Yes & No
Catalyst C	0.6% Au/TiO_2	37.3 & 29.5	449	No & No
Catalyst D	0.6% Au/TiO_2	33.5 & 12.2	440	No & No
Catalyst E	0.3% Au/TiO_2	31.4 & 28.9	427	No & No
Catalyst O	0.6% Au/TiO_2	23.1 & 34.8	NA	No & No

Coating of the microreactor plates

Plates were coated with prepared suspension with a disposable 10 ml pipette. The suspension was taken with the pipette from the vial and added dropwise on the micro channels of the microreactor plates. The suspension was spread evenly in the channels and excess suspension was swiped away. Viscosity of the suspension varied between the catalysts. When the microreactor plates were coated, excess amount of suspension was spread on blank plates to be dried and used for characterization. The coated plates were dried overnight at room temperature. Also, some of the suspension were left in the vial and stored. While drying, the color of the suspension turned dark purple.

Calcination of the microreactor plates

Dried plates were placed in an evaporating dish and then in the oven (Nabertherm, controller P 330) with air (synthetic) flow of 50 l/min and a heating program was used for controlled calcination. The heating program is shown in Figure 16.

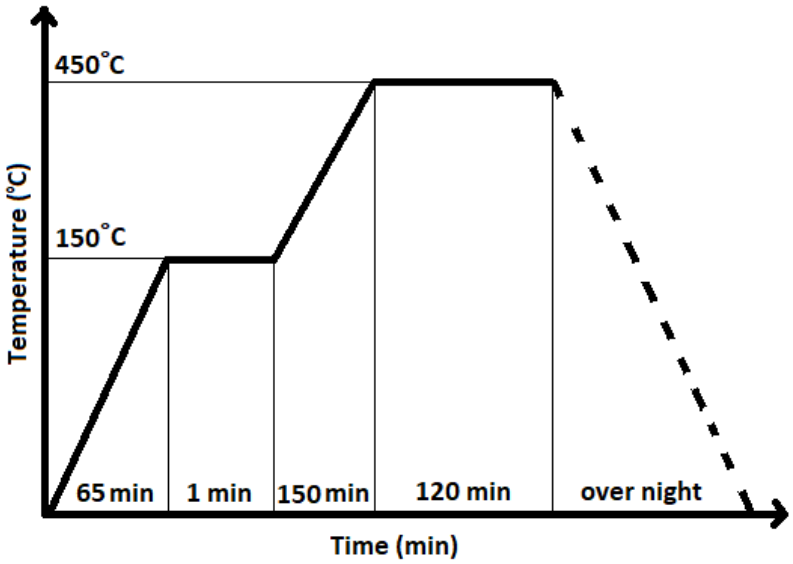

Figure 16. Heating program for the calcination of coated microreactor plates and blank plates (picture is not in scale).

After the calcination step the plates were taken from the oven and weighted. Coated and calcined microreactor plate Catalyst A and B, and coated and the calcined blank plate (Catalyst B) are shown in Figure 17. Catalyst A was smoothly dried and shows no cracks or deformity. Blank plate of Catalyst B had been cracked and deformation. Catalyst B microreactor plated had dots on the channels. The microreactor plates were stored for the later use in the microreactor. The coating of the blanks plates was scratched off, crushed to powder with a magnetic stirrer and stored in a vial.

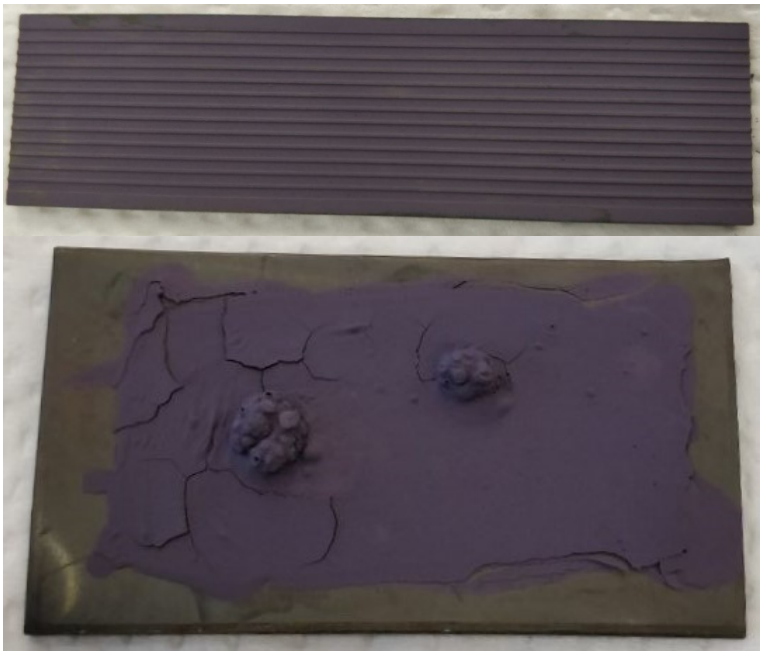

Figure 17. A calcined microreactor plate and a blank plate. On the top, coating on the microreactor plate (Catalyst A). On the bottom, coating on the blank plate (Catalyst B). (Pictures are not in the same scale)

3.2 Characterization

This section is about characterization equipment and methods, detailed information is found in subsections. By applying several characterization methods, it was possible to obtain crucial information about the catalysts. Most important method was TEM in order to obtain data from median Au particle size. Performed characterization experiments for each catalyst is shown in Table 8.

Table 8. Performed characterization analyses for each catalyst.

Name	Amount of gold	TEM	EDS	XRF	TGA	XPS	Rheology
Catalyst A	1.0% Au/TiO_2	X	X	X	X	X	
Catalyst B	1.0% Au/TiO_2	X	X	X			
Catalyst C	0.6% Au/TiO_2	X		X		X	
Catalyst D	0.6% Au/TiO_2	X		X			X
Catalyst E	0.3% Au/TiO_2	X		X		X	X
Catalyst O	0.6% Au/TiO_2	x	x	x			

3.2.1 Transmission electron microscope and Energy Dispersive Spectroscopy

For calcined powders of all catalysts, TEM was used to obtain pictures from the gold nanoparticles and EDS data. The model of the TEM was JEOL-2200FS FEG TEM/STEM. Particle sizes for all catalyst were measured manually from the pictures with Gatan DigitalMicrograph (version 2.32.888.0) program. The amount of the sample was around few milligrams. TEM was operated by Jiang Hua[19] in facilities of Aalto University at OtaNano - Nanomicroscopy Center (Aalto-NMC).

3.2.2 X-ray fluorescence

XRF was used to analyze the amounts of different elements on the calcined catalyst powder. PANanalytical Axios mAX was utilized for the XRF measurements. Samples were placed on specific sample holder for the equipment. XRF measurement is not harmful for the sample. XRF equipment was operated by Giovanni Marin in facilities at Aalto University School of Chemical Engineering.

3.2.3 Thermogravimetric analysis

Thermogravimetric analysis was applied to make sure that all added PVA has been combusted during the calcination from the catalyst. TGA analysis was only used for Catalyst A, because of the clear result of combustion of the PVA (see section 4.1.4). The model of the equipment was TA Instruments Q500. An amount of 7.8 mg sample was taken from dried and uncalcined Catalyst A suspension and put on the instrument. Heating program was 5 °C per minute from room temperature to 700 °C in air flow of 40 ml/min. Although the calcination temperature for the catalyst is 450 °C, the temperature was increased up to 700 °C to a obtain wider range of data from the catalyst, if it is needed later. Measurements were performed by the author with help of Phan Huy Nguyen in facilities at Aalto University School of Chemical Engineering.

3.2.4 X-ray photoelectron spectroscopy

X-ray photoelectron spectroscopy (XPS) was utilized in order to see if there is any differences between the oxidation state of gold and the amount of gold. The XPS measurements were made using Kratos Axis Ultra system, equipped with a monochromatic AlKα X-ray source. All measurements were performed with 0.3 mm x 0.7 mm analysis area and the charge neutralizer on, the overall spectra with 80 eV pass energy and the high-resolution spectra with 20 eV pass energy. The energy calibration was made using one of the C1s components at 284.4 eV. Measurements were done Dr. Jouko Lahtinen in facilities of Aalto University at OtaNano - Nanomicroscopy Center (Aalto-NMC). Amount of the given sample was a few dozen of milligrams.

3.2.5 Rheology

While spreading suspension to microreactor plates, there were noticeable differences on the viscosity between the catalysts. An attempt was made to test and compare, if it is possible to measure the viscosity of the suspension. The viscosity analysis was made with Ta Instruments ARG2 by taking a sample from different stages of the stirring. Viscosity tests during the stirring are shown in Table 9. Analysis were made by taking a ~1 ml sample with a 10 ml disposable pipette from the stirring solution and then taking the sample quickly to the analytical device, so the sample would not cool down, if heated or dried during exposure to air. Viscosity test for PVA in water was taken from reference sample, which was made for the measurement in order to save catalyst suspension. Samples were taken from Catalysts D and E, because of the late idea and the possibility of taking viscosity tests. Taken samples could not be used anymore. Measurements were performed by the author with help of Steven Spoljaric in facilities at Aalto University School of Chemical Engineering.

Table 9. Planned viscosity tests on different stages of the stirring.

Sample	Stage of the stirring	Stirring time
1	Only PVA on water at 90 °C, 800 rpm	2 h
2	Au/TiO2 in PVA water at 65 °C , 500 rpm	2 h
3	Suspension at room temperature, 300 rpm	6-8 h
4	Suspension at room temperature, 300 rpm	24 h
5	Suspension at room temperature, 300 rpm	48 h
6	Suspension at room temperature, just before spreading	72 h

3.3 Microreactor activity tests

In this section microreactor and parameters of the operation are described in detailed. Microreactor was applied to obtain data for the activity of the catalysts coated microreactor plates in the partial oxidation of 1-butanol. Effect of the reactor conditions and effect of the gold loading and other preparation parameters conditions were tested. Detailed amounts of the catalyst are show in Table 7.

3.3.1 The reactor setup

Microreactor activity tests were performed with a catalyst testing microreactor (CTMR). The microreactor was manufactured and customized for the need of the Catalysis research group in Aalto University by IMM (Institut Für Mikrotechnik Mainz GmbH, Mainz, Germany). Experimental setup of the microreactor is shown in Figure 18.

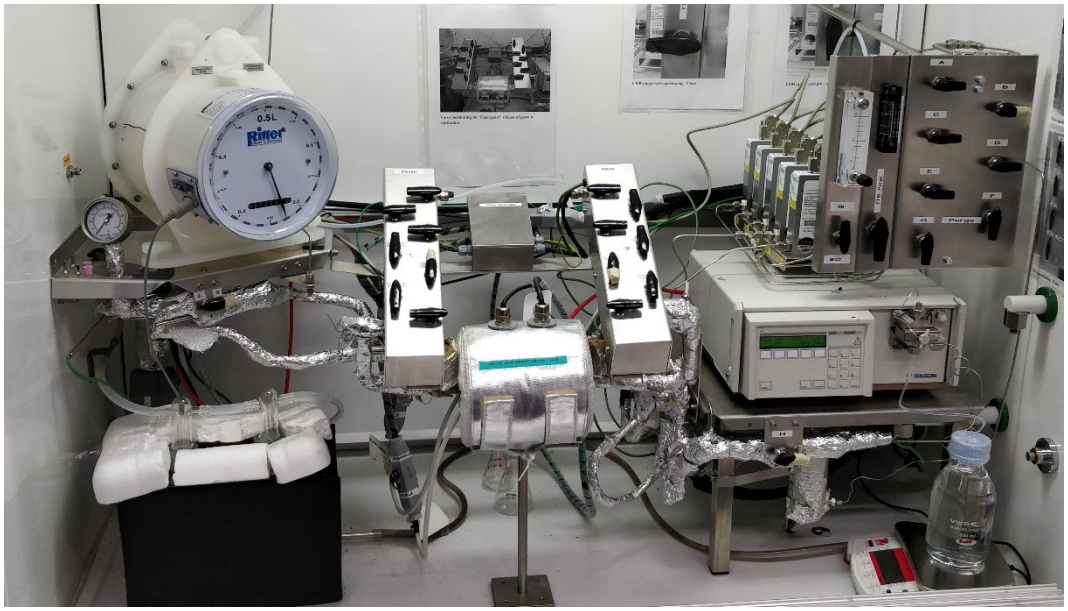

Figure 18. Experimental setup of the microreactor in fume hood.

The reactor was used for partial oxidation of 1-butanol (VWR, 99.9%), with synthetic air (AGA, 5.0) as an oxidizer in a stoichiometric ratio and N_2 (AGA, 5.0) as the carrier gas in atmospheric pressure with partial pressure of 13.5 kPa of butanol. A Gilson 307 pump was used to pump 1-butanol from an external container. 1-Butanol was evaporated and mixed with the gases. After mixing, the flow went through either the microreactor or a by-pass line to an online Fourier-transform infrared spectrometer (Gasmet instruments CR 5000). Passing through FTIR mixed gas flow went to a cold trap, where all condensable compounds were trapped and left-over air and N_2 went to ventilation through a volumetric gas meter (Ritter). The schematic experimental setup is shown in Figure 19.

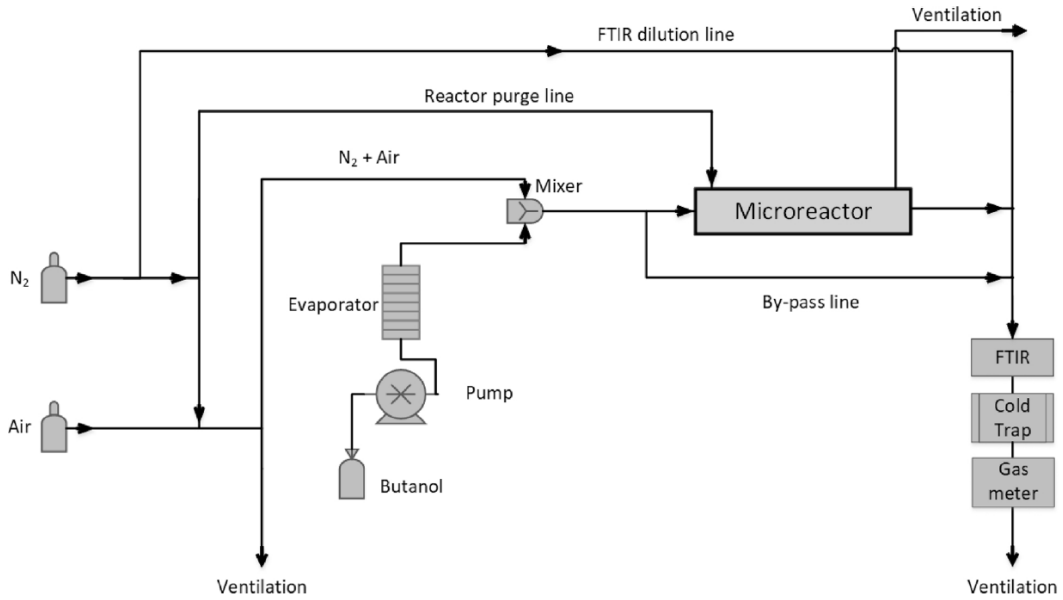

Figure 19. Schematic experimental setup of the microreactor. [17]

The reactor setup was controlled by hand and computer software. Mass flows of the gases were controlled with BROOKS (version 1.01.0) program, reactor temperature controlled with eLabs (version 3.0.2.0.) program, FTIR spectra was observed with CALMET (version 4.5.4) program and dry gas flow with Rigamo (version 3.1) program. FTIR spectra and description to obtain data are presented in Appendix A.

The reactor contains set of ten microreactor plates (10 pairs), in two different compartments, of which 9 pairs were kept as a filling and 1 as a catalyst, where the flow was directed. Plates were placed in the microreactor on top of each other and the catalyst containing channels facing each other. The reactor and plates were isolated with graphite sealings and gaskets. The reactor without the insulation and the inside of the reactor with microreactor plate set up and isolation is shown in Figure 20. The microreactor plates in more detailed are shown in Figure 21.

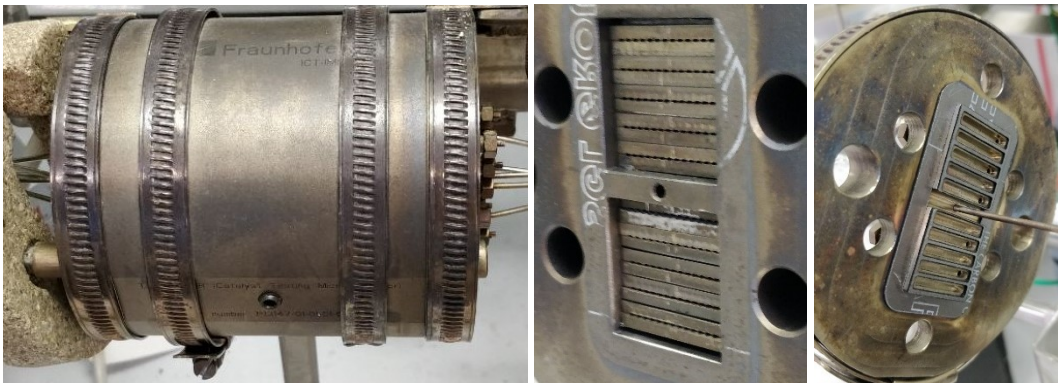

Figure 20. Reactor setup. In the left, microreactor without the insulation. In the middle, inside of the reactor 10 set of microreactor plates visible. In the right, graphite sealing and gaskets of the reactor. (Pictures are not in the same scale)

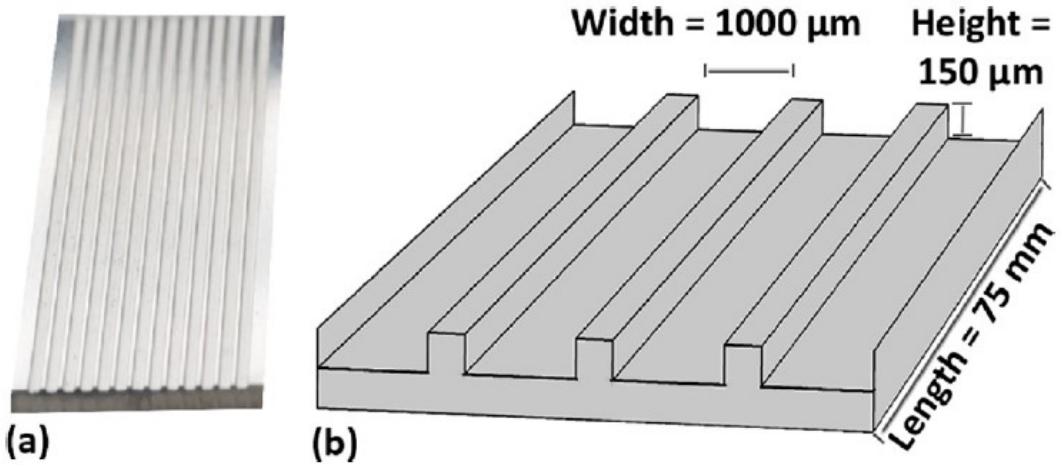

Figure 21. Detailed information of the microreactor plates. Plates had 13 channels. A) An uncoated microreactor plate. B) Schematic picture of the microreactor plate with dimensions shown.[17]. (Pictures are not in the same scale)

3.3.2 Operating procedure for the reactor

Operating the reactor for one experiment took one working day (8 hours). Depending on the day and the catalyst, different steps took different times and were run by case by case. Flows varied depending on the steps and experiment. Example procedure of each reactor experiment is shown in Figure 22. Subsections explain steps in more detail and parameters used are shown in Table 10 (section 3.3.4).

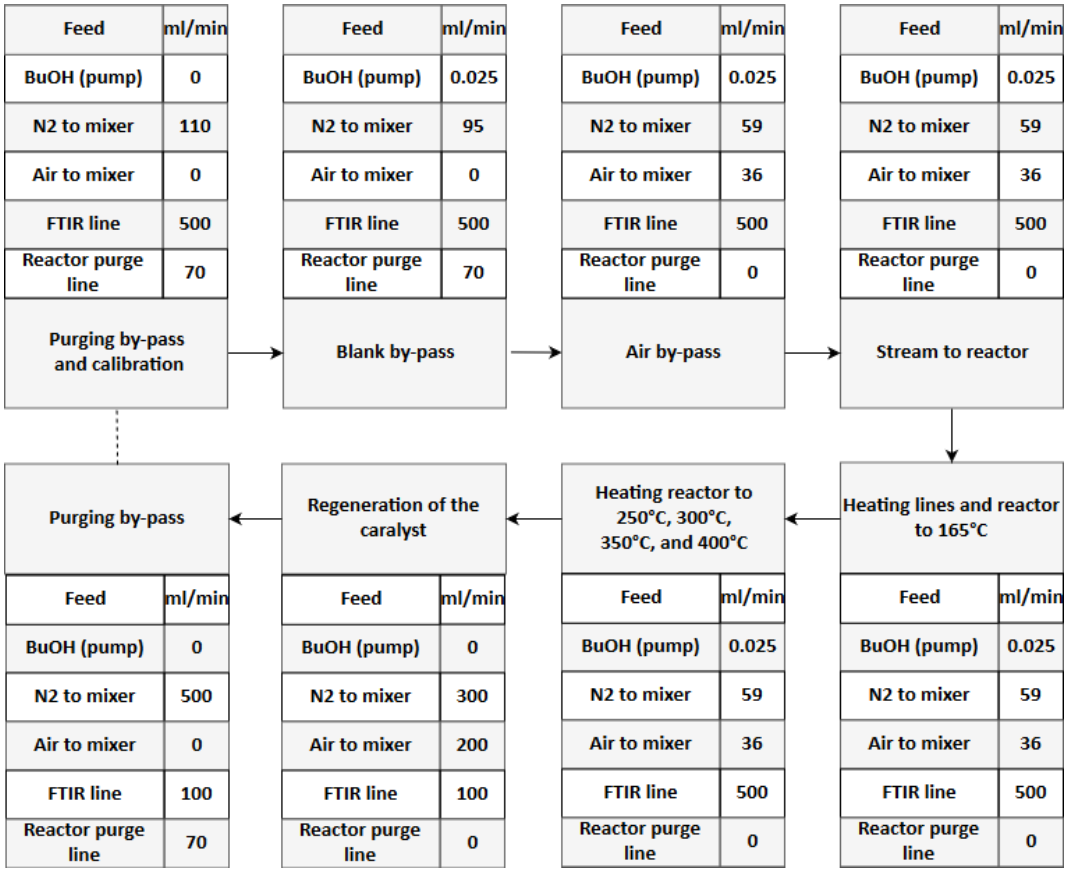

Figure 22. Example reactor experiment (experiment 3 in Table 10). Different steps of the experiment and parameters of the feeds.

Purging and calibration

In the beginning of every experiment, the reactor and by-pass line were heated to 130 °C and purged with a N_2 gas flow. At this step, the mixer line was going through by-pass line to FTIR. After reaching the temperatures, FTIR was calibrated to N_2 volum flow.

Blank by-pass

1-Butanol was added to stream and flow of the N_2 was decreased to match overall flow of 110 ml/min. FTIR spectra was stabilized by time and reference data was collected from by-pass. Flow of 1-butanol is taken as a reference point to calculate conversion of 1-butanol and selectivities of compounds in every temperature. No reaction was occurred in by-pass.

Air to by-pass

Air was added to stream and flow of the N_2 was decreased to match overall flow of 110 ml/min. FTIR spectra was stabilized by time and reference data was collected from air by-pass. No reaction was occurred in air by-pass.

Stream to reactor

The streams of 1-butanol, N_2 and air were changed from the air by-pass lines to reactor. FTIR spectra was stabilized by time and reference data was collected from the reactor at 130 °C. No reaction occurred in the reactor at 130 °C. Amount of 1-butanol decreases during the change of the flow from by-pass line to reactor.

Heating the lines and the reactor

The reactor, by-pass line and valves were heated to 165 °C and reactor output line to 168 °C, but keeping the reactor input line at the 130 °C. FTIR spectra was stabilized by time and reference data was collected from the reactor at 165 °C. No reaction was occurred in the reactor at 165 °C

Heating the reactor

The reactor was heated to 250 °C, 300 °C, 350 °C and 400 °C in different stages and waited the reactor to reach the wanted temperature. FTIR spectra was stabilized by time and reference data was collected from the reactor at wanted temperatures. Reaction occurred in the reactor and butyraldehyde and other products were formed.

Regeneration of the catalyst

Feed of the 1-butanol was stopped. Feed of the oxygen raised radically in order to burn any organic residues from the reactor and in order to regenerate the reactor.

Purging by-pass

Reactor, by-pass and other lines were purged with nitrogen to avoid any unwanted accumulation on the system. System ready was for next experiment.

3.3.3 Reactor parameters to catalysts A-E and O

For testing the effect of the gold loading and preparation parameter, same reactor parameters were used to have similar reaction conditions and create comparable data. Same partial pressure and residence time of 1-butanol were used. These experiments were done to Catalyst A-E and O. Parameters for the gold loading and preparation conditions are under “Experiment 3” in Table 10.

3.3.4 Reactor parameters by reactor condition parameter

Effect of the reactor condition to activity was tested with Catalyst O by changing the reaction conditions. Experiments were done in different partial pressures of 1-butanol and different residence times. Parameters only for the reactor condition experiments performed to Catalyst O are shown in Table 10. Effect of the partial pressure is most comparable with experiments with same residence time and effect of the residence time by comparing different residence times. Partial pressure of experiment 8 and residence time of experiment 9 are the most comparable with experiment 3 in order to see the effect of the individual parameter.

Table 10. Effect of the reaction parameters to activity. Used parameters for Catalyst O in different experiments.

Experiment	Partial pressure (kPa)	Residence time (s)	Pump flow (l) (ml/min)	BuOH (g) (ml/min)	N_2 (ml/min)	Air (ml/min)
1	13.5	0.193	0.015	10	41	23
2	13.5	0.165	0.020	12.2	49	29
3	**13.5**	**0.137**	**0.025**	**15.0**	**59**	**36**
4	13.5	0.104	0.035	20.0	78	48
5	13.5	0.080	0.050	26.0	100	62
6	13.5	0.052	0.075	40.0	154	96
7	18.0	0.193	0.020	12.2	29	29
8	18.0	0.165	**0.025**	17.2	41	37
9	18.0	**0.137**	0.035	20.0	48	42
10	18.0	0.104	0.050	26.0	54	62
11	18.0	0.080	0.065	35.0	72	84
12	18.0	0.052	0.080	42.5	88	101

3.4 Used equations

For calculating conversion *(X)* of 1-butanol, selectivity *(S)* and yield *(Y)* of the products, the following equations (3.1), (3.2) and (3.3) were used.

$$X_{\text{Butanol}} = \frac{\dot{n}_{\text{butanol,in}} - \dot{n}_{\text{butanol,out}}}{\dot{n}_{\text{butanol,in}}} \qquad (3.1)$$

$$S_{\text{product}} = \frac{\dot{n}_{\text{product,out}}}{\dot{n}_{\text{butanol,in}} - \dot{n}_{\text{butanol,out}}} \qquad (3.2)$$

$$Y_{\text{product}} = \frac{\dot{n}_{\text{product,out}}}{\dot{n}_{\text{butanol,in}}} \qquad (3.3)$$

Where $\dot{n}$ is in molar flow (mol/s) of 1-butanol or product either in or out.

4. Results

This chapter shows the results of the experimental work. Results are discussed in chapter 5. Discussion, and the error analysis is examined in chapter 6. Error estimation

4.1 Characterization

4.1.1 Transmission electron microscope

Over 150 pictures were obtained by TEM imaging from different regions of the samples. Scale of the regional pictures was 20, 50 or 100 nm depending on the region and sample. Different regions were also divided to areas where the scale was 5, 10, or 20 nm, depending on the region and sample. Every catalyst contained regions with Au particles, without particles and intermediate of these. From these pictures, best pictures were chosen by the practicality to calculate the particle size distribution and deviation. Around 200 particles from each catalyst were calculated.

The chosen pictures for the particles measurements A-G and zoomed picture H for particles are shown in Figure 23, larger pictures are shown in Appendix B. For Catalyst A two pictures were chosen to be used for the mean average particle size analysis. Measured mean average particle sizes are shown in Table 11. Particle size distributions of the catalysts are shown in Figure 23. Effect of the parameters to particle distribution are shown in Figure 24 - Figure 26.

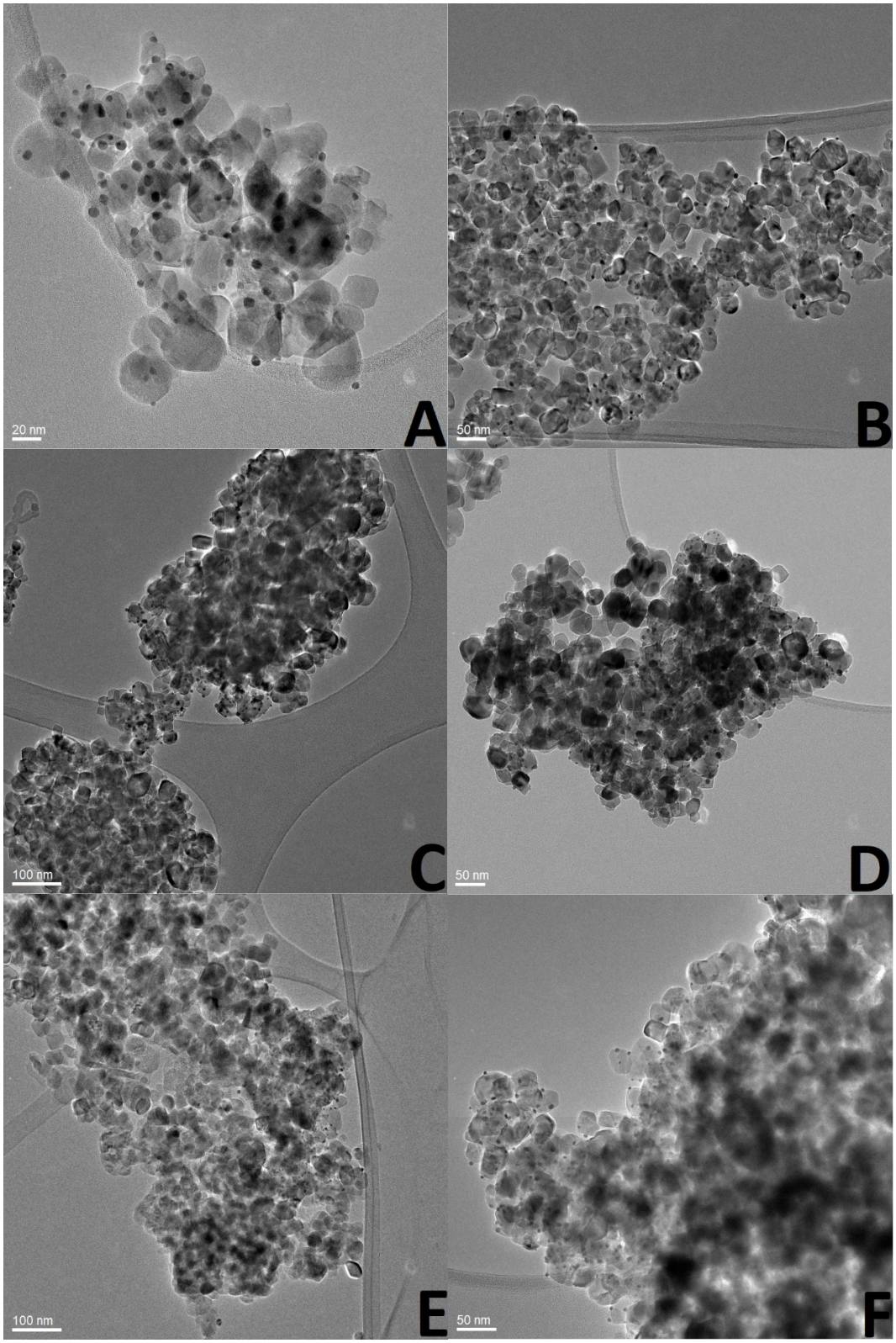
20 nm
A
50 nm
B
100 nm
C
50 nm
D
100 nm
E
50 nm
F

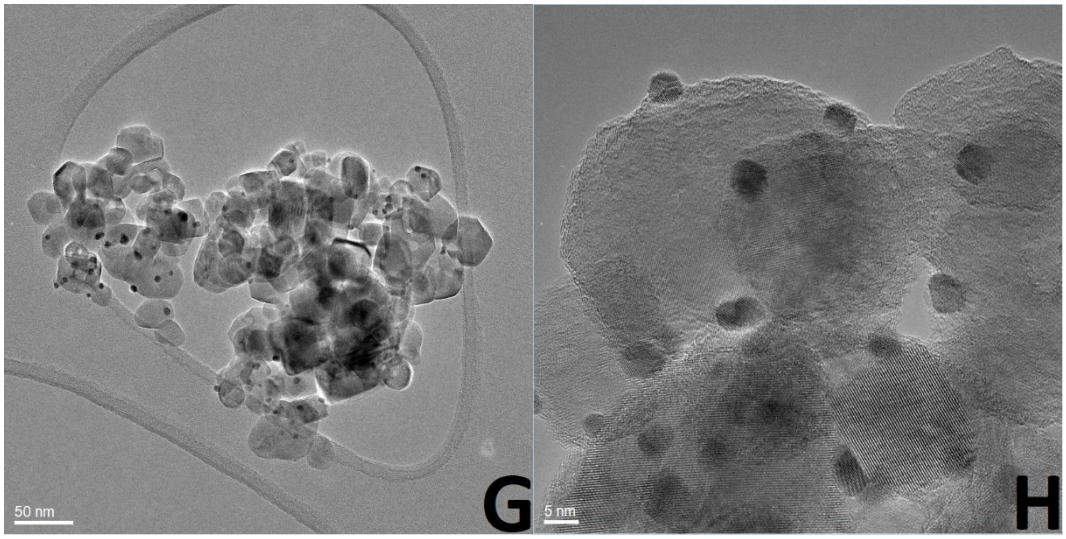

Figure 23. TEM pictures from the Au/TiO_2 catalysts the particles size for measurements. A) Catalyst A, 20 nm. B) Catalyst B, 50 nm. C) Catalyst C, 100 nm. D) Catalyst D, 50 nm. E) Catalyst E, 100 nm. F) Catalyst O, 50 nm. G) Catalyst A picture 2, 50 nm. H) Catalyst O picture zoomed to particles, 5 nm.

Table 11. Particle sizes, errors and calculated particles of the catalysts.

Name	Amount of gold	Mean average particle size (nm)	Standard deviation (nm)	Number of the measured particles
Catalyst A	1.0% Au/TiO_2	3.86	1.39	201
Catalyst B	1.0% Au/TiO_2	3.21	1.68	196
Catalyst C	0.6% Au/TiO_2	2.66	1.67	198
Catalyst D	0.6% Au/TiO_2	3.79	1.88	216
Catalyst E	0.3% Au/TiO_2	2.02	1.17	195
Catalyst O	0.6% Au/TiO_2	2.67	1.25	205

Effect of the gold amount to the particle size and distribution

Catalyst A, C and E were produced to compare the effect of the gold amount to particles size distribution (also to activity, see section 5.1.1). Comparing A, C and E, they are prepared similar having only different amount of gold in them (Table 11); there is clearly a visible trend of decreasing particle size and decreasing amount of gold. The amount of the gold affects also the particle distribution. Combined particle size distributions of Catalysts A, C and E are shown in Figure 24.

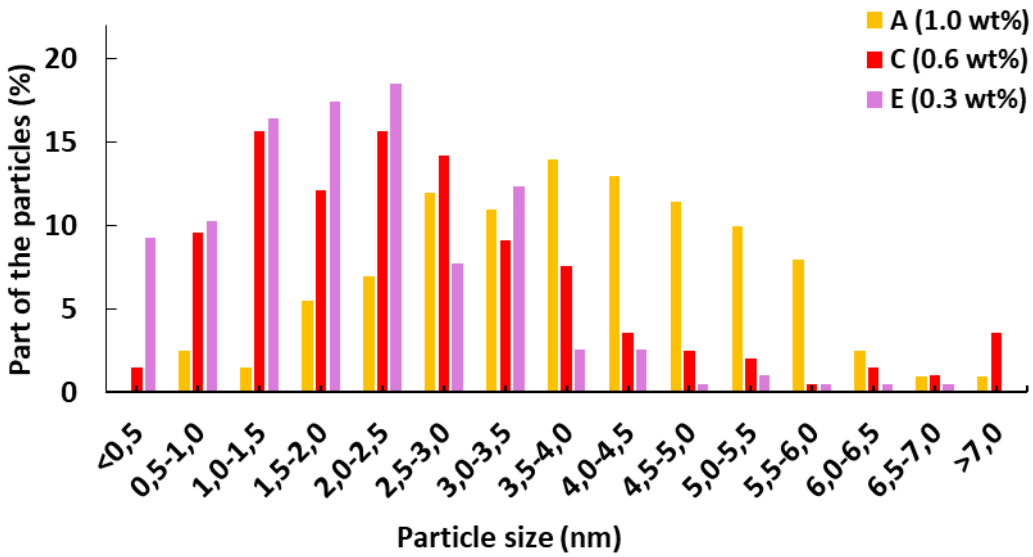

Figure 24. Particle size distribution of Catalysts A, C and E. Effect of amount of gold to particle distributions.

Catalyst A had most of the particles between 2.5 and 5.5 nm, but still quite evenly spread between 0.5 and 7.0 nm looking like shaped as normal distribution. For comparison, by assuming the particle distribution of the Catalyst A is concentrated in the center of the graph, as a flat triangle.

In Catalyst C the distribution had moved more towards range 0.5 – 4.0 nm, not evenly distributed. There were quite many particles over 7 nm, but not at all under 0.5 nm. The distribution has moved around ¼ of the graph to left but has long "tail" on the right side.

In Catalyst E more than 50% of the particles are between 1.0 and 2.5 nm and most of the particles are less than 3.5 nm in size. Around 10% of the particles are smaller than 0.5 nm in size, which Catalyst A and Catalyst C did not have at all. Distribution is moved ¼ to the left, like with Catalyst C, but Catalyst E has a more intense concentration and no "tail". This clearly indicates that there is correlation between amounts of gold with size and particle distribution of the catalysts in these preparation conditions. Catalyst B, D and O are not directly comparable to Catalysts A, C and E, having different preparation steps, but they still lead to same results.

Effect of the pH adjustment to particle size and distribution

Catalyst A and B were produced to compare the effect of pH adjustment timing to particle size. Catalyst A and B particle distributions are shown in Figure 25. Comparing particle size of A and B to each other, there are a noticeable difference between average particle size of 3.86 and 3.21 nm. There were also differences between the distributions of the particles.

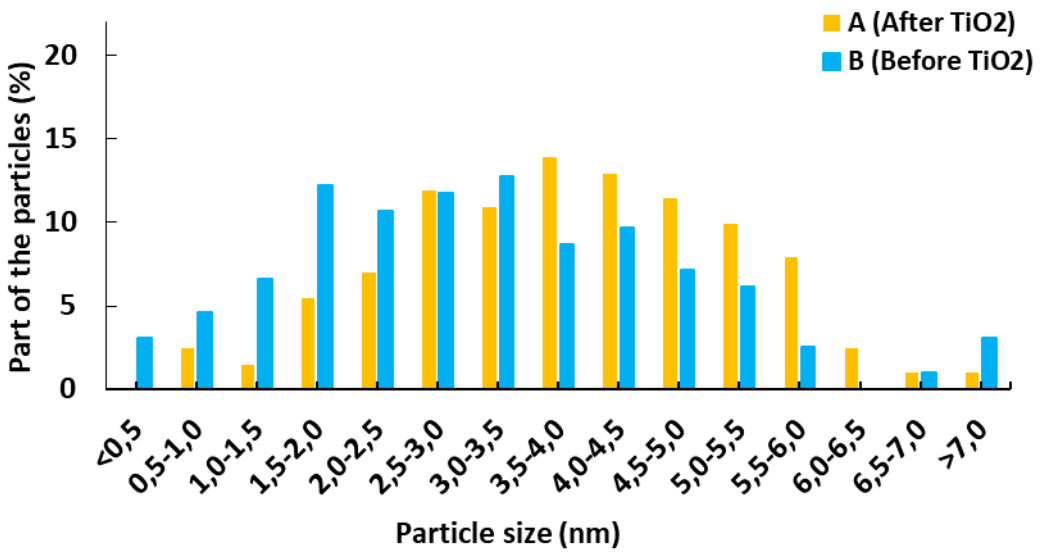

Figure 25. Particle size distribution of Catalyst A and B. Effect of pH adjustment timing to particle distributions, before and after TiO_2 addition.

Average particle size distribution of Catalyst B has been slightly moved to the left of the graph and the shape of the "triangle" has also been flattened. Catalyst B has most of the particles between 1.5 - 5.5 nm, which is roughly a 1 nm shift more to left. There is also a notable amount of more under 0.5 and over 7.0 nm particles. This shows that adjusting pH before or after adding TiO_2 has some effect on the particle distribution.

Effect of the pH level to particle size and distribution

Catalysts C (pH 1) and D (pH 3) were produced to compare the effect of pH to the Au particle size and distribution. Combined particle distribution of catalysts C, D and O are shown in Figure 26.

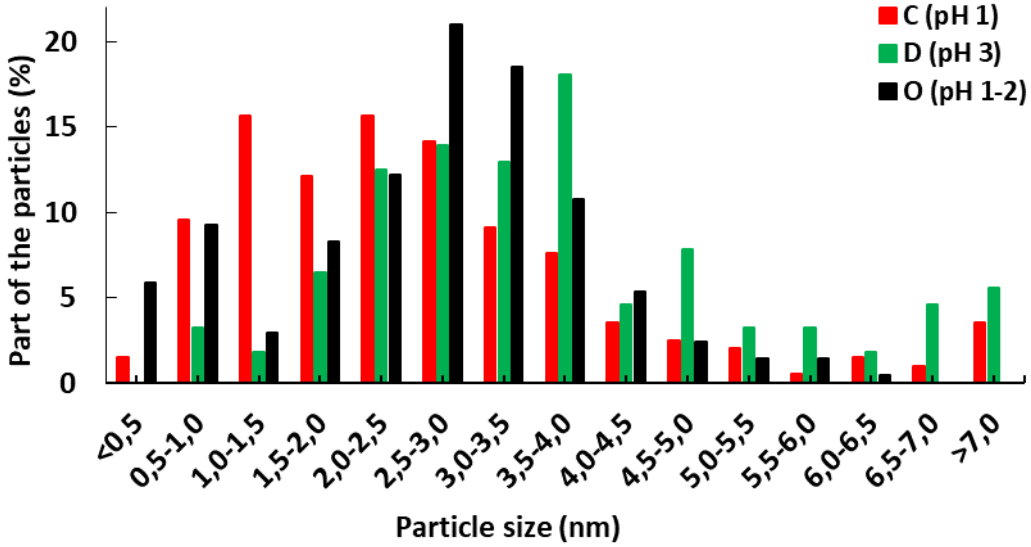

Figure 26. Particle size distribution of Catalysts C, D and O. Effect of pH to particle distribution.

It seems that the shape of the Catalyst D graph did not move as much to the left side as with the Catalyst C. Intensity of the triangle are almost the same, but the "tail" is also stronger to the right. Most of the particles are between 1.5 – 5.0 nm. There are no under 0.5 nm particles in Catalyst D, but more 6.5 – 7.0 nm than in Catalyst C. There are much less particles between 0.5 - 1.5 nm in Catalyst D, which tells that a higher pH level gives larger particles than a lower pH. Effect of the higher pH is similar to higher amount of gold.

Comparing Catalysts D and O (pH 1-2), their triangles are located in the same region, but Catalyst O is more intense and has the majority of its particles under 2.0 nm and not much particles in the region over 5.0 nm, like Catalyst D. Slightly lowered pH might have kept the distribution in a narrow area, which is like combining Catalyst E, low amount of gold to catalyst D relatively sharp triangle together.

4.1.2 Energy Dispersive Spectroscopy

Energy dispersive spectroscopy (EDS) measurements were performed on Catalysts A, B and O. According to the results, the catalysts contains only gold and TiO_2. Traces of copper comes from the TEM grip, which was made of copper. EDS results

for Catalysts A, B and O contains different amount of gold and TiO_2, due to the different amount of gold and the spot, where the EDS was taken. In samples of Catalyst O, there is no gold visible, because the EDS was taken from on TiO_2. As an example, EDS result for Catalyst A is shown in Figure 27, whereas results for Catalysts B and O are showing in Appendix C.

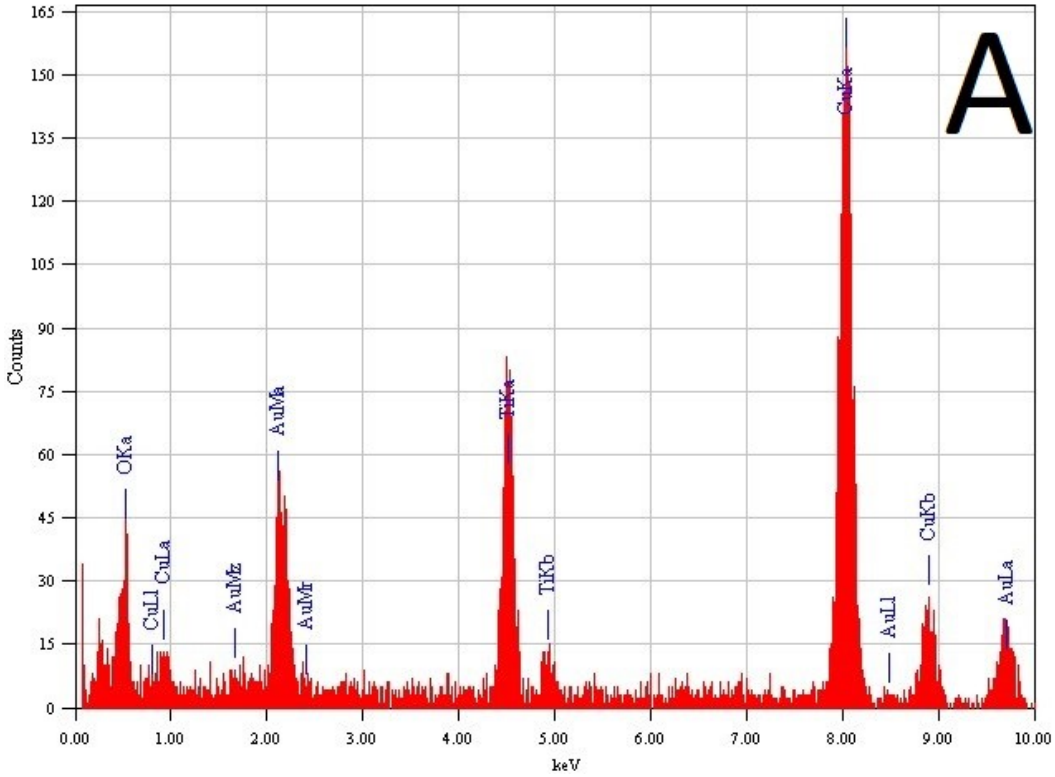

Figure 27. Results of the EDS measurements. Catalyst A, EDS from gold particle.

4.1.3 X-ray fluorescence

The results from the XRF measurements are shown in Table 12. Catalyst A and B might have been changed during the measurements. There is some variation in the amount of gold, compared to the calculated nominal amount. This was probably due to the very difficult weighing of the $HAuCl_4$. There is variation on the residues of Cl, Na and S, but the traces are very small. Na and S are calculated from Na_2O and SO_3, which were used for calibration. It is possible that traces can affect the catalytic activity somehow. The most outstanding result is the absence of Na on Catalyst E. This might be an analytical error or the amount of Na was so small that it was washed away during the filtering and rinsing. Other deviation is in the

amount of gold in Catalyst D and Catalyst B, it is 0.1% units more than it was supposed to be. XRF results also showed residues from other compounds, but they were left out, due to low amounts.

Table 12. XRF results.

	Target Au (%)	Obtained Au (%)	TiO2 (%)	Cl (%)	Na (%)	S (%)
Catalyst A*	1.0	1.0	98.0	0.0	0.1	0.0
Catalyst B*	1.0	1.2	97.6	0.0	0.1	0.0
Catalyst C	0.6	0.6	97.7	0.0	0.2	0.0
Catalyst D	0.6	0.7	98.2	0.0	0.1	0.1
Catalyst E	0.3	0.3	98.6	0.0	-	0.1
Catalyst O	0.6	0.6	98.3	0.0	0.1	0.1

* Catalyst A and B might have been mix together during the XRF measurement.

4.1.4 Thermogravimetric analysis

The weight loss (3% - 4%) of the sample occurs at around 200 °C, which is melting point of PVA. According to this analysis, there should be no PVA left on the calcined catalyst, because it is heated up to 450 °C. The results of the TGA analysis is shown in Figure 28. TGA was done only for Catalyst A, due to the very clear result of combustion of PVA.

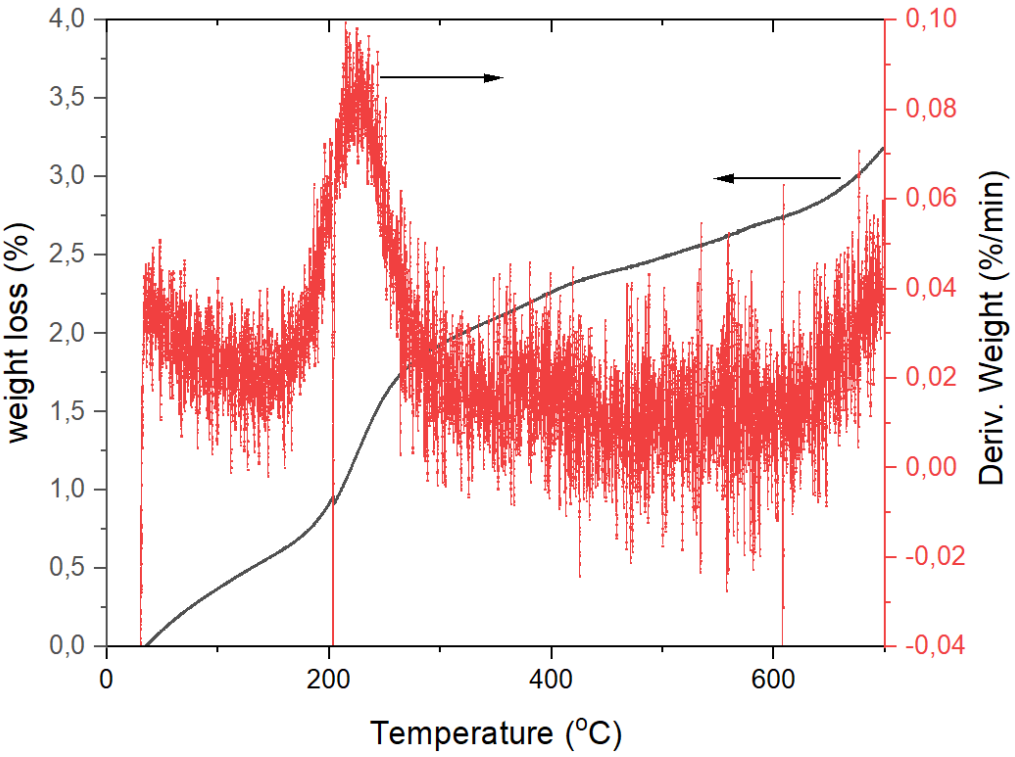

Figure 28. TGA results for Catalyst A.

4.1.5 X-ray photoelectron spectroscopy

Result of gold form XPS experiments from Catalysts A, C, E and calcined TiO_2 are shown in Figure 29. Other results are shown in Appendix D. The XPS equipment was not calibrated for the metals, so the results are only comparable with each other. There are no differences between the oxidation state and the amount of gold, according to this analysis. However, gold peaks are at 83 eV, which is close to zerovalent gold binding energy, and 87 eV.

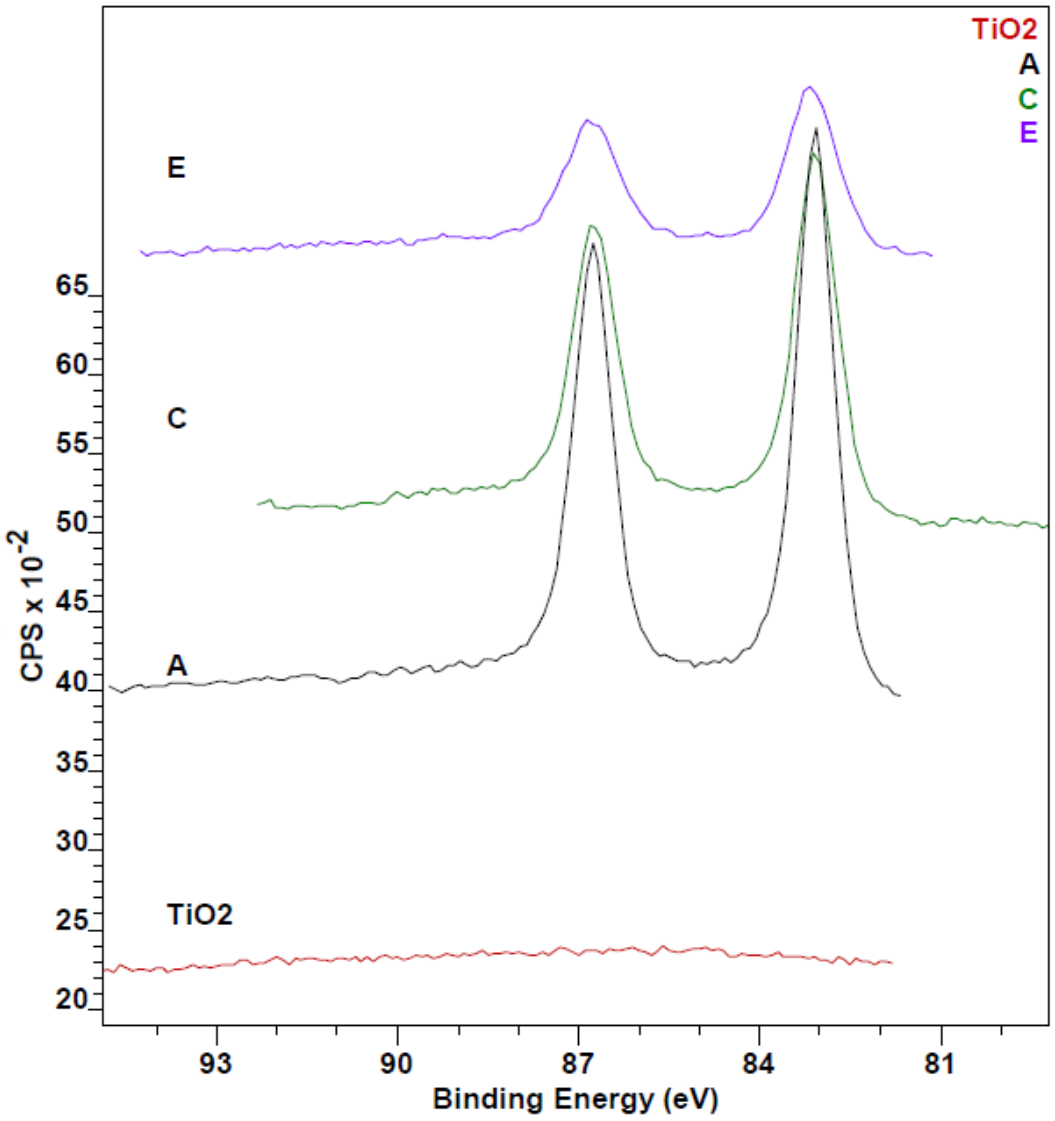

Figure 29. XPS results for the gold peak from Catalysts A, C, E and calcined TiO_2, the relative amount of gold.

4.1.6 Rheology

Viscosity tests did not go as planned. Due to the low amount of the catalyst suspension, therefore some data points needed to be left out from the experiment. The results for references (water and water + PVA) are shown in Figure 30 and for Catalyst D and Catalyst E are shown in, Figure 31. Because of human error Catalyst E analysis was on different mode, where the sensor rotated and pulled instead just pulling. As can be seen from the results, the viscosity test did not give clear result. However, it can be concluded that viscosity increased, when catalyst was added to water-PVA solution. Viscosity might have some dependence on the spreading ability of the catalyst suspension and the amount of the catalyst on the channels of the microreactor plate.

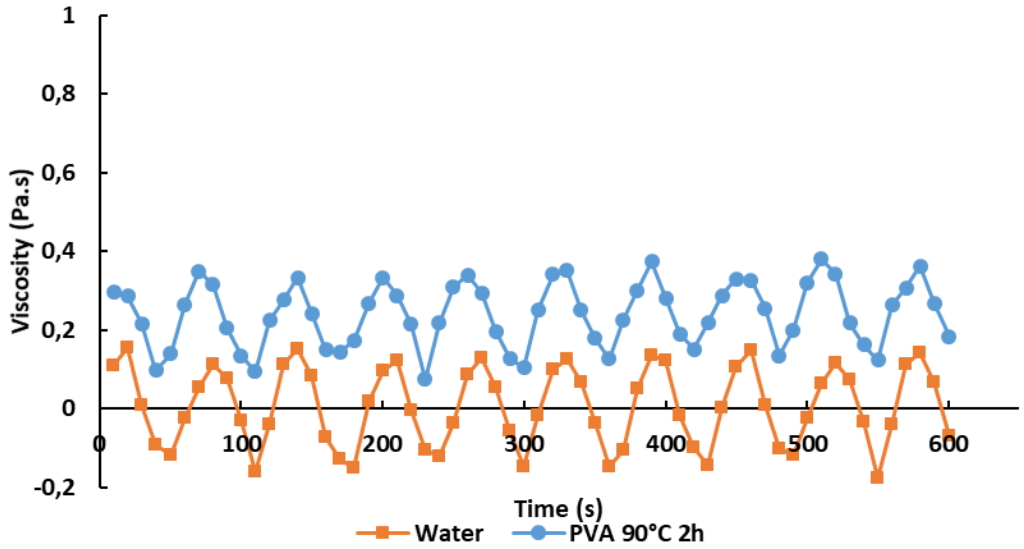

Figure 30. Reference results from viscosity analysis, water and PVA.

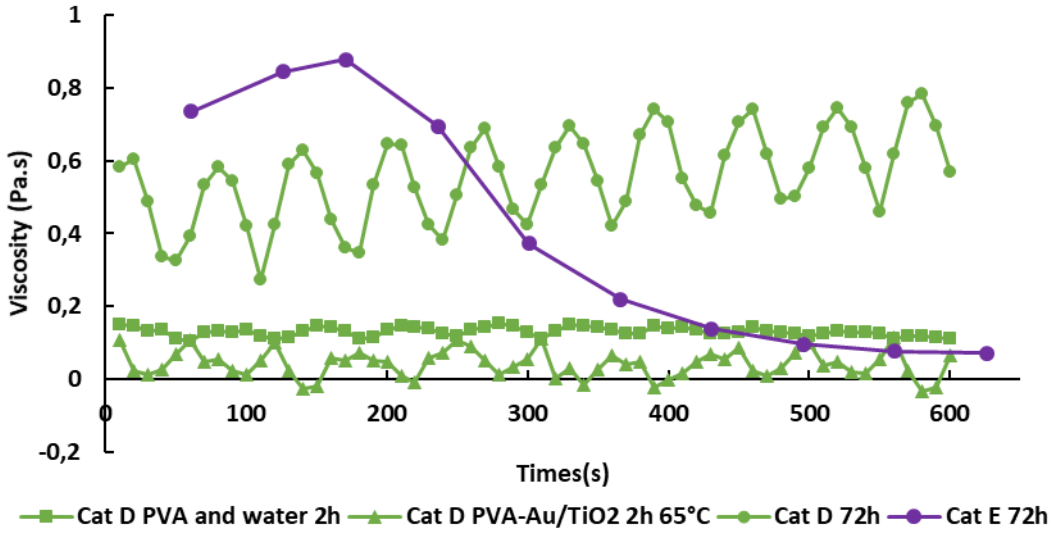

Figure 31. Catalyst suspension results from viscosity analysis.

4.2 Microreactor activity tests

A total of 27 experiments were performed to analyze the effect of the gold loading and preparation parameters on the activity of catalysts and 29 experiments to analyze the effect of the reactor condition on the activity of the catalysts, 4 experiments were possible to include in both sets (“Experiment 3”). Performed experiments for catalysts in order to obtain data from effect of the gold loading and preparation parameters to the activity are shown in Table 13. Experiments with Catalyst O, in order to obtain data from the effect of the reactor parameters to the activity are shown in Table 14. Observed products in term of yields from the partial oxidation of 1-butanol, are marked by volume percentage to give scale of the amounts (Table 15). Those products, which were produced more than 1 vol %, on different catalysts or in different reactor conditions, are graphically presented. Products, with yield lower than 1%, are presented numerically in Appendix E - Appendix G, with all other products. Detailed volume percentages of the organic compounds are presented in Subsections 4.2.1 and 4.2.2. Volume percentages amounts of water and 1-butanol are not presented in graphs.

There is drop in amount of 1-butanol when flow is changed from by-pass line to reactor. Due to the calculation method and properties of the system, data of conversion and selectivity are not exactly correct, but comparable to each other.

Table 13. The number of performed experiments to all catalysts in order to obtain data from the effect of the gold loading and preparation parameters to activity.

Name	Amount of gold	Amount of experiments
Catalyst A	1.0% Au/TiO_2	6
Catalyst B	1.0% Au/TiO_2	5
Catalyst C	0.6% Au/TiO_2	4
Catalyst D	0.6% Au/TiO_2	4
Catalyst E	0.3% Au/TiO_2	4
Catalyst O	0.6% Au/TiO_2	4

Table 14. The number of performed experiments to Catalyst O, in order to obtain data from the effect of the reactor parameters to activity. Yields of partial oxidation of 1-butanol to products are marked by volum percentage.

Experiment	Partial pressure (kPa)	Residence time (s)	Pump flow (l) (ml/min)	Amount of experiments
1	13.5	0.193	0.015	2
2	13.5	0.165	0.020	2
3	**13.5**	**0.137**	**0.025**	**4**
4	13.5	0.104	0.035	2
5	13.5	0.080	0.050	2
6	13.5	0.052	0.075	2
7	18.0	0.037	0.020	2
8	18.0	0.165	**0.025**	3
9	18.0	**0.137**	0.035	4
10	18.0	0.104	0.050	2
11	18.0	0.080	0.065	2
12	18.0	0.052	0.080	2

Table 15. Observed compounds with FTIR from all of the microreactor activity tests. Yields of all compounds are given with percentages.

Compound	Structure	Catalysts A-E and O	Experiments 1-6	Experiments 7-12
1-Butanol	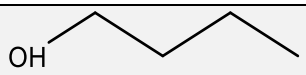	-*	-	-
Butyraldehyde	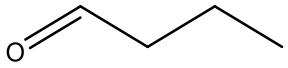	20% - 55%	50% - 65%	45% - 60%
CO	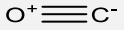	3% - 10%	3% - 5%	3% - 5%
CO2	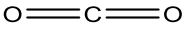	5% - 25%	15% - 30%	15% - 25%
Water	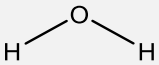	-	-	-
Trans-2-butene		1% - 10%	0% - 10%	<1%
1-Butene	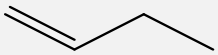	1% - 5%	<2%	<1%
Propene	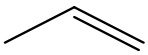	0% - 5%	<1%	<1%
Butyric acid	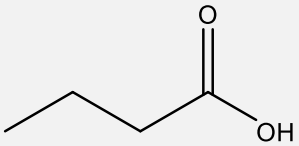	0% - 2%	<1%	<1%
2-Butene		<1%	<2%	<1%
Isobutene	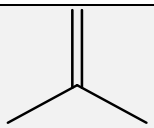	<1%	<1%	<1%
Butyl butyrate	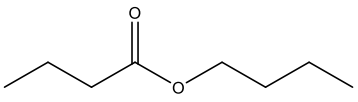	<1%	<1%	<1%
Methane	CH_4	<1%	<1%	<1%

* yield was not considered

4.2.1 Effect of gold loading and preparation parameters on activity of the catalyst

From every experiment of the catalyst, average of the results were taken. Results have been collected to observe the effect of gold amount, adjustment step of pH and level of pH to activity. Average selectivity, conversion and yields of partial oxidation of 1-butanol to butyraldehyde as a desired product from the partial oxidation are presented. Yield graphs give the best overall picture from the catalysts. Average yields from CO and CO_2, which both were produced more than 10% in the temperature range, as a normal oxidation product are presented. Average yields of the major side products such as t-2-butene, 1-butene, propene and butyric acid in range of 1% - 15% are presented. Specific reaction parameters are shown in Table 10 and number of experiments in Table 13.

Effect of gold amount to activity

Conversion of 1-butanol

Conversion of 1-butanol over Catalysts A, C and E with different amounts of gold in them are shown in Figure 32. Conversion of 1-butanol increases with increasing temperature. Amount of gold effects quite much to conversion, Catalyst E has the highest conversion with smallest amount of gold, but Catalyst C has almost the same conversion at 400 °C. Conversion over Catalyst E separates already at 250 °C from those of Catalysts A and C. Conversion over catalysts A and C separates at 300 °C, when conversion over Catalyst C increases more. A lower amount of gold is converting more than a higher amount of gold.

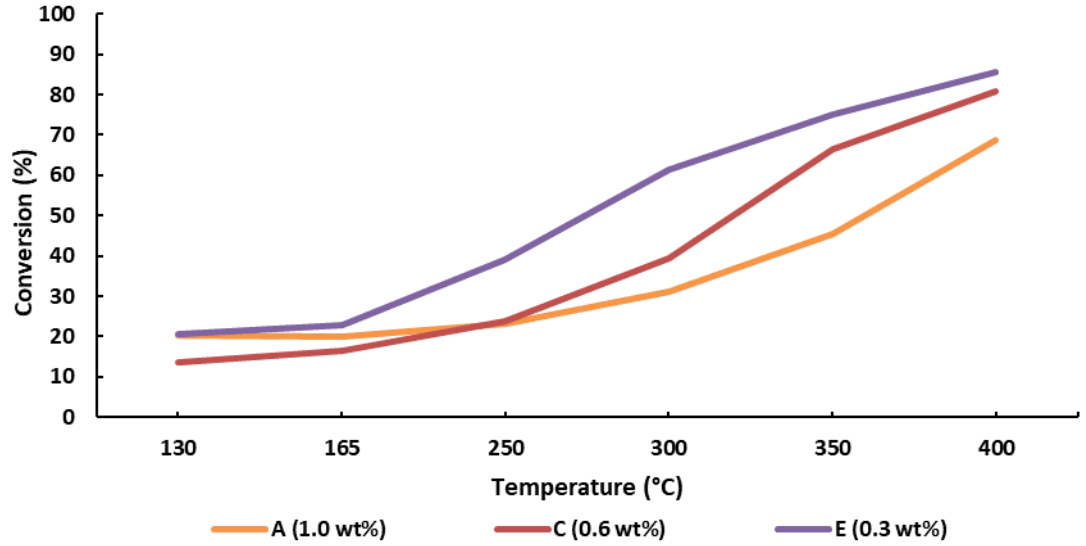

Figure 32. Conversion of 1-butanol Catalysts A, C and E. Effect of the amount of gold to activity.

Selectivity to butyraldehyde

Selectivity to butyraldehyde over Catalysts A, C and E to butyraldehyde, with different amount of gold is shown in Figure 33. In terms of selectivity, to butyraldehyde, the effect of gold loading is not clear. Selectivity over Catalyst C is the highest in every temperature and selectivity over Catalyst E is the second highest. Selectivities over Catalyst C and E increase much faster than selectivity over Catalyst A. The selectivity to butyraldehyde is not in line with the amount of gold, even though conversion was. It seems that there is more an optimal amount of gold between 0.3% and 1.0% with respect of selective to butyraldehyde.

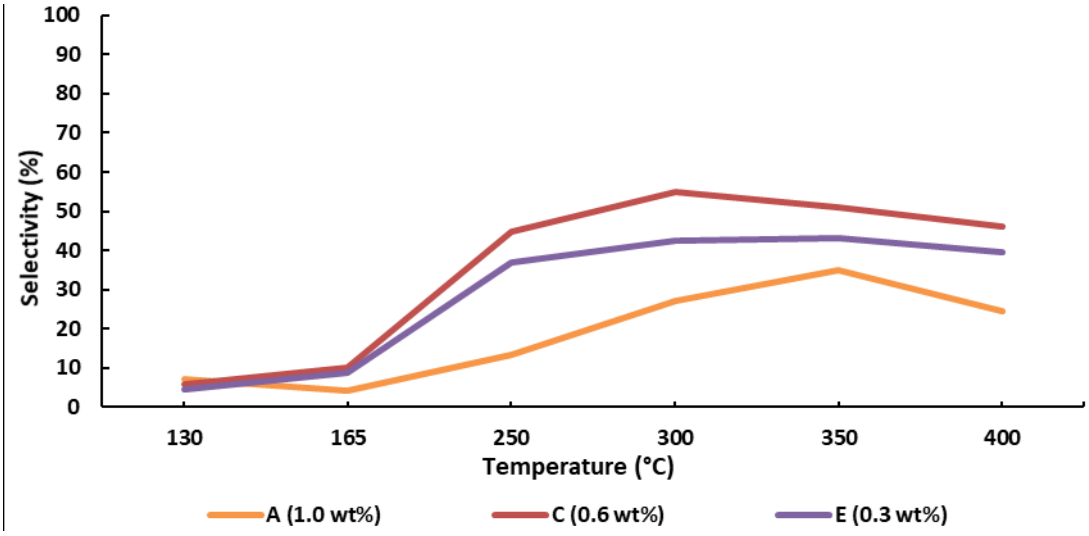

Figure 33. Selectivity to buturyaldehyde over Catalysts A, C and E. Effect of the amount of gold to activity.

Yield of butyraldehyde

Yields of Catalysts A, C and E to butyraldehyde, with different amount of gold are shown in Figure 34. The yield of butyraldehyde over Catalysts C and E was similar, but effect of the temperature changes the yield. Yield of butyraldehyde over Catalyst E is higher than over Catalyst C at temperatures below 300 °C. However, at temperatures above 350 °C, higher yield was achieved over Catalyst C compared to that of Catalyst E. The effect of gold loading is a combination of selectivity and conversion, and in this case Catalyst C and E are very close to each other even if there was a clear difference in conversion and selectivity. There is a major decrease on the percent, when comparing conversion over 80% to yield of under 40%. Even amount percent's of Catalyst A are decreased from conversion around 70% to as low as selectivity of 20%. It would seem that there is correlation between gold loading and yield, but it is affected by selectivity more than conversion. For yield there seems not to be as much difference to yield of butyraldehyde with amount of gold. Of course, in this case it was better to have less than 1% by weight of gold.

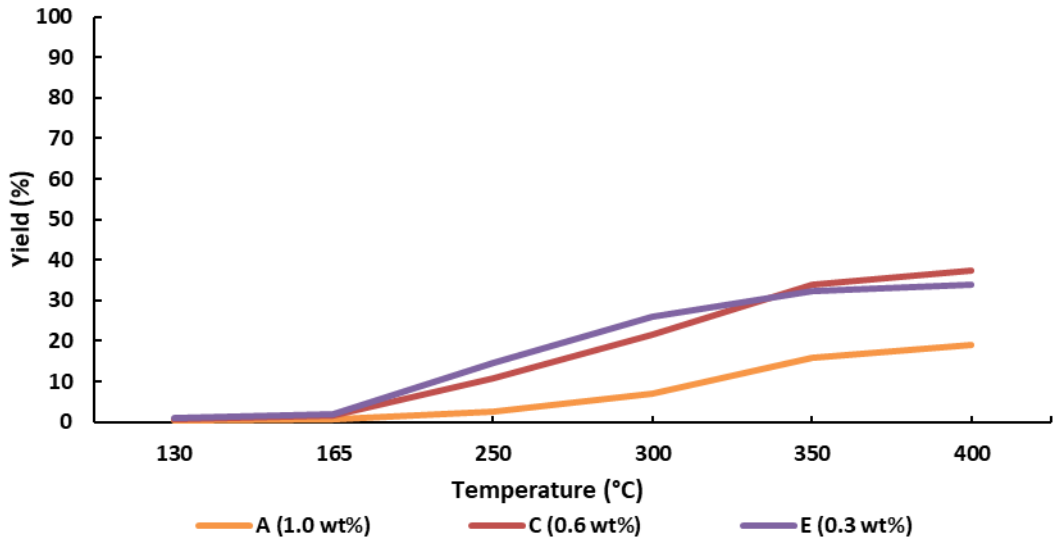

Figure 34. Yield of 1-butanol to butyraldehyde, Catalysts A, C and E. Effect of amount of gold to activity.

Yield of CO and CO_2

Yields of Catalysts A, C and E to CO and CO_2, with different amount of gold are shown in Figure 35. In yield of CO and CO_2 smaller amount of gold increases the yield. The yield of CO_2 and CO is correlated with amount of gold as was conversion of 1-butanol, the lower the amount of gold, the higher the yield. There are similarities on the trends, lower amount of gold increases the yield at lower temperatures and increasing overall production of the CO_2 and CO. CO_2 and CO are increasing with same style, however when the temperature increases, CO_2 changes the rate of increase, when curve of CO stays more constant.

At Catalyst E the yield of butyraldehyde was changing at 300 °C, when the yield of CO_2 increased. Same occurs with Catalysts A and C at 350 °C. It is possible that smaller particle size and distribution controls the yield to CO_2 and CO. The yield of CO seems to be ½ yield of the CO_2, but in Catalyst C it is around ¼ of the yield.

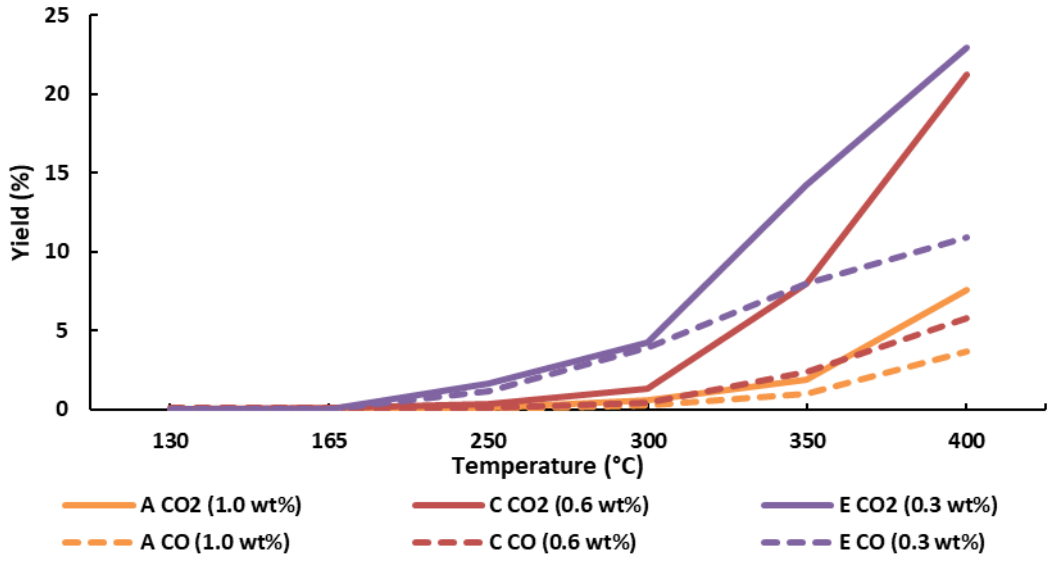

Figure 35. Yield of 1-butanol to CO_2 and CO, Catalysts A, C and E. Effect of amount of gold to activity.

Major side products

Yield of t-2-butene

Yields of Catalysts A, C and E to t-2-butene, with different amount of gold are shown in Figure 36. The amount of gold affect significally to yields, higher amount of gold yields, higher amount of t-2-butene and in lower temperatures.

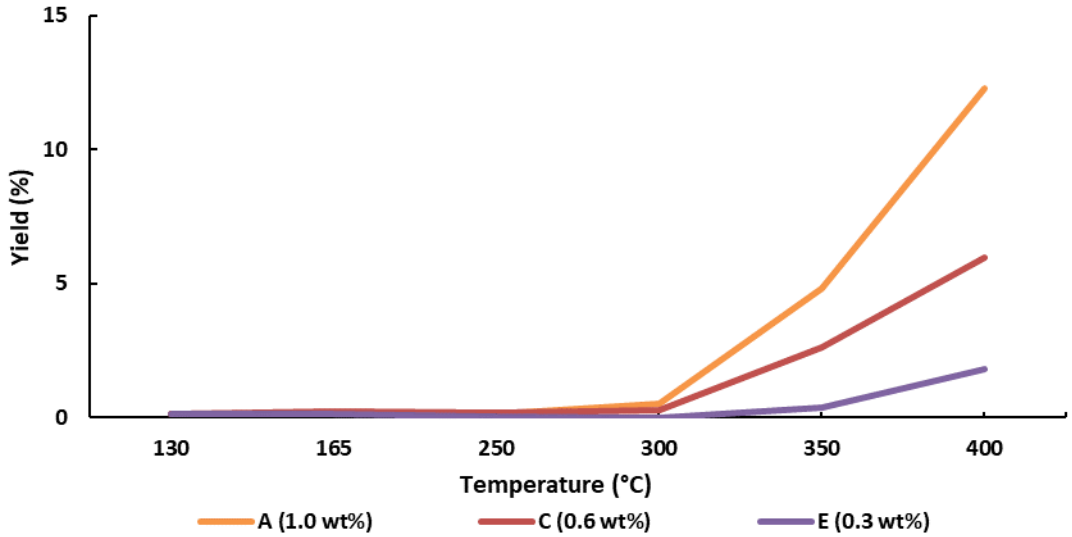

Figure 36. Yield of 1-butanol to t-2-butene, Catalysts A, C and E. Effect of amount of gold to activity.

Yield of 1-butene

Yields of Catalysts A, C and E to 1-butene, with different amount of gold are shown in Figure 37. The amount of gold affecting the yield of 1-butene much differently than in the yield of butyraldehyde. A higher amount of gold is producing more 1-butene that a lower amount of gold. Catalysts C and E have similar trends, but also some variation in the yield and temperatures. Catalyst E includes the lowest amount of gold and it starts to produce 1-butene at 250 °C and the yield stay constant between 300 - 350 °C and the yield decreases. While Catalysts A and C starts to produce 1-butene at 300 °C and yield of Catalyst A increases constantly to 400 °C, Catalyst C is having similar trend to Catalyst E at 350 °C.

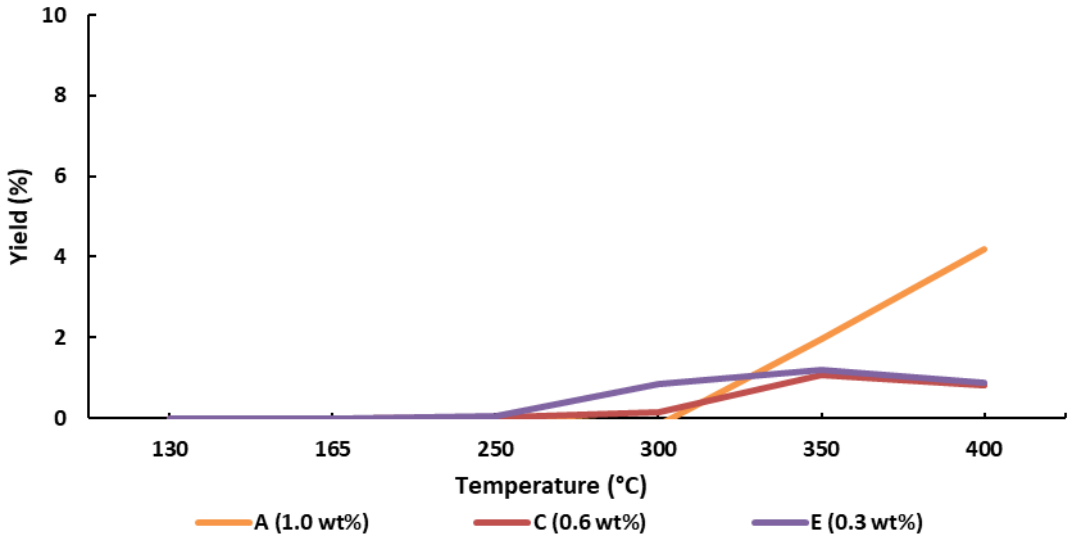

Figure 37. Yield of 1-butanol to 1-butene, Catalysts A, C and E. Effect of amount of gold to activity.

Yield of propene

Yields of Catalysts A, C and E to propene, with different amount of gold are shown in Figure 38. Catalyst E was only catalyst to yield propene more than 1%. Catalyst A and C barely yield any propene, but Catalyst E is yielding quite much. Graph of the Catalyst E starts to increase already at 165 °C and increases to 300 °C, where it increases even more. Graphs of Catalyst A and C are increasing slightly at 400 °C. The amount of gold is affecting the yield of propene significally.

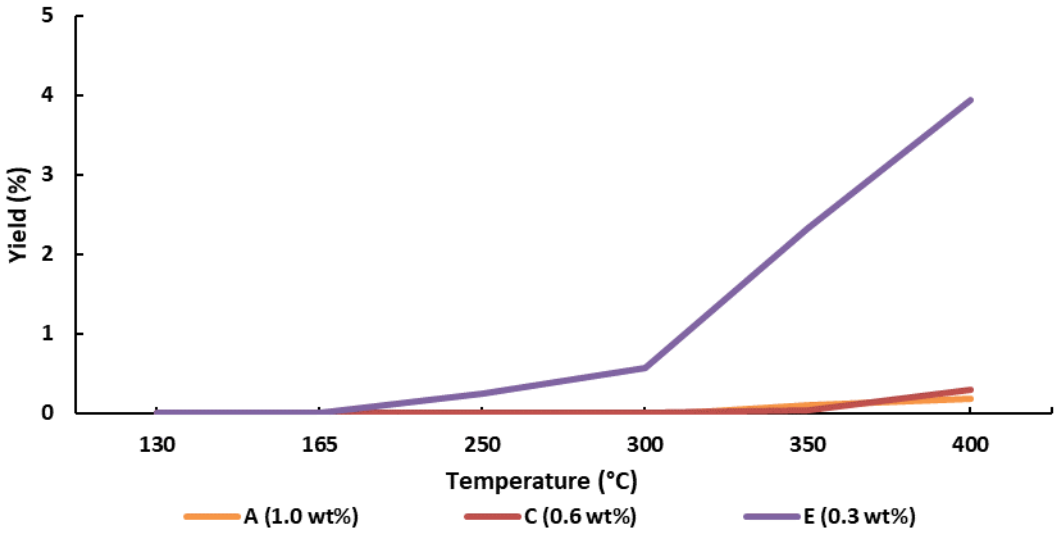

Figure 38. Yield of 1-butanol to propene, Catalysts A, C and E. Effect of amount of gold to activity.

Yield of butyric acid

Yields of Catalysts A, C and E to butyric acid, with different amount of gold are shown in Figure 39. Catalyst E was the only catalyst producing more than 1% of butyric acid. Yield of butyric acid starts at 250 °C and increases to 300 °C. After 300 °C yield of butyric acid decreases. Yields of Catalysts A and C are not very reliable due to small amount.

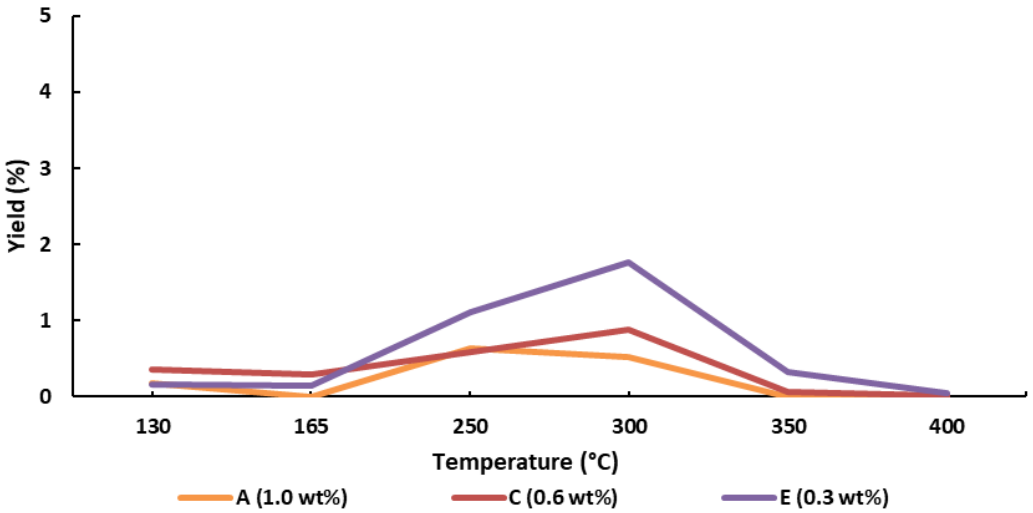

Figure 39. Yield of 1-butanol to butyric acid, Catalysts A, C and E. Effect of amount of gold to activity.

Effect of the pH adjustment to activity

Conversion of 1-butanol

Conversion of Catalysts A and B, with different pH adjustment step are shown in Figure 40. Catalysts A and B have the same amount of gold, but Catalyst B is converting less 1-butanol.

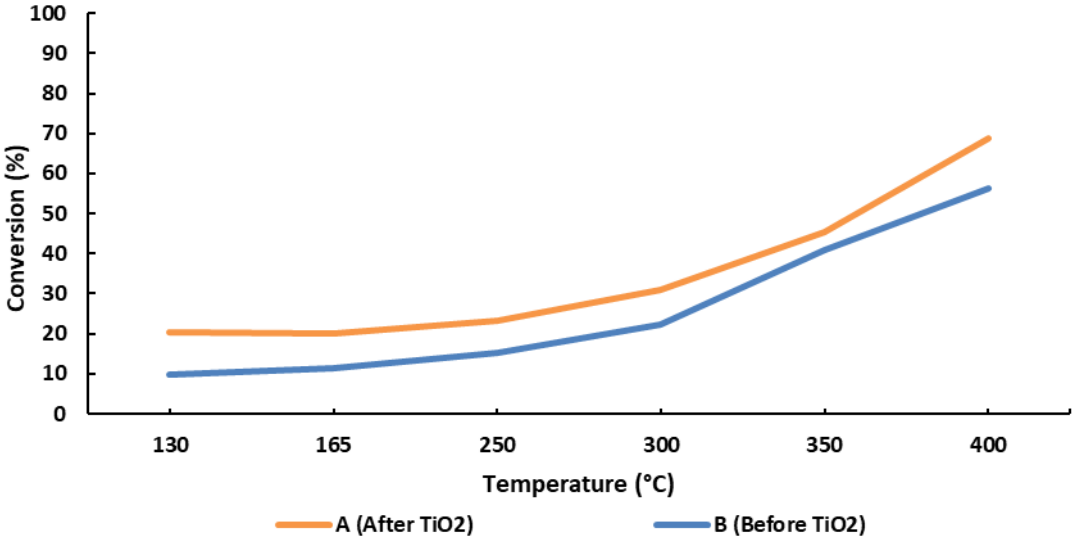

Figure 40. Conversions of 1-butanol Catalyst A and B. Effect of the pH adjustment step to activity.

Selectivity to butyraldehyde

Selectivity of Catalyst A and B, which explain more of the selectivity between same amount of gold, but different size and distributions of the particles are shown in Figure 41.

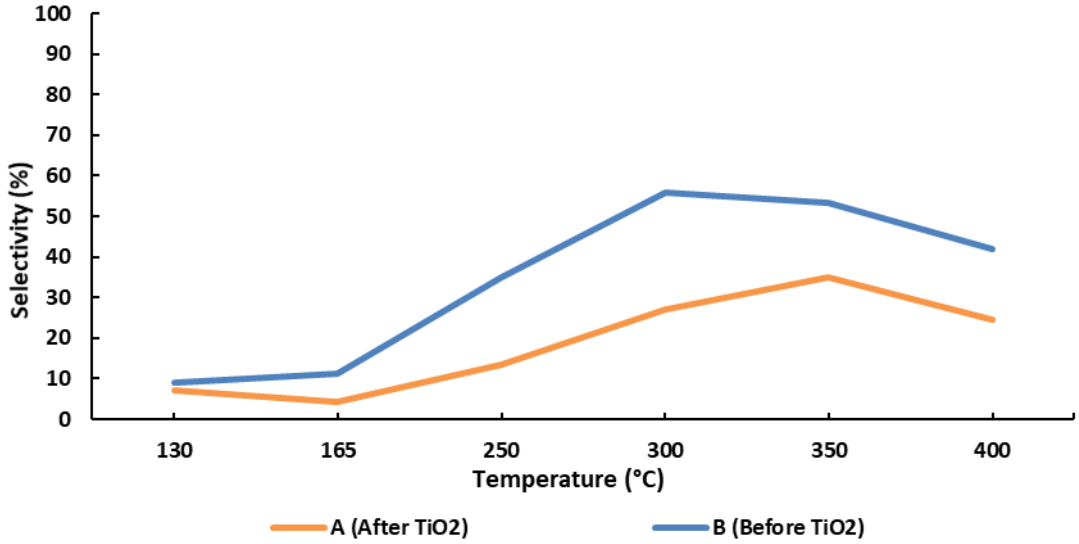

Figure 41. Selectivities of Catalysts A and B to butyraldehyde. Effect of the pH adjustment step to activity.

Yield of butyraldehyde

Yields of butyraldehyde of Catalyst A and B, with different pH adjustment step are shown in Figure 42. Yield is affected by conversion and selectivity, as did the other parameters. Yield shows that there is some difference between Catalyst A and B in producing butyraldehyde. Much better selectivity is exceeding slightly higher conversion in the yield.

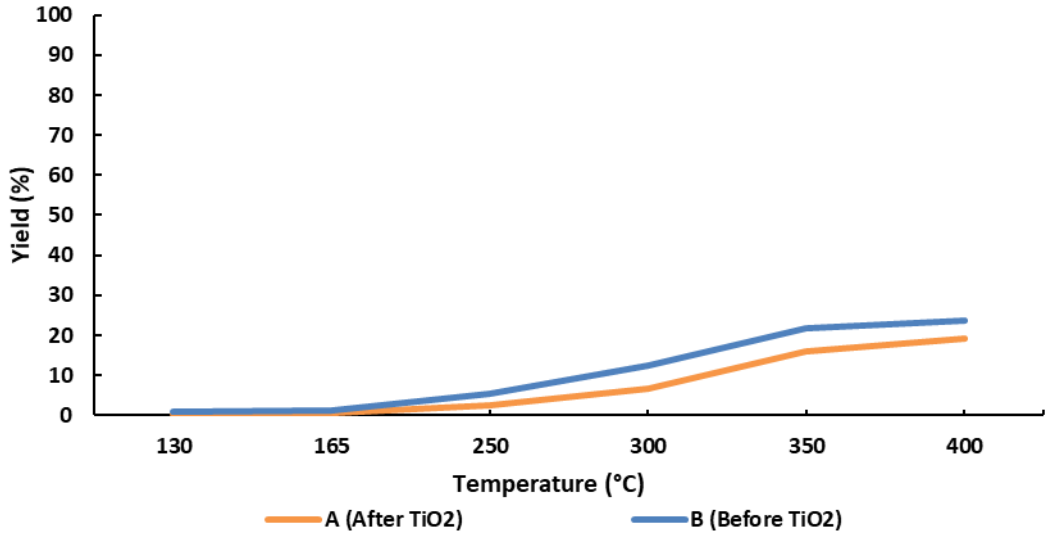

Figure 42. Yield of 1-butanol to butyraldehyde, Catalysts A and B. Effect of the pH adjustment step to activity.

Yield of CO and CO_2

Yields of Catalysts A and B to CO_2 and CO, with different amount of gold are shown in Figure 43. The differences between Catalysts A and B are as small as were the differences between yields of butyraldehyde, the trend is same, but the amounts are slightly different. As for the yields of CO_2 and CO, they develop at same rate to 350 °C and separate slightly after that.

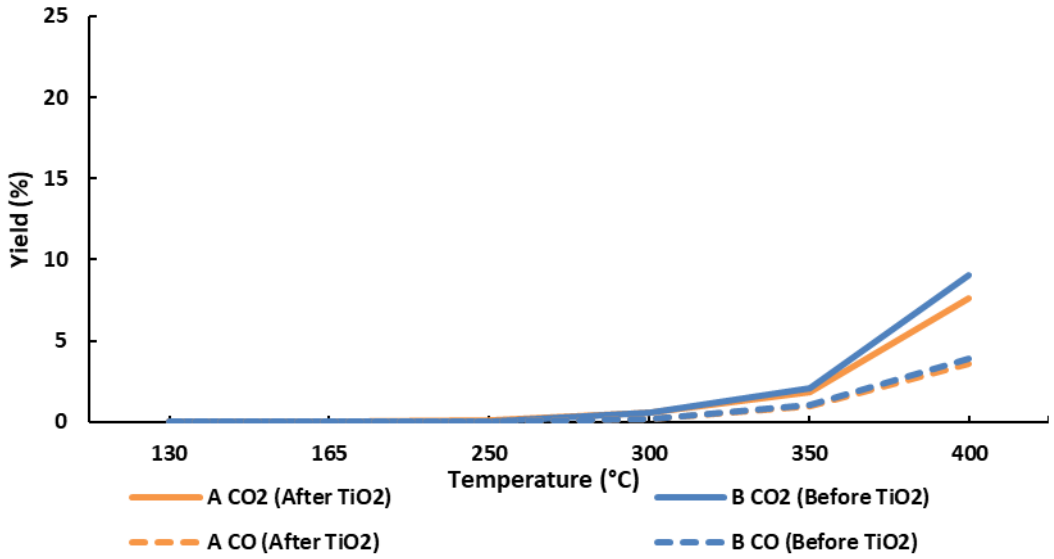

Figure 43. Yield of 1-butanol to CO_2 and CO, Catalysts A, C and E. Effect of the pH adjustment step to activity.

Major side products

Yield of t-2-butene

Yields of t-2-butene of Catalyst A and B, with different pH adjustment step are shown in Figure 44. The effect of the pH adjustment step decreased the yield of 1-butene, but keeps the starting temperature and trend same.

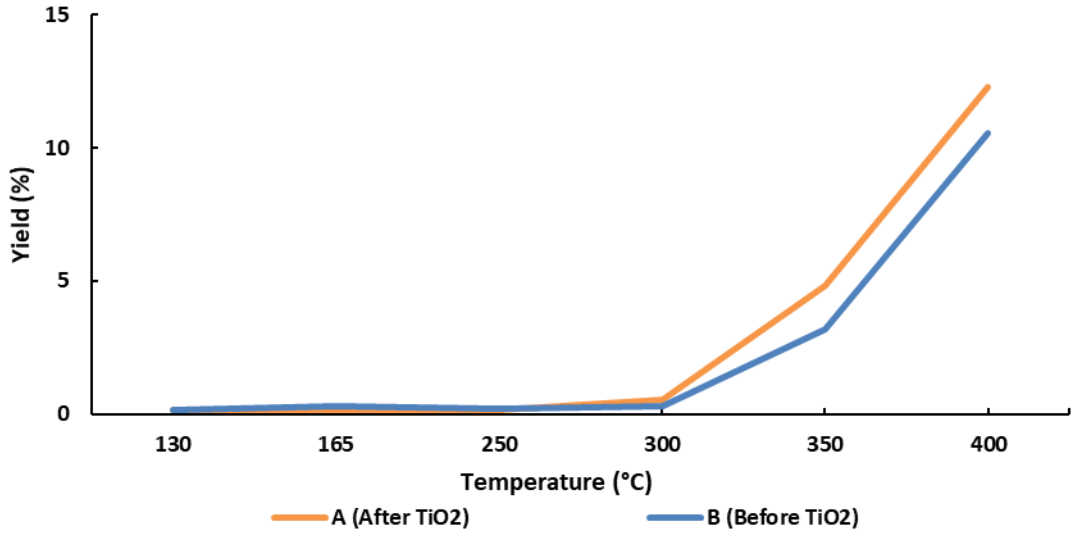

Figure 44. Yield of 1-butanol to t-2-butene, Catalysts A and B. Effect of the pH adjustment step to activity.

Yield of 1-butene

Yields of 1-butene of Catalyst A and B, with different pH adjustment step are shown in Figure 45. The effect of the pH adjustment step increased the yield of 1-butene and decreases the starting temperature slightly, while keeping the trend same.

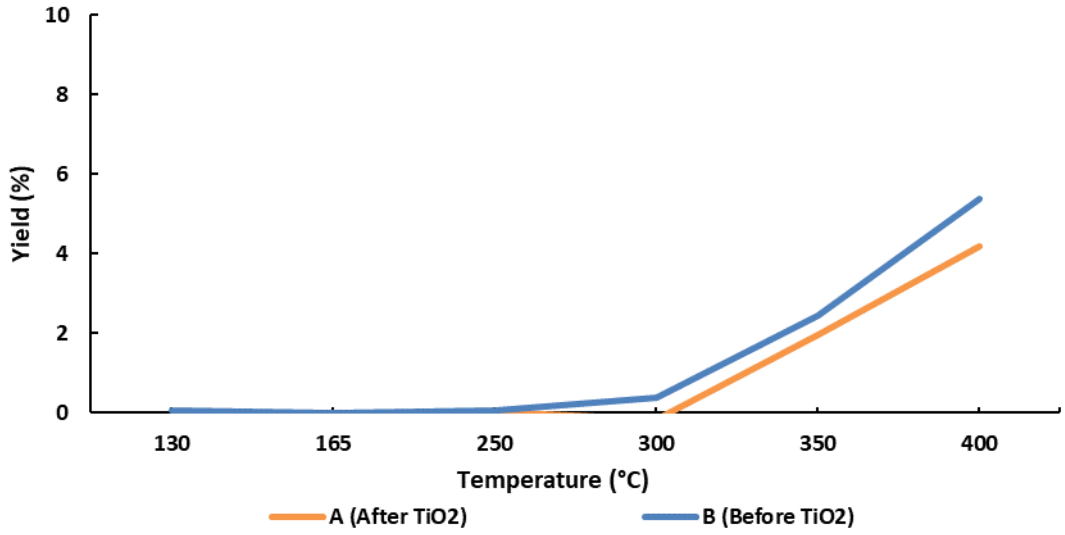

Figure 45. Yield of 1-butanol to 1-butene, Catalysts A and B. Effect of the pH adjustment step to activity

Effect of the pH level to activity

Conversion of 1-butanol

The conversion of Catalysts C, D and O are shown in Figure 46. The trend of the conversion of the Catalyst C, D and O are similar and the difference between the catalysts at the 400 °C looks very even, as the Catalyst D followed Catalysts C and O lower temperatures, before graph of C and O separated. It seems that lower pH gives higher conversion at high temperatures.

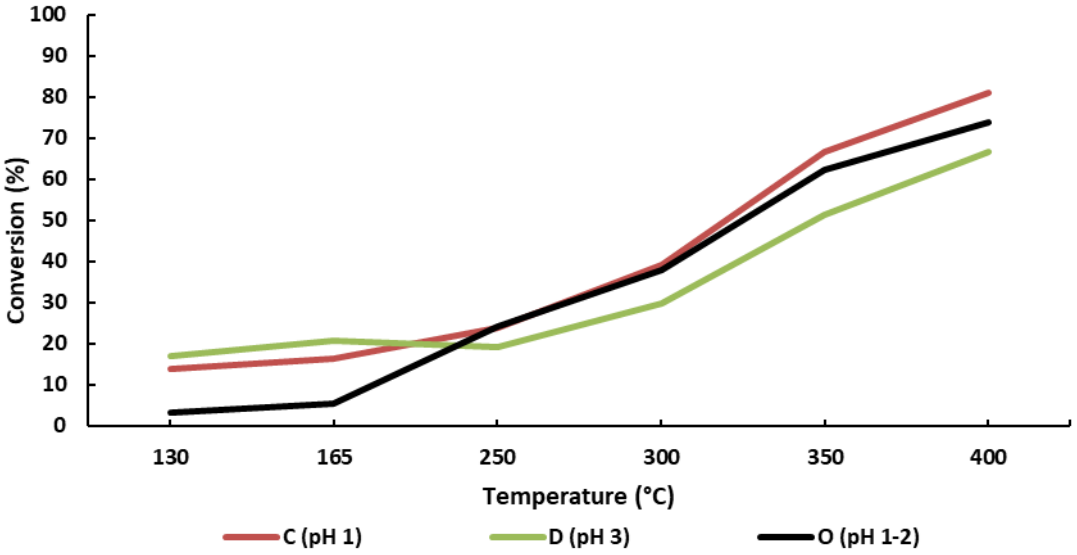

Figure 46. Conversions of 1-butanol Catalysts C, D and O. Effect of the pH level to activity.

Selectivity to butyraldehyde

Selectivities of Catalysts C, D and O, with different pH level are shown in Figure 47. There is a difference between the selectivities and pH level with same catalysts, same amount of gold and even particle size. The most interesting feature is decrease of Catalyst O between 300 °C and 350 °C and then increasing back and even more to 300 °C, when the selectivity of Catalysts C and D are decreasing after 350 °C.

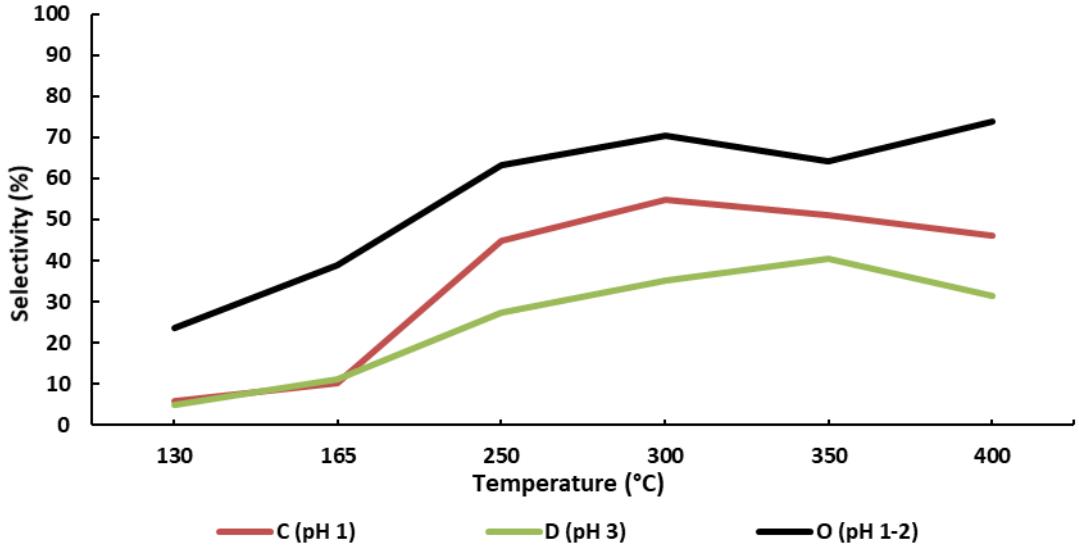

Figure 47. Selectivities of Catalysts C, D and O. The effect of pH level to activity.

Yield of butyraldehyde

Yields of butyraldehyde of Catalysts C, D and O, with different pH level are shown in Figure 48. Graph of Catalyst O continues linear, while C and D have a linear part of increasing yield, but yield changes at 350 °C. Comparing yield to conversion, graphs of all three catalysts were increasing, but the difference comes in selectivity. Selectivity decreases with C and D and this affects the yield also. There must be something in the particle size and distribution, which keeps the selectivity and this way yield stable all the way to 400 °C.

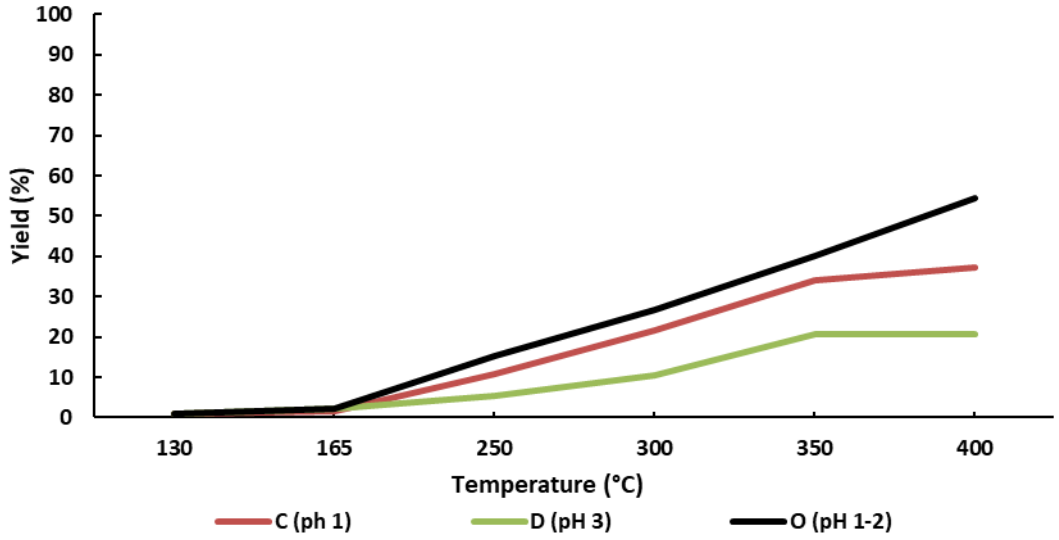

Figure 48. Yield of 1-butanol to butyraldehyde, Catalysts C, D and O. Effect of pH level to activity.

Yield of CO and CO_2

Yields of Catalysts C, D and O to CO_2 and CO are shown in Figure 49. The trend of Catalyst O is different than Catalyst C and D in yields of CO_2 and CO. An interesting observation was the change in the rate of CO and CO_2 yield after 350 °C. Catalyst C is the only one with yield of CO is half the amount from CO_2, which was trend with A, B and E. Catalyst O and C are having yield of CO one quarter yield of CO_2.

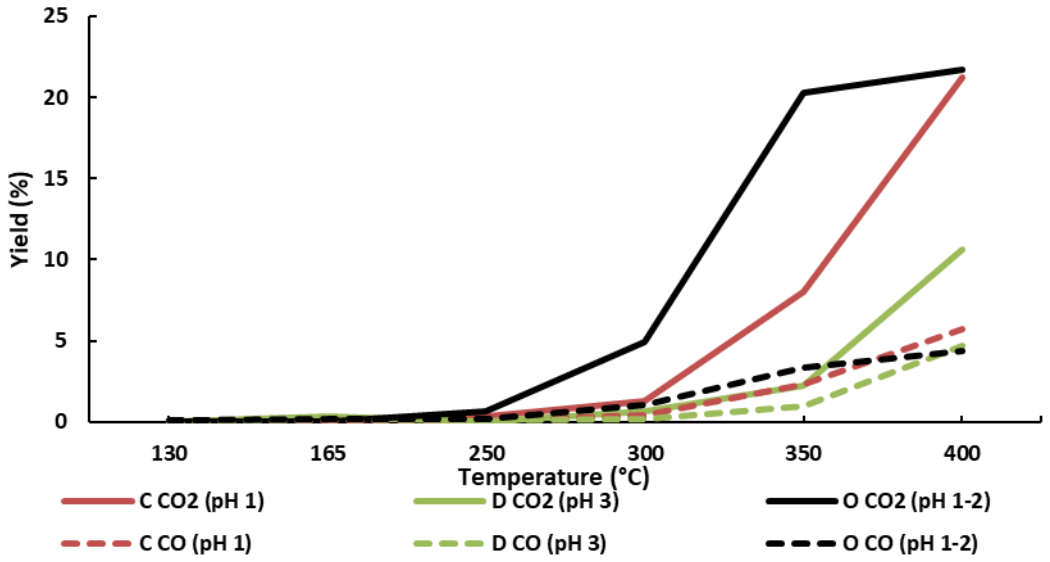

Figure 49. Yield of 1-butanol to CO_2 and CO, Catalysts C, D and O. Effect of pH level to activity

Major side products

Yield of t-2-butene

Yields of t-2-butene of Catalysts C, D and O, with different pH level are shown in Figure 50. The pH changes the yield and starting temperature of the t-2-butene, and it also effects the trend. Catalysts C and D have a similar trend and the yield starts at 300 °C, but differs by yields at 400 °C. Catalyst O already starts to yield at 250 °C, but after 350 °C the yield decreases.

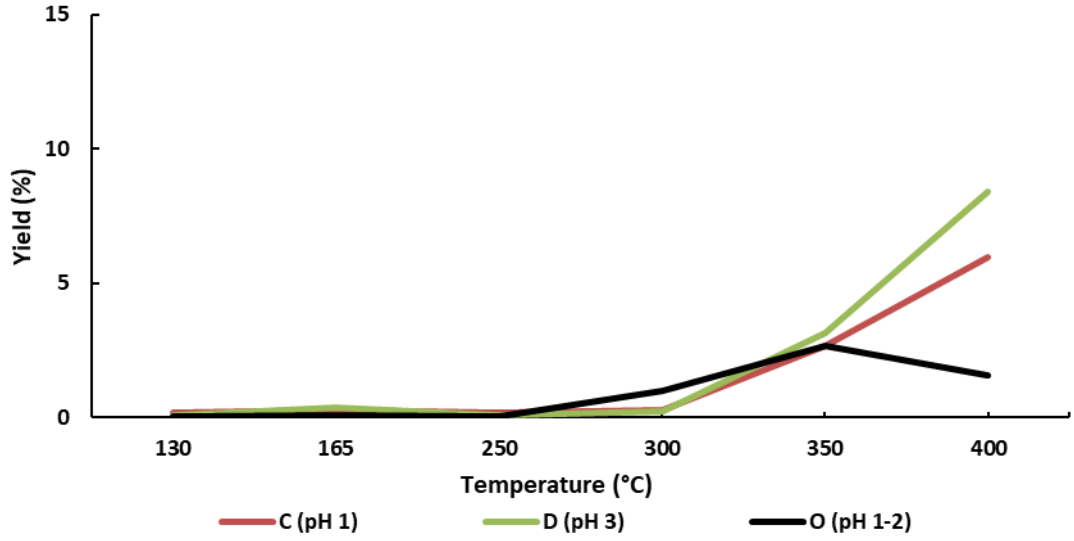

Figure 50. Yield of 1-butanol to t-2-butene, Catalysts C, D and O. Effect of pH level to activity.

Yield of 1-butene

Yields of 1-butene of Catalysts C, D and O, with different pH level are shown in Figure 51. The pH affects to the yield of 1-butene by opposite way than in the yield of butyraldehyde. Catalyst D has the highest yield of 1-butene, by yield increasing linear from 300 °C. Also yield of Catalyst C starts to increase at this point, but increasing stops, while Catalyst O is at its lowest. Yield of 1-butene was at its highest between 250 °C and 300 °C with Catalyst O, dropping almost to zero after that.

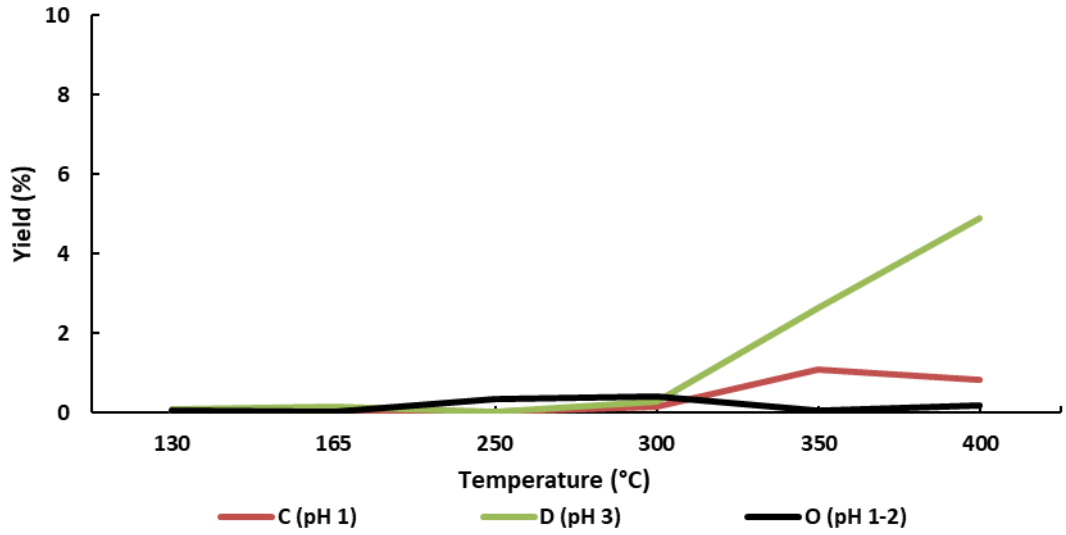

Figure 51. Yield of 1-butanol to 1-butene, Catalysts C, D and O. Effect of pH level to activity.

4.2.2 Effect of the reactor conditions on activity of the catalyst

From every experiment of the reactor condition for Catalyst O, average of the results were taken. Average conversions, selectivities and yields of the partial oxidation of 1-butanol to butyraldehyde at partial pressures of 1-butanol 13.5 kPa and 18.0 kPa at experiments 1-12 (Table 10 and Table 14) are shown in Figure 52- Figure 57. Yields of CO and CO_2 at partial pressures of 1-butanol 13.5 kPa and 18.0 kPa in experiments 1-12 are shown in Figure 58 - Figure 61. The other product, which was t-2-butene produced by both partial pressured more than 1% by volume, in partial pressures of 1-butanol 13.5 kPa and 18.0 kPa in experiments 1-12 is shown in Figure 62 and in Figure 63.

Conversion of 1-butanol

Conversions of 1-butanol to butyraldehyde in 13.5 kPa are shown in Figure 52 and 18.0 kPa are shown in Figure 53. The conversion of the 1-butanol to butyraldehyde is varies between 65% and 75% in 13.5 kPa and between 60% and 75% in 18.0 kPa at 400 °C. There are no optimal parameters for getting the best conversion from the Catalyst O, but higher conversions come with higher residence time, in experiments 1-3 and 7 and 8. Experiment are dividing to two different groups: low and high residence times. Main differences between the experiments are that higher residence are rising more linearly until they change direction at 350 °C. While experiments of lower residence time go with smaller rate to 300 °C, then having a big leap to 350 °C and after that, ratio of yield stabilizes. To have higher conversion, use of higher residence time is better. In 18.0 kPa experiments, experiment 9 have moved from “higher” residence time to closer pile of “lower” residence time.

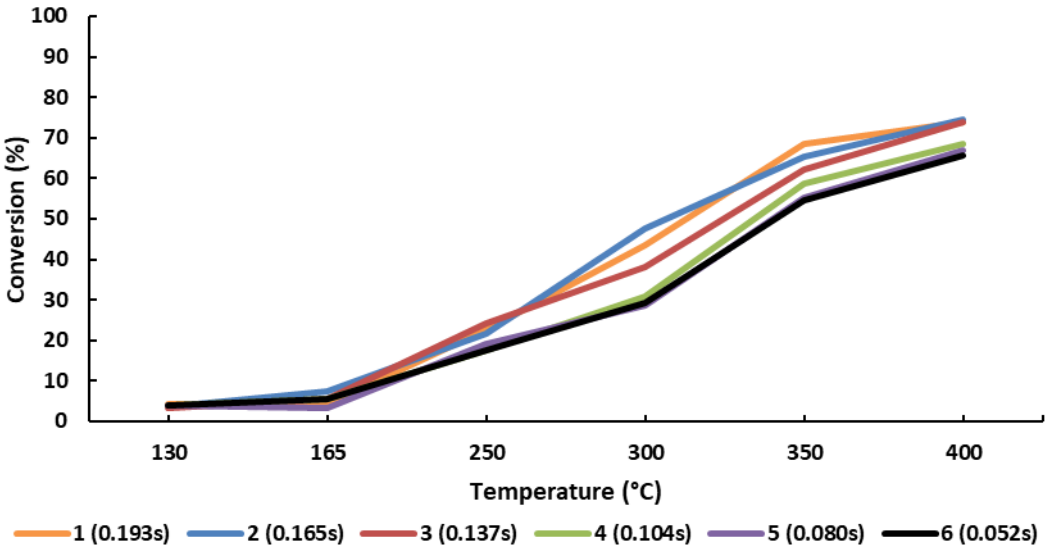

Figure 52. Conversion of 1-butanol to butyraldehyde in 13.5 kPa, experiments 1-6. Effect of the reactor parameters.

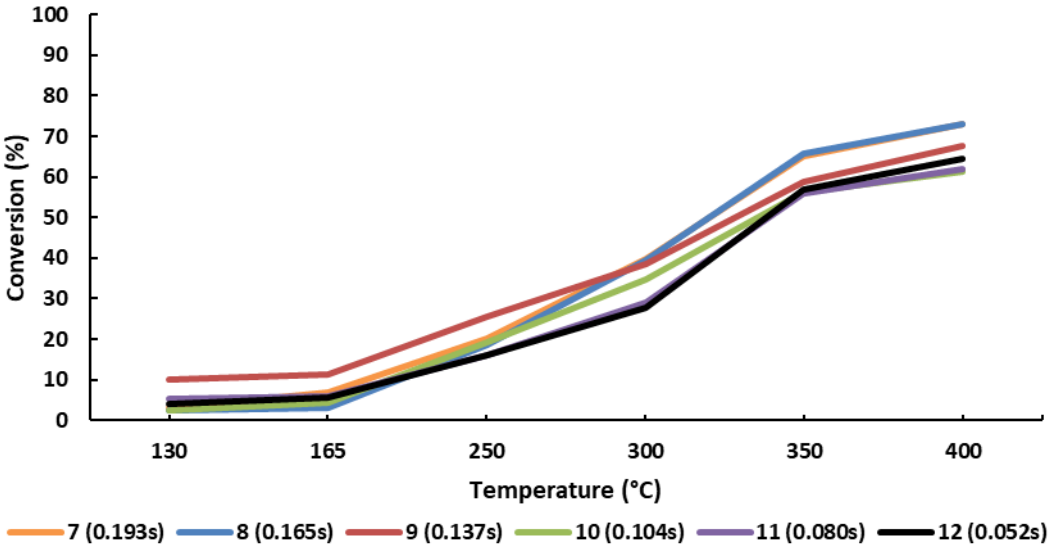

Figure 53. Conversion of 1-butanol to butyraldehyde in 18.0 kPa, experiments 7-12. Effect of the reactor parameters.

Selectivity to butyraldehyde

Selectivities of 1-butanol to butyraldehyde in 13.5 kPa are shown Figure 54 in and 18.0 kPa are shown in Figure 55. The selectivity of butyraldehyde varies 65% - 100% at 400 °C with both partial pressures. There are no clear pattern to describe all of the experiments. There are some similarities, such as that lower residence times are more selective to butyraldehyde than experiments with higher residence times. Experiment 1 and 4 are starting with the same type, all the way to 300 °C, but after that the lower residence time experiment 4 increases again and higher residence time experiment 1 decreases. Similar thing is occurring with experiment 2 and 3, but already at 250 °C. Experiment 2 stays quite stable after 250 °C, which is somehow similar to Catalyst E selectivity. Experiments 9 and 12 have a similar trend, but lower residence time in experiment 12 is much selective. The same occurs with experiments 10 and 11.

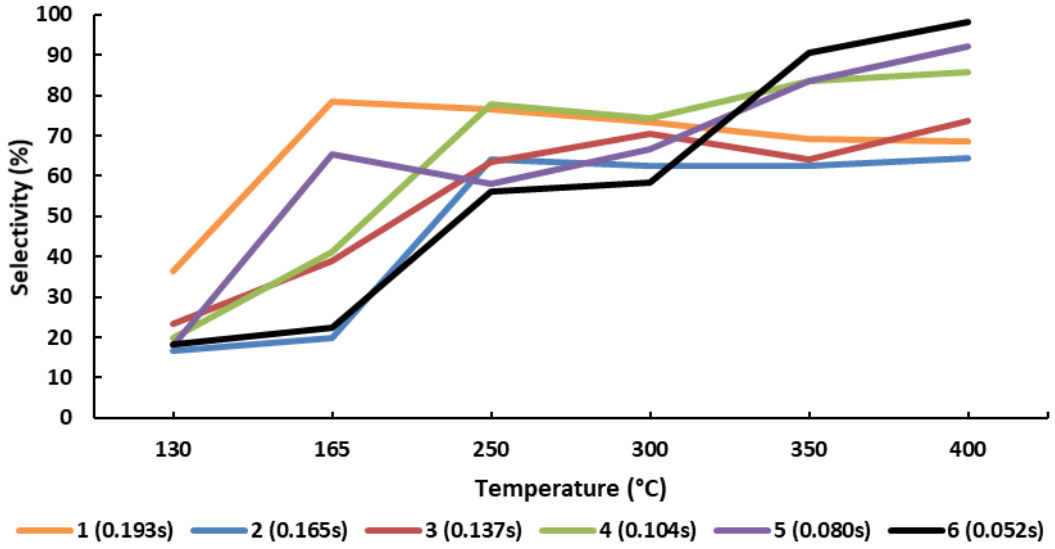

Figure 54. Selectivity of 1-butanol to butyraldehyde in 13.5 kPa, experiments 1-6. Effect of the reactor parameters.

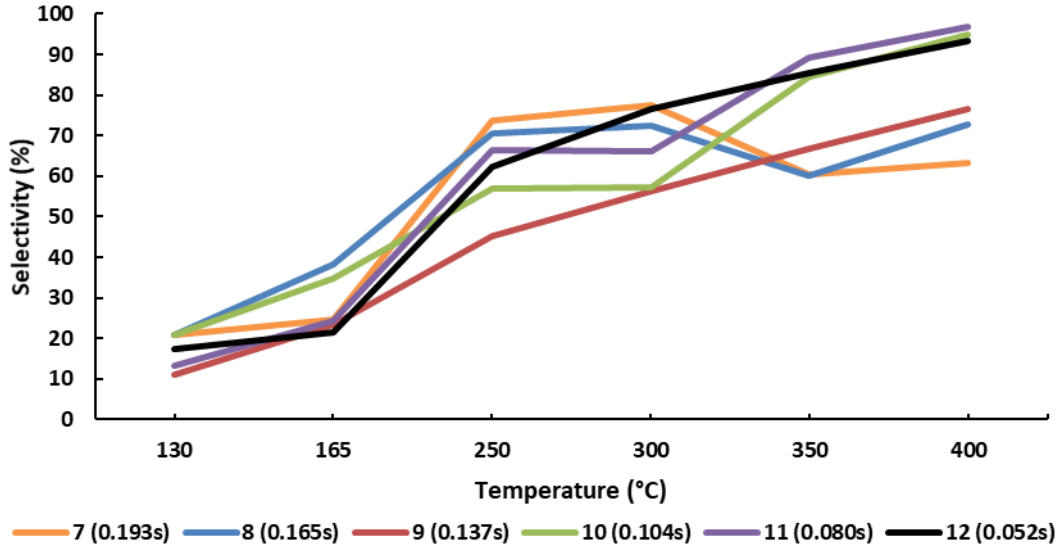

Figure 55. Selectivity of 1-butanol to butyraldehyde in 18.0 kPa, experiments 7-12. Effect of the reactor parameters.

Yield of butyraldehyde

Yields of 1-butanol to butyraldehyde in 13.5 kPa are shown in Figure 56 and in 18.0 kPa are shown in Figure 57. Yields of the experiments are also following the trend from the conversion graph, as previous. At 13.5 kPa, the separation of lower and higher residence times, has been turned upside down and also the cap is not as clear. At 18.0 kPa the separation of the lower and higher residence times has been also turned upside down as in the 13.5 kPa. But the difference is clearer and residence times are more in their own groups. The cap between the lower and higher residence times are clearer at 18.0 kPa at 300 °C, even experiment 9 has moved to group of lower residence times. Experiments with same residence time at 13.5 kPa and 18.0 kPa have similar trend, with small variation between increasing yield and temperature. Yield is a combination of conversion and selectivity, which was at this case affected more by the selectivity. Increased partial pressure decreased selectivity at 250 – 350 °C, which is now visible at the yield curve.

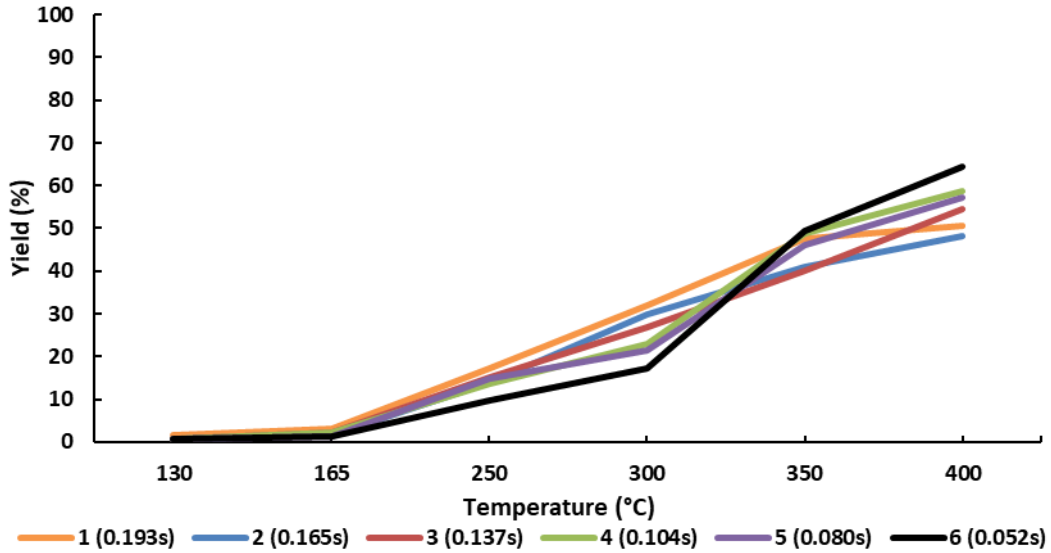

Figure 56. Yield of 1-butanol to butyraldehyde in 13.5 kPa, experiments 1-6. Effect of the reactor parameters.

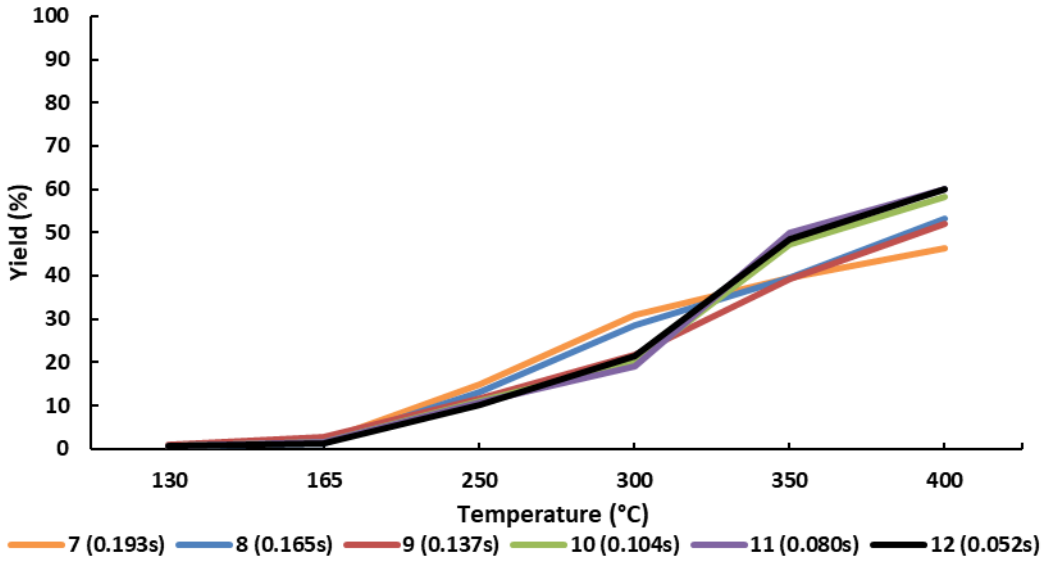

Figure 57. Yield of 1-butanol to butyraldehyde in 18.0 kPa, experiments 7-12. Effect of the reactor parameters.

Yield of CO and CO_2

Yields of 1-butanol to CO at 13.5 kPa are shown in Figure 58 and at 18.0 kPa are shown in Figure 59. Yields of CO are varying between 1% and 6% at partial pressure of 13.5 kPa and between 3% and 5% at partial pressure 18.0 at 400 °C. At 13.5 kPa it seems that higher residence time gives a higher yield of CO. At 18.0 kPa the order is not as clear, because experiment 9 has dropped under the lower residence time experiments. It also might be an experimental error, otherwise the experiments seem to be in their own groups. At both partial pressures, experiments with higher residence time start to rise more at 250 °C than experiments with lower experiments, which start to rise at 300 °C. Both residence times stabilize after 350 °C.

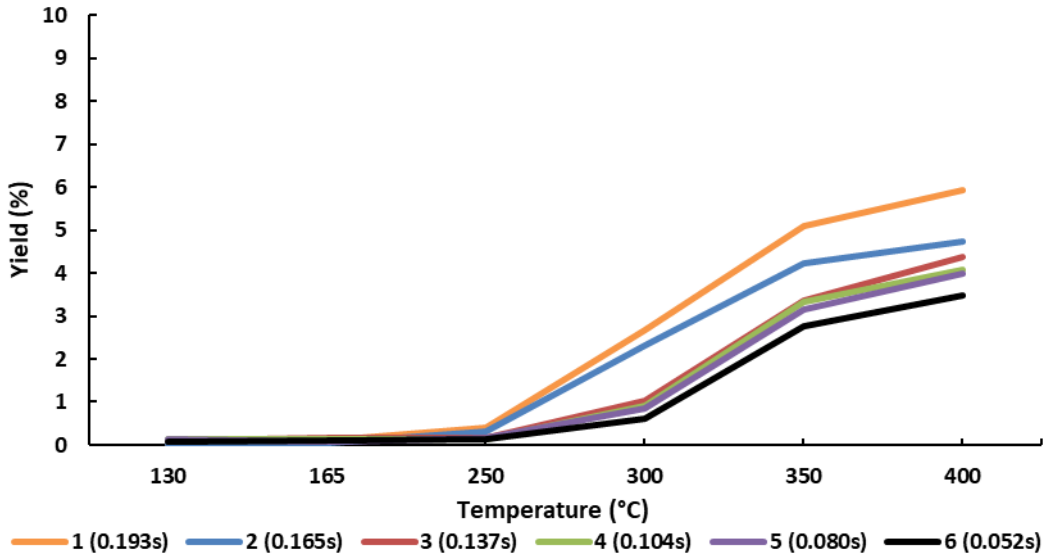

Figure 58. Yield of 1-butanol to CO in 13.5 kPa in experiments 1-6. Effect of the reactor parameters.

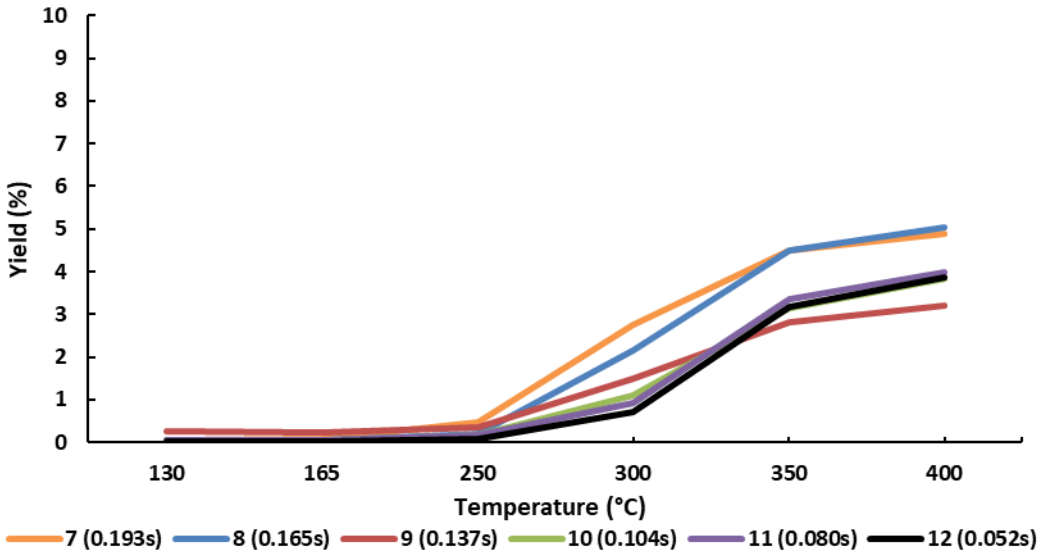

Figure 59. Yield of 1-butanol to CO in 18.0 kPa in experiments 7-12. Effect of the reactor parameters.

Yields of 1-butanol to CO_2 at 13.5 kPa are shown in Figure 60 and at 18.0 kPa are shown in Figure 61. In the yield of CO_2 experiments seem to also have higher yield of CO_2 with lower residence time. At partial pressure of 13.5 kPa it seems, that experiments with lowest and highest pump flows are separating the from the medium pump flows (0.025 - 0.05 ml/min). At partial pressure 18.0 kPa yield, difference is even larger at lower residence times, but the highest are yielding 10% units more.

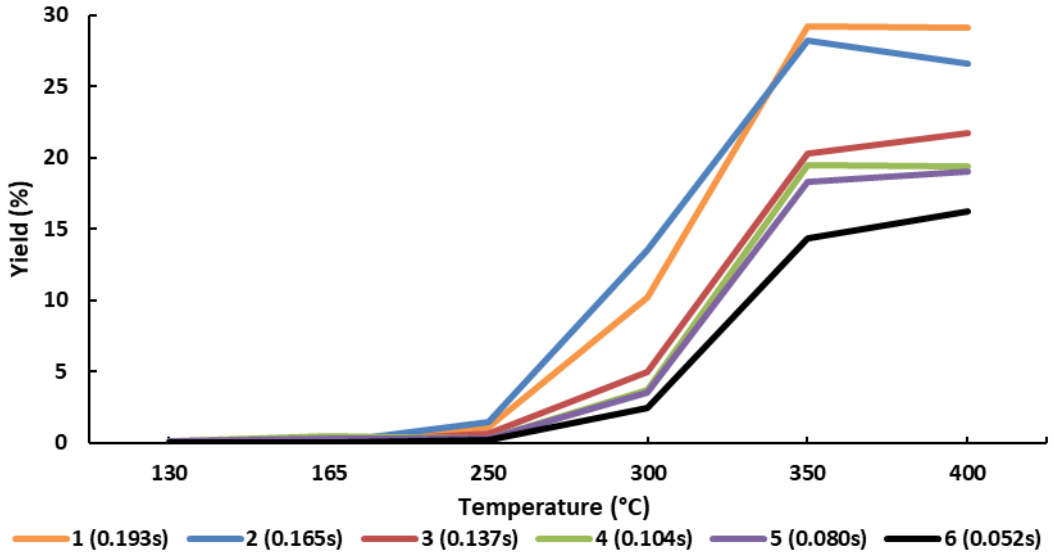

Figure 60. Yield of 1-butanol to CO2 in 13.5 kPa in experiments 1-6. Effect of the reactor parameters.

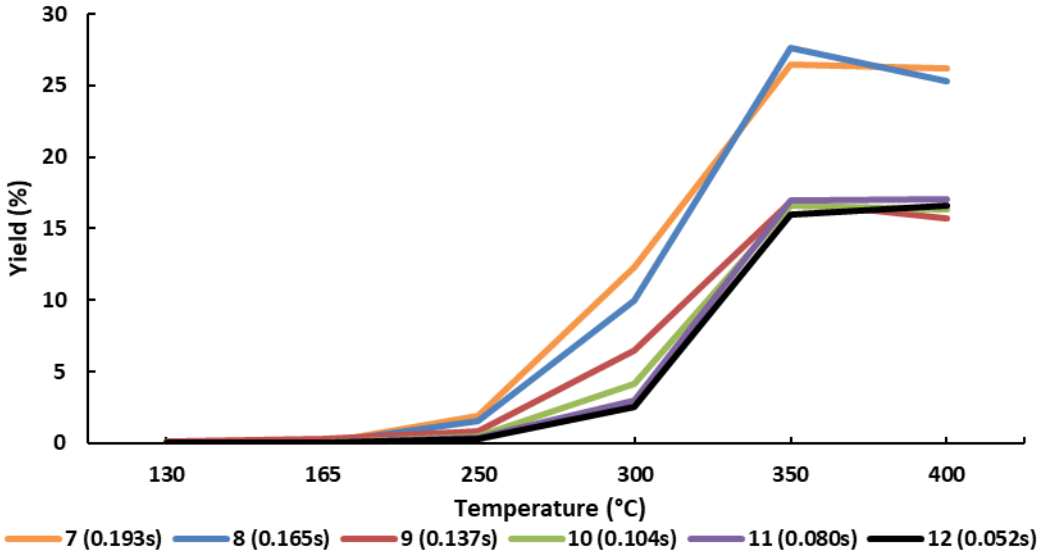

Figure 61. Yield of 1-butanol to CO_2 in 18.0 kPa, experiments 7-12. Effect of the reactor parameters.

Major side products

The yield of major side products varies depending on partial pressure and residence time. There are similarities and differences in yields of t-2-butene (0% - 10%), 1-butene (0% - 2%) and 2-butene (0% - 2%). Variation in t-2-butene are shown graphically. Yields of 1-butene and 2-butene are not compared graphically due to small amounts of yield.

Yield of t-2-butene

Yields of 1-butanol to t-2-butene at 13.5 kPa are shown in Figure 62 and at 18.0 kPa are shown in Figure 63. The yield of t-2-butene has a similar trend in 13.5 kPa and in 18.0 kPa, lower residence time and higher partial pressure seem to have higher yields, but experiments 6, 11 and 12 are not the most reliable results, due the fluctuation, so it is better to compare medium pump flows.

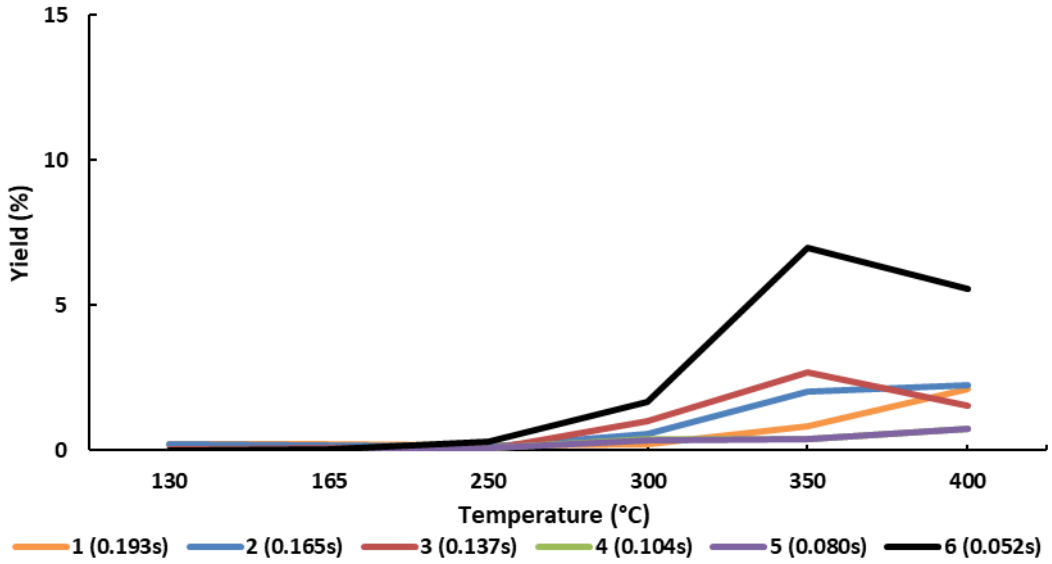

Figure 62. Yield of 1-butanol to trans-2-butene in 13.5 kPa, experiments 1-6. Effect of the reactor parameters.

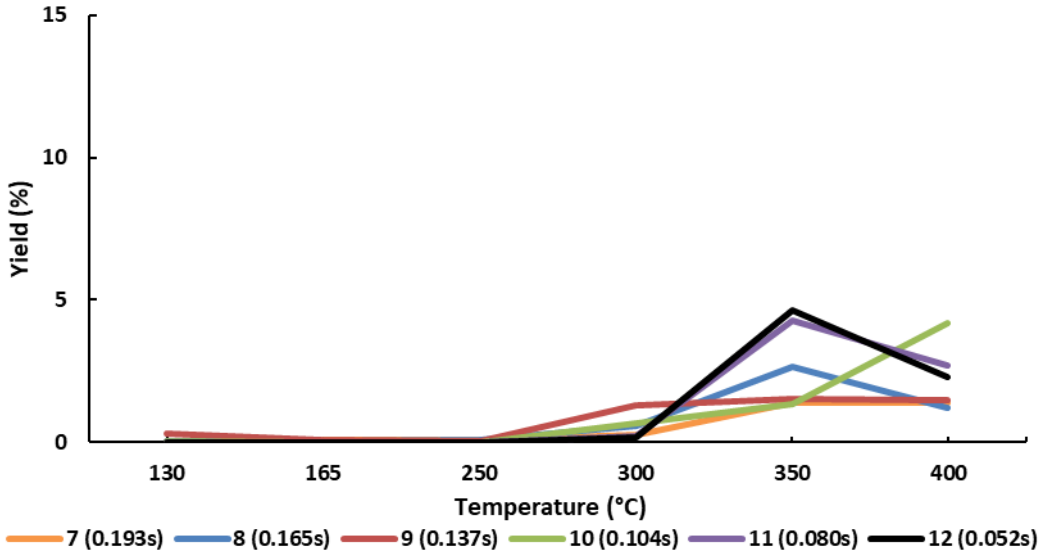

Figure 63. Yield of 1-butanol to trans-2-butene in 18.0 kPa, experiments 7-12. Effect of the reactor parameters.

Yield of 1-butene

In the yield of 1-butene, which is not a considerably large amount, has still some trend between both partial pressures. Higher residence times seem to yield more 1-butene than lower residence times. The amounts are small and the flows of experiment 1 and 2 are not so reliable, but ones again the amount of product was still noticeable.

Yield of 2-butene

In the yield of 2-butene, the amount is very low, but still noticeable. It seems that t-2-butene is much more favored product.

5. Discussion

In this chapter, the experimental part and results are discussed.

5.1 Microreactor activity tests

Many experiments were done to reliable data from the catalyst and reactor conditions, which are shown in Table 13 and Table 14. Amount of four to six experiments were good amount of experiments from the different catalysts. There were clear trends in each catalyst, which made taking average values easier. The reason for the Catalyst A and B amount of five to six experiments was problems with microreactor, which gave unreliable results so more experiments needed to be done. Catalyst A and B were placed two times in the microreactor, which may have caused more out wearing to the catalyst coating.

Amount of two to four experiment from the reactor conditions was just enough to see the trend within and between the experiments, but more would have been better. Experiment 3 was done 4 times, because of the reference catalyst for gold loading and preparation parameters and reactor condition experiments. Experiments 8 and 9 were done more than twice, because of the errors in the microreactor run, so more data was needed to get a better result. It is possible that experiments with only 2 runs are not accurate.

With every catalyst, data obtained at 130 °C is not reliable and it is somehow reliable at 165 °C. This is because of the uneven fluctuation of the FTIR spectra. At temperatures 250 - 350 °C the data obtained is more reliable, due to the better FTIR-spectra. As temperature rises to 400 °C, FTIR spectra becomes again a little bit uncertain, but not as much as 130 and 165 °C. FTIR spectra affects every result obtained from the microreactor experiments. Also the pump had a major influence to FTIR spectra. Flows under 0.025 ml/min (experiments 1, 2 and 7) were not quite reliable and pump flows more than 0.050 ml/min (experiments 5, 6, 11 and 12) were not reliable, because of the fluctuation. It was necessary to increase the temperature of the evaporator and lines to 140 °C instead of 130 °C to reduce

the fluctuation, but experiments give a direction at the results, even not being exactly the same conditions as the others.

Experiments gave different amount of different products, which was expected, because of the different gold loadings and partial pressures. Butyraldehyde started to form after 165 °C in every experiment. See detailed discussion on subsections 5.1.1 and 5.1.2.

5.1.1 Effect of gold loading and preparation parameters on activity of the catalyst

As seen in Figure 32 - Figure 51, gold loading and preparation parameters have a a lot of effect to activity, by varying the conversion, selectivity and yield of different side products. Depending on the desired products and operating temperatures, optimal catalyst can be obtained by optimizing these parameters, but before that it is necessary to understand their effects on catalyst.

Conversion of 1-butanol

As seen in Figure 32, Figure 40 and Figure 46, the conversion of 1-butanol increases with increasing temperature in every catalyst. Conversions vary between 55% and 85% at 400 °C. With lowest amount of gold, 0.3% (also smallest particle size 2.02 nm, Catalyst E) was most active to convert 1-butanol, in all temperatures.

The next ones were Catalyst C and O, with the next lowest amount of gold, 0.6% (also second smallest particle size, 2.66 and 2.67 nm), even if they had slightly different conversions at 350 °C and after. Conversion of Catalyst C reached conversion of Catalyst E little bit at 400 °C. Catalyst A had the same conversion as C and O at 250 °C, but then conversion started to differ.

The third highest active for conversion were Catalysts A and D, having most amount of gold (Catalyst A, 1 wt.%) and highest pH (Catalyst D, pH 3), but similar size of the particles (3.86 and 3.79 nm). In development of the conversion, Catalysts A and D are more or less the same at every temperature, with little variations, which might even go to error range of the experiments.

Smallest conversion of 1-butanol was Catalyst B, which had 1 wt.% of gold (particle size of 3.21 nm), but still had a similar trend to Catalysts C, D and O. Although it is not directly only for the amount of gold or size of the particle, because Catalyst B is having smaller particle size than Catalysts A and D. It is possible that the dots in catalyst B plates are disturbing the microreactor experiments. Adjustment of the pH may have altered the activity of the Catalyst B, since it was noticeable that pH has an effect on the activity in Catalysts C, D and O.

Selectivity to butyraldehyde

As seen in Figure 33, Figure 41 and Figure 47, Catalyst O is the most selective towards to butyraldehyde compared to Catalysts A-E in all temperatures. Selectivities vary between 25% and 75%.

Every catalyst has the same trend to 300 °C, selectivity increases. After this, there is larger differences. While the selectivity of Catalysts A-E decreases after 300 °C or 350 °C, the selectivity of Catalyst O increases at 400 °C back to where it was at 300 °C. Catalysts B and C are most selective at 300 °C and almost as selective at 350 °C. In Catalyst E there are no big change after 250 °C to 400 °C, which is unique compared to others. Graph of Catalysts B and E develop at the same time to 250 °C, then selectivity increases until selectivities are almost the same again at 400 °C.

There is some correlation between the amount of gold and the selectivity, which concentrates more on the particle size and distribution. It seems that selectivity of butyraldehyde is more favored for particle sizes of around 2.6 – 3.2 nm (Catalysts C, O and B), but cannot be explained only with that because, they have similarities on the particle distributions with other catalysts and they are not as selective.

There should be more experiments to find out the optimal gold amount for the most selective amount of gold in the catalyst. Smaller particle size in the same amount of gold is better for selectivity of butyraldehyde. Particle size closer to 3 nm seems to lower the temperature and increasing the yield at the same time,

with these two catalysts. This might not only be due to the particle size and the distribution, but it is at least one effecting factor.

Differently size distributed particles in the catalysts gave different amount of butyraldehyde in different temperatures, by lowering temperature and increasing the selectivity. Level of the pH must be one factor to effect to the selectivity, or it effects to particle distribution, which effects to selectivity.

Yield of butyraldehyde

As seen in Figure 34, Figure 42 and Figure 48, the yield of butyraldehyde with all catalysts increases with increasing temperature, as did their conversion. Conversion and selectivity are combined in the yield, so their trend affect the yield. Catalyst O is yielding the most 1-butanol to butyraldehyde, which graph is very linear starting from the 165 °C all the way to 400 °C. Yield of Catalyst E is the same as yield of Catalyst O until to 300 °C, then it changes. Graphs of Catalysts A, B and D have also very much similarities in the trend, but differences in the activity on different temperatures. The yield of Catalyst D stays the same after 350 °C, which is out of the overall trend.

Yield of CO and CO_2

As seen in Figure 35, Figure 43 and Figure 49, there is a connection between conversions of 1-butanol and yields of CO and CO_2. Yield of CO varies between 1% and 10% and the yield of CO_2 varies between 5% and 25%. Catalyst E is at its own category in the yield of CO, while yield of CO_2 is around same level as Catalyst O and C. Catalysts A-D and O are having group of their own in yield of CO, and Catalyst A, B and D have very much similarities with the yield of CO and CO_2.

In the yield of CO Catalyst E already starts to separate from other catalysts early at 250 °C, and rises even two time higher than the others. Catalyst C and O separate from the other catalysts at 300 °C, but not as much as catalyst E. Catalysts A, B, and D start to really increase at 350 °C, while Catalyst O stabilizes to same level at 400 °C.

In the yield of CO_2, Catalysts E and O start to clearly separate from the other catalysts again at 250 °C. At 300 °C E and O are giving 3 and 4 times more CO_2 than at 250 °C, which is a huge increase in the yield. The yield of CO_2 in Catalyst C increases significantly at the yield at 300 °C, but the yield does not increase as much as Catalysts E and O, however yield reaches yield of Catalysts E and O at 400 °C. Catalyst O is having big changes at 350 °C at the yield and the increasing almost stops. At 350 °C Catalyst A, B and D are starting to really increase. At Catalyst A, B, D and E the yield of CO seems to be ½ of the yield of CO_2.

The order of the graphs are alignment with conversion and yield of CO_2 and CO, but not completely. There are major changes in place of Catalyst O and minor changes with Catalyst B, otherwise the order is the same. Observing changes of parameters might reveal the cause of the changes.

Major side products

The yields of major side products are varying significantly, depending on the catalyst. There are some similarities in yields of t-2-butene (2%-12%), 1-butene (0% - 6%), propene (0% - 4%) and butyric acid (0% - 2%).

Yield of t-2-butene

In yield of t-2-butene Catalysts A - E have the same trend, but major variation in the yield and temperatures. Catalyst O has a trend of its own after 350 °C otherwise quite similar, but higher yield in lower temperatures.

Yield of 1-butene

In yield of 1-butene Catalyst A, B and D have similar trend, but some variation in the yield and temperatures. Mean average particle size of Catalyst A, B and D are more than 3 nm, which may affect to the yield of 1-butene.

Yield of propene

In the yield of propene Catalyst E was the only catalyst having more than 1% of propene. Production starts at 250 °C and yield increases from 300 to 400 °C constantly. Catalysts A, B, C, and O start to have some production at 350 °C and

slightly increasing to 400 °C. It is very difficult and inefficient to compare other catalysts, because the amount is not enough to be very reliable. Yield of propene might have something to do with yield of CO in Catalyst E, since both graphs are clearly out of the trend. There might be correlation with a small particle size and size distribution of Catalyst E and yields on propene and CO.

Yield of butyric acid

In the yield of butyric acid, Catalyst E was the only catalyst producing more than 1% of butyric acid. Producing starts at 250 °C and is at its highest at 300 °C and decreases after that. There are some traces of butyric acid in every catalyst at 130 and 165 °C, since the amount is small and these two temperatures are not as reliable, so there might be residues in lines from previous experiments or just error in FTIR.

Minor side products

The yield of 2-butene was under 1%, but yield was higher in reactor condition experiments. There was still some traces of 2-butene, which is structurally very similar with t-2-butene. This tells that t-2-butene isomer is more favored with these catalysts and reactor conditions.

5.1.2 Effect of the reactor conditions on activity of the catalyst

As seen in Figure 52 - Figure 63, effect of the reactor conditions on activity is mostly by increasing or decreasing the yield and/or temperature. Different reaction conditions drive reaction to different products.

Conversion of 1-butanol

As said earlier, for lowest and higher pump rate (also higher and lower residence times) there was quite much fluctuation which definitely has affected the results. This why it is easier to compare the change of the partial pressure and pump flow, with experiment 8, which has same pump flow and experiment 9 residence time. Effect of the reactor conditions to conversion, in experiments 3, 8 and 9 are shown in Figure 64. Increasing residence time, experiment 8, lowers the conversion at

lower temperatures, then rises a little bit until it stabilizes back to same as the experiment 3, at the 400 °C. Keeping the residence time same, but increasing partial pressure, experiment 9, affect conversion only at higher temperatures by lowering the conversion around 5% units.

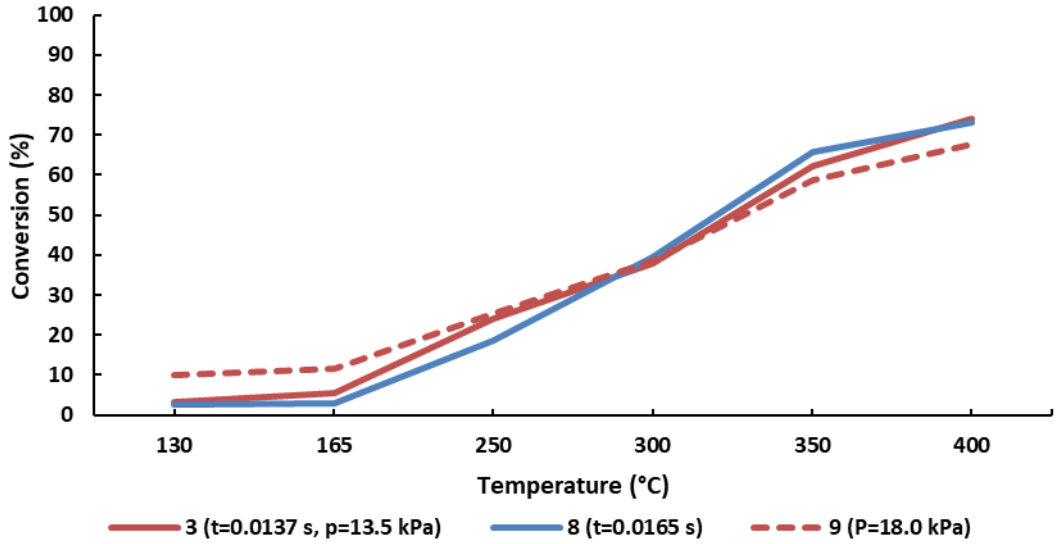

Figure 64. Effect of reactor conditions to conversion, experiments 3, 8 and 9.

Selectivity to butyraldehyde

Effect of the reactor conditions to selectivity, in experiments 3, 8 and 9 are shown in Figure 65. Increasing partial pressure lowers the selectivity at lower temperature, but increases selectivity at 400 °C. It also alters the trend of the graph quite much, being more stable as having too growing linear part. Increasing residence time, strengthens the curves of the graph, making it more dependent on the temperature. Selectivity is still remaining same at the 400 °C. This is quite valuable information, if operating at lower temperatures optimize the selectivity.

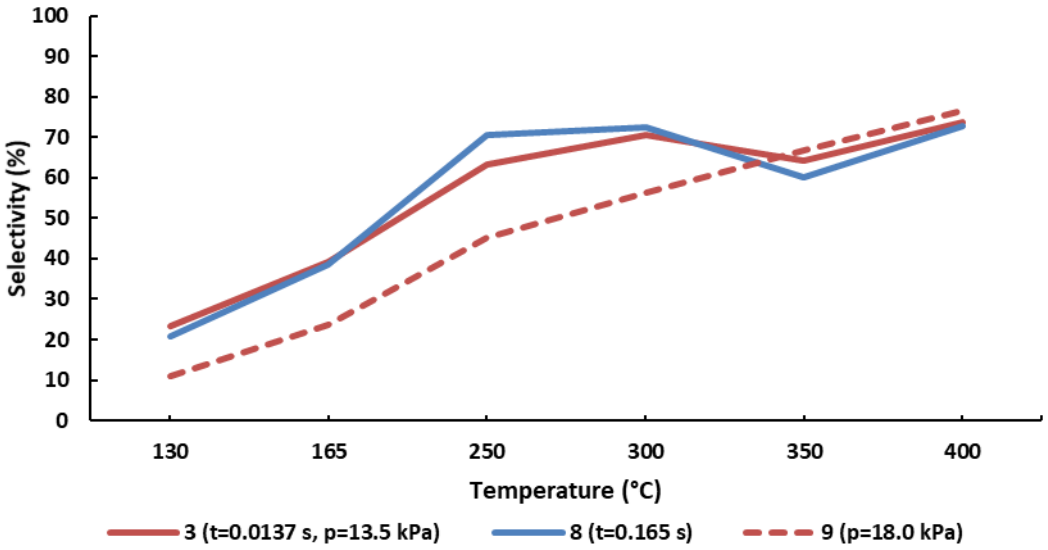

Figure 65. Effect of reactor conditions to selectivity, experiments 3, 8 and 9.

Yield of butyraldehyde

Effect of the reactor conditions to yield, in experiments 3, 8 and 9 are shown in Figure 66. Increased residence time did not affect the yield as much as pressure, as seen in the similarities of conversion and selectivity curves with the experiment 3.

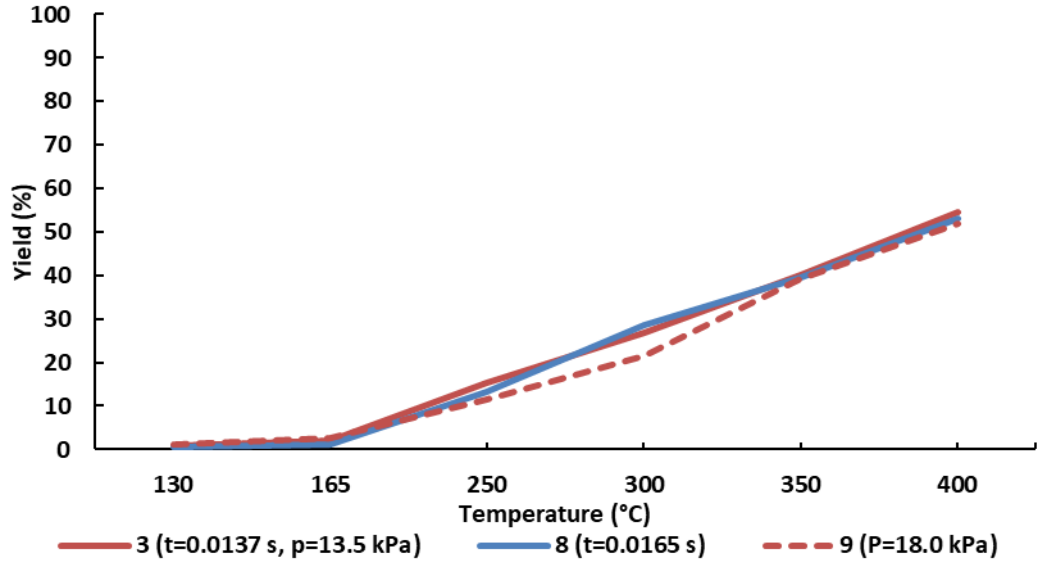

Figure 66. Effect of reactor conditions to yield of butyraldehyde, experiments 3, 8 and 9.

Yield of CO and CO_2

Effect of reactor conditions to yield of CO in experiments 3, 8 and 9 are shown in Figure 67. Increasing residence time increases the yield of CO at all temperatures. The increasing partial pressure increases the yield at lower temperatures, and decreases the yield of CO at higher temperatures.

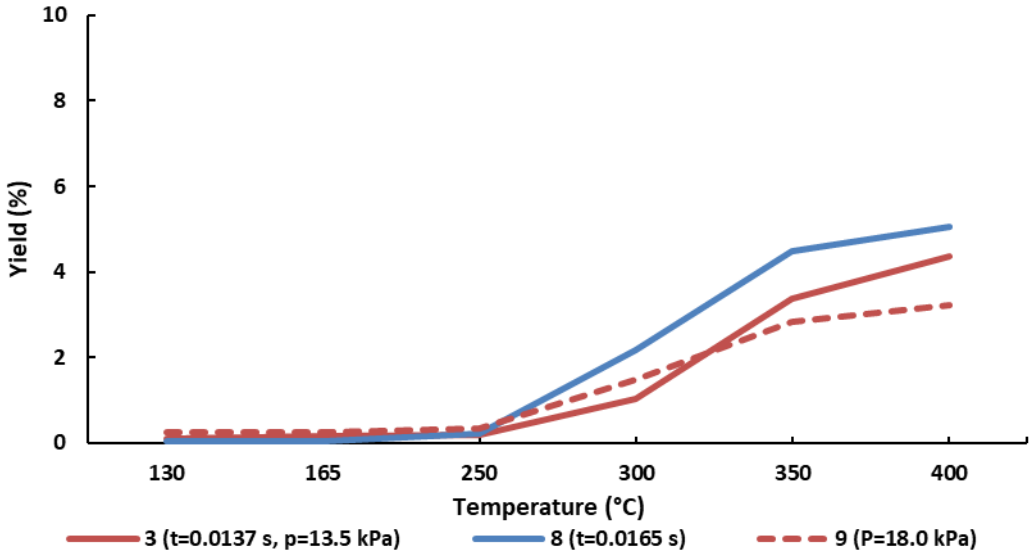

Figure 67. Effect of reactor conditions to yield of CO, experiments 3, 8 and 9.

Effects of reactor conditions to yield of CO_2 in experiments 3, 8 and 9 are shown in Figure 68. Increasing residence time increases the yield of CO_2 at all temperatures. The increasing partial pressure increases the yield at lower temperatures, and decreases the yield of CO_2 at higher temperatures.

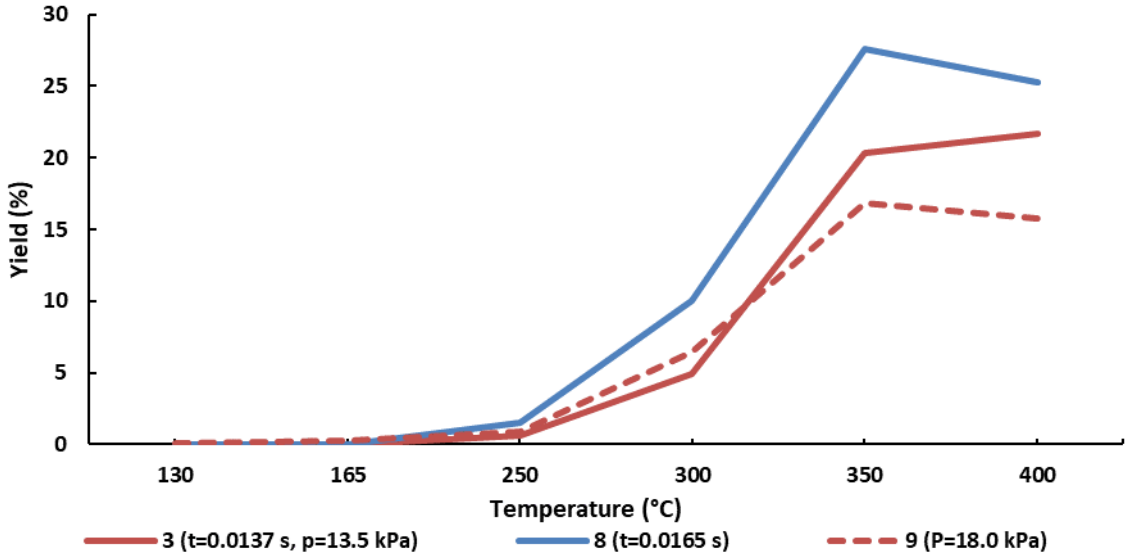

Figure 68. Effect of reactor conditions to yield of CO_2, experiments 3, 8 and 9.

Major side products

Not many side products were yielded, but they are still briefly discussed since there some similarities with Catalyst A-E.

Yield of t-2-butene

Effect of the reactor conditions to yield, in experiments 3, 8 and 9 are shown in Figure 69. By increasing residence time, it is actually possible to lower the yield of t-2-butene. Increasing partial pressure, yield of t-2-butene can be decreased at lower and higher temperatures.

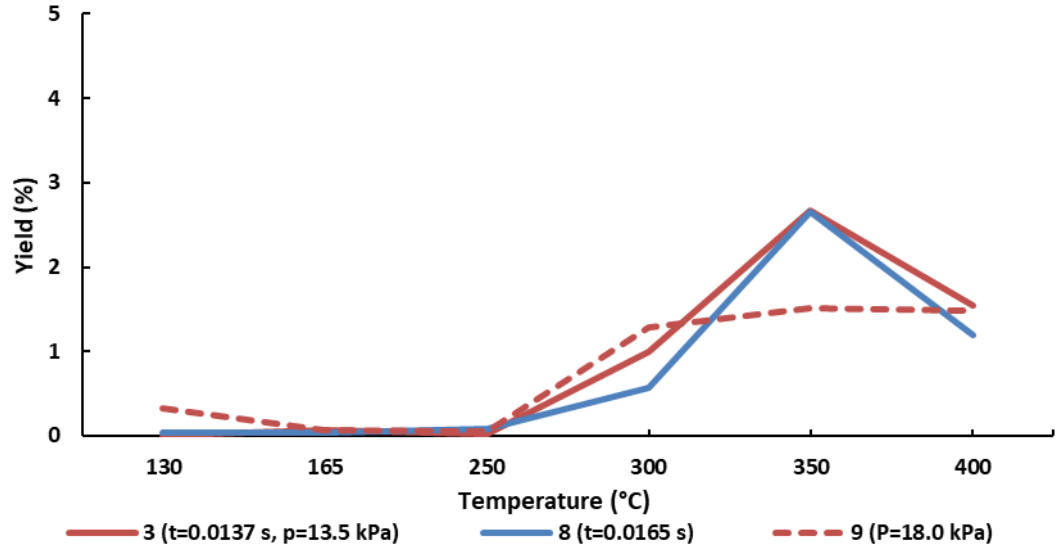

Figure 69. Effect of reactor conditions to yield of t-2-butene, experiments 3, 8 and 9.

Yield of 1-butene and 2-butene

Yield of 1-butene and 2-butene were not so much with Catalyst O, but it would have been interesting to compare with catalysts, especially with Catalyst A, B and C. Catalysts A, B and C yielded most 1-butene and 2-butene

Minor side products

Yield of butyric acid was much more noticeable with Catalyst E and C, it would have been interesting to make pressure experiments to them and then compare.

In the yield of propene there is almost nothing visible until at higher pressures and lower residence times. It would have been very interesting to see reactor condition effect on Catalyst E.

5.2 TEM Characterization

The size of the particles were measured visually, so there is some variation on the measurement of the particles between particles and between pictures. Pictures with different scale were also used, which itself caused some error on the measurements (particles seem bigger in 20 nm scale compared to 100 nm scale even if the picture is zoomed). Not every particle was shaped as a circle or uniform, which made the measuring prone errors.

Pictures and graphs still give good information about the catalysts and particles. As seen from the Table 11 and in Figure 24 - Figure 26, every catalyst have their own fingerprint on the particle size and distribution, even if there are similarities. It is possible that there are many variables that have an effect on the size of the gold particles.

Comparing Catalysts A, C and E to O, Catalysts A, C and E are having some trend in the sift of the peak by amount of gold, Catalyst O is having the clearest peak of particles between 2.5 – 3.5 nm and a sharp triangle between 1.0 – 4.5 nm and a quite large “tail” at the left side of the graph. Even if the Catalyst C and D have the same amount of gold and same particle size, the particle distribution is different.

6. Error estimation

In this chapter largest errors in the experimental part are estimated

6.1 Errors of microreactor system

As already mentioned in Subsections 3.3.2 and 4.2, also discussed in Subsection 5.1, there are some errors in the microreactor results. Due to the calculation method and properties of the system, data of conversion and selectivity are not exactly correct. Conversion and selectivities effects to yields, which were widely presented in this thesis. However results are still comparable to each other from the same system.

Reference point of 1-butanol flow is taken from the blank by-pass (flow is not in the microreactor) at 130 °C to calculate conversion of 1-butanol and selectivities of compounds in every temperature at the reactor. Flow of the 1-butanol decreases after taking the reference point, when the flow is directed to reactor from the by-pass line. No reaction occur at temperatures 130 and 165 °C, which can be verified with FTIR spectra. However the calculated average results shows some conversion of 1-butanol and selectivity of other compounds at these temperatures. This is only because of the misleading reference point and calculation method. These numbers have been used to make the conversion, selectivity and yield graphs. Yield is close to zero, which is closer to reality, but it is not exactly correct. Conversion and selectivity cannot be marked as zero at 130 and 165 °C, because it would have given false information from the development of the graph and result from temperatures at 250 – 400 °C.

This property of the microreactor system effects to the all results obtained from the microreactor, with different catalysts and different partial pressures. Taking reference point from the by-pass line gives comparable data before the microreactor and it is not varying depending on the catalyst.

6.2 Microreactor plates

There are differences between the microreactor plates, before and after the microreactor. Catalysts A-D calcined plates before are shown in Figure 70 and Catalysts A-E and O after the microreactor experiments are shown in Figure 71.

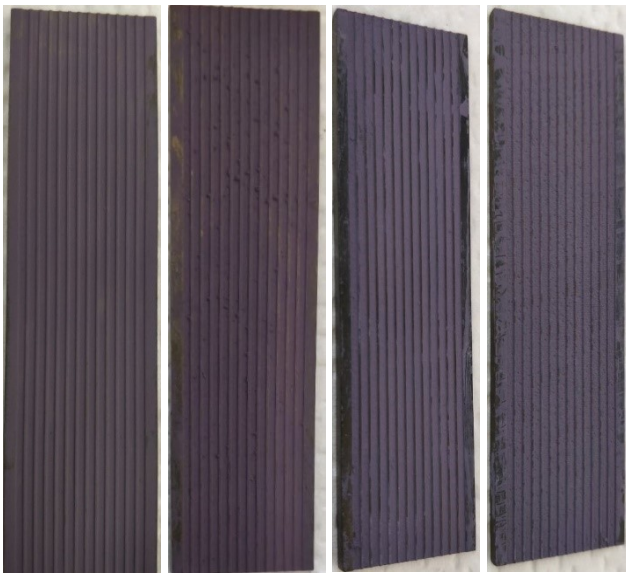

Figure 70. Catalysts A-D plates before microreactor experiments. In order from left to right: A, B, C and D. Pictures are no exactly in the same scale.

Figure 71. Plates of Catalyst A-E and O after the microreactor experiments. In order from left to right: A, B, C, D, E and O. The top sides of the plates were on inlet and bottom side no the outlet of the reactor. Catalysts A and O were put 2 time in the reactor, others 1 time. Selected plates were on the top. Pictures are not exactly in the same scale.

As seen from Figure 70 and Figure 71 the out wearing of each catalyst is different, least out wearing as seen in Catalyst D. The color of Catalyst D plates was still quite purple. Catalyst O is the most damaged, due to the several experiments and scratching of the plates when taking the plates out from the microreactor. The color of the Catalyst O was the darkest. There might be some correlation with wearing out and pH, but this cannot be said for sure.

Amount of the catalyst on microreactor plates

The amount of catalyst on the microreactor plates (Table 7) might have some effect on the yields. The largest difference between the plates is with Catalyst D. There is roughly 3 times more catalyst on the other plate

Dots on Catalyst B microchannels

If suspension dried too fast, bubbles with solid particles and cracks was formed. This occurred only for blank plates with suspension area of few centimeters and thickness of a few millimeters. But in Catalyst B suspension there was some solid particles, which got to microreactor plates. Particles were not removed during the microreactor experiment. The dots on the microchannels of the Catalyst B is shown in Figure 72.

Figure 72. Dots on the Catalyst B microchannels.

Old and new plates

It is possible that new and old plates had slightly different properties compared to each other due to having more oxidation layer. In Figure 15 it was visible that the plate that was used is still darker than the new ones after pretreatment.

Placing plates to reactor

The microreactor holds only one catalyst plates at time. Plates were changed after every experiment set for each catalyst. Plates did not fit perfectly to the reactor, so some filing was needed on end and edges of the plates to fit them in the reactor. Some of the catalysts needed to be scratched away from the top of the plates. Plates needed to be placed carefully to the reactor, in order not to scratch off the catalyst from the channels.

Graphite sealing and gasket

The reactor contains graphite sealing and gaskets, which were changed to new ones before starting all experiments. One gasket was changed during the experiment, since it was damaged. This was noticed after experiments of the Catalyst E. This might have affected the experiments. Since nothing suspicious was noticed during the experiments, the effect is probably minor. The broken gasket is shown in Figure 73.

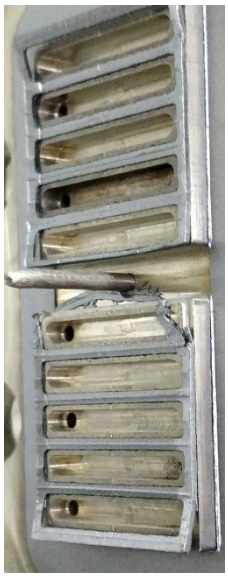

Figure 73. The broken gasket.

6.3 Catalyst preparation

The preparation of the catalyst is an important step for the success of the catalyst. There are variables in many areas, which would have affected the result. Here are collected a few things that might have affected the outcome.

The pH of the solution

The pH of the solution where TiO_2 particles are added, strongly affects how Au nanoparticles attach on the TiO_2 surface. The pH in this work was measured by dipping a pH paper in to the solution. This might have affected to the preparation solution. This could have been prevented by using pH paper meant for acidic solutions, with better scale to get more accurate pH reading. Or using pH meter, also taking samples from the solution in order not to effect on solution, would increase the accuracy of the pH adjustment.

Filtering and particles

Particles could be analyzed from the filtration solution, but visual analysis was good enough for this work. There might have been some particles passing through the membrane filter. But further on, it would be good to check, if there are any particles on the filtrated solution, depending purpose and the schedule of the work. Spectrophotometry, electrical conductivity meter or other suitable analyze device would do well.

H_2SO_4

Used H_2SO_4 was already prepared previously and might have already diluted, which might have affected to the pH adjustment. This might have led to adding excess amount of SO_4^{-2}, which maybe influences to the particles.

7. Future recommendations

Here are collected some thoughts, which came up during the writing of the thesis and which could help proceed in the future.

Chemisorption and physisorption

It would be interesting to analyze chemisorption and physisorption of the catalysts, but it was not possible for this thesis due to schedule. Results would give more information about the catalyst and properties about the activity.

Amount of water

It would be interesting to test effect of the water amount to particle size and particle distribution. This could be easily tested by changing the amount of the water on the catalyst preparation and keeping other parameters as same as tested on this thesis. It might affect the particle size.

Amount of the catalyst on the microreactor plates

It would be interesting to test the same catalyst with different coating thicknesses on the plates. Thinner film could be obtained by spreading suspension to two different pairs of plates instead of one pair of plates and test how much they differ on the microreactor. Still there should be enough of catalyst for the characterizations.

Rheology

The rheology tests were failed, however viscosity changes was a good observation, which is good to keep on mind when doing further experiments. First development proposal is to have more suspension to test, used amounts were too small. It also would be beneficial to have more optimized method parameters and more experience on the viscosity measurements and data analysis.

8. Conclusions

Five nano gold catalysts supported on titania (TiO_2) were prepared with the sol-immobilization method. Catalysts were prepared to observe the effect of catalyst preparation parameters to nanoparticle size distribution of the gold nanoparticles and activity of the catalyst. The varied preparation parameters were amount of gold, pH adjustment and pH level. 1-Butanol was partial oxidized to butyraldehyde with the catalysts in a microreactor.

Catalysts contained 0.3, 0.6 and 1.0% of gold by weight. Particle size of gold vary between 0.5 – 7.0 nm, particle size of titania was less than 25 nm. One catalyst had different pH adjustment in the catalyst preparation step. Catalyst was acidified before adding the support instead of acidifying after adding the support. One catalysts had pH level 3 instead of 1 in order to observe the difference effect to activity.

1.0 wt.% amount of gold gave 3.9 nm average size of particles and 0.3 wt.% amount of gold gave 2.0 nm average size of particles. Acidifying catalyst preparation solution before adding TiO_2 affected size of the particles by reducing their size from 3.9 nm to 3.2 nm. Acidifying catalyst preparation solution to pH 3, affected size of the particles by increasing their size from 2.7 to 3.8 nm with 0.6 wt.% of gold containing catalyst.

All catalysts yielded 20% - 55% of butyraldehyde at 400 °C. Yields of other products such as CO (3% - 10%), CO_2 (5% - 25%), trans-2-butene (1% - 10%), 1-butene (1% - 5%) and propene (0% - 5%) at 400 °C. Highest conversion (85%) of 1-butanol was achieved with 2.0 nm average particle size and highest selectivity (74%) of butyraldehyde with 2.7 nm at 400 °C. Decreasing the residence time and increasing the partial pressure of 1-butanol it was possible to have more selective reactor conditions to the butyraldehyde.

Information about the effect of the preparation step and effect of the reactor conditions to activity of the catalyst was obtained. Catalyst preparation procedure was made to consume less active time, by pump and semi-automated water dropper.

References

1. Haruta, M. When gold is not noble: Catalysis by nanoparticles. *Chem. Rec.* **3,** 75–87 (2003). DOI 10.1002/tcr.10053

2. Hvolbæk, B., Janssens, T.V.W., Clausen, B.S., Falsig, H., Christensen, C.H., Nørskov, J.K.. Catalytic activity of Au nanoparticles. *Nano Today* **2,** 14–18 (2007). DOI 10.1016/S1748-0132(07)70113-5

3. Chen, C. Wanga L., Xiao G., Liu Y., Xiao z., Deng Q., Yao P. Continuous acetone-butanol-ethanol (ABE) fermentation and gas production under slight pressure in a membrane bioreactor. *Bioresour. Technol.* **163,** 6–11 (2014). DOI 10.1016/j.biortech.2014.04.004

4. Knözinger, H. Heterogeneous catalysis and solid catalysts. *Ullmann's Encyclopedia of Industrial Chemistry* (2009). DOI 10.1002/14356007

5. Mascal, M. Chemicals from biobutanol: technologies and markets. *Biofuels, Bioprod. Bioref.* **6,** 483–493 (2012). DOI 10.1002/bbb.1328

6. Khan, Y., Marin, M., Karinen, R. & Lehtonen, J. 3D simulations of a microchannel reactor with diffusion inside the catalyst layer for 1-butanol dehydration reaction in gas phase. *Chem. Eng. Process.* **110,** 97–105 (2016). DOI 10.1016/j.cep.2016.07.002

7. Khan, Y., Marin, M., Karinen, R., Lehtonen, J. & Kanervo, J. 1-Butanol dehydration in microchannel reactor: Kinetics and reactor modeling. *Chem. Eng. Sci.* **137,** 740–751 (2015).DOI 10.1016/j.ces.2015.07.026

8. Horn, M., Schwerdtfeger, C F; Meagher, E. P. Zeitschrift fuer Kristallographie, Kristallgeometrie, Kristallphysik, Kristallchemie 5000223 @ www.crystallography.net. 273–281 (1972). Date accessed 20.02.2018

9. Comotti, M., Li, W.-C., Spliethoff, B. & Schüth, F. Support Effect in High Activity Gold Catalysts for CO Oxidation. *J. Am. Chem. Soc.* **128,** 917–924 (2006). DOI 10.1021/ja0561441

10. Liu, X. Y., Wang, A., Zhang, T. & Mou, C. Y. Catalysis by gold: New insights into the support effect. *Nano Today* **8,** 403–416 (2013). DOI 10.1016/j.nantod.2013.07.005

11. Sobolev, V. I., Koltunov, K. Y., Simakova, O. A., Leino, A. R. & Murzin, D. Y. Low temperature gas-phase oxidation of ethanol over Au/TiO 2. *Appl. Catal. A Gen.* **433–434,** 88–95 (2012). DOI 10.1016/j.apcata.2012.05.003

12. Prati, L. & Martra, G. New Gold Catalysts for Liquid Phase Oxidation. *Gold Bull.* **32,** 96–101 (1999). DOI 10.1007/BF03216617

13. Haruta, M. Size- and support-dependency in the catalysis of gold. *Catal. Today* **36,** 153–166 (1997). DOI 10.1016/S0920-5861(96)00208-8

14. Villa, A., Wang, D., Veith, G. M., Vindigni, F. & Prati, L. Sol immobilization technique: a delicate balance between activity, selectivity and stability of gold catalysts. *Catal. Sci. Technol.* **3,** 3036 (2013). DOI 10.1039/c3cy00260h

15. Hallensleben, M. L. Polycarbonates. *Ullmann's Encycl. Ind. Chem.* **29,** 603–611 (2000). DOI 10.1002/14356007.a21

16. Kemira Sodium Borohydride NaBH4 An effective reducing agent Sodium Borohydride NaBH 4. Date accessed 30.07.2018 http://www.ecochem.com.co/pdf/Hydrifin%20Brochure.pdf

17. Khan, Y. Marin M., Viinikainena T., Lehtonen J., Puurunen R.L., Karinen R. Structured microreactor with gold and palladium on titania: Active, regenerable and durable catalyst coatings for the gas-phase partial oxidation of 1-butanol. *Appl. Catal. A Gen.* **562,** 173–183 (2018). DOI 10.1016/j.apcata.2018.06.010

18. Lopez-Sanchez, J. A. *et al.* Au–Pd supported nanocrystals prepared by a sol immobilisation technique as catalysts for selective chemical synthesis. *Phys. Chem. Chem. Phys.* **10,** 1921–1930 (2008). DOI 10.1039/b719691a

19. Jiang, H. Ruokolainen J., Young N., Oikawa T., Nasibulin A.G., Kirkland A., Kauppinen E.I. Performance and early applications of a versatile double aberration-corrected JEOL-2200FS FEG TEM/STEM at Aalto University. *Micron* **43,** 545–550 (2012). DOI 10.1016/j.micron.2011.10.004

Appendices

Appendix A Explained FTIR picture from Calmet

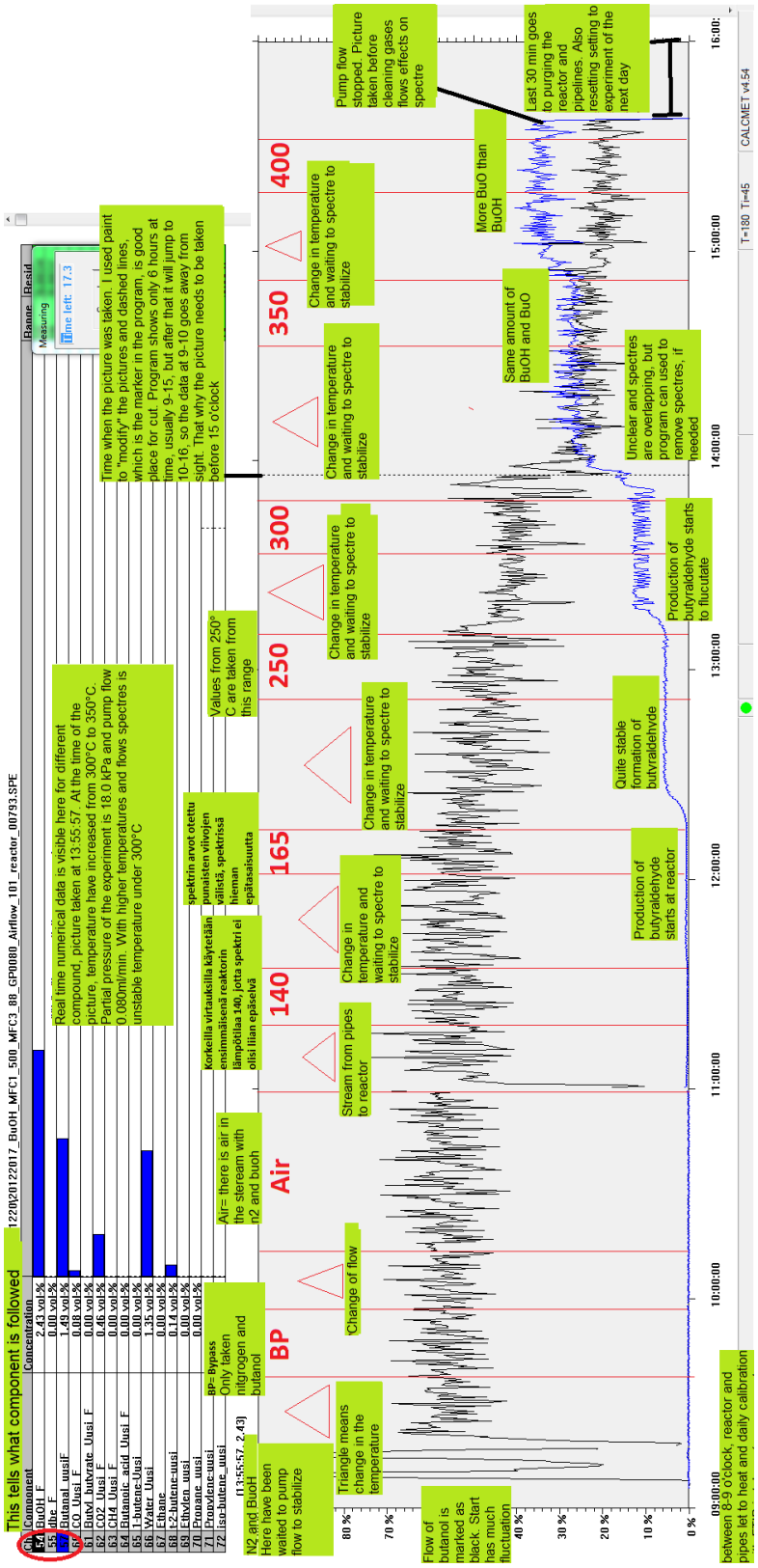

Figure 1. Explained FTIR picture from Calmet with partial pressure of 18.0 kPa and pump flow of 0.080 ml/min of 1-butanol (l).

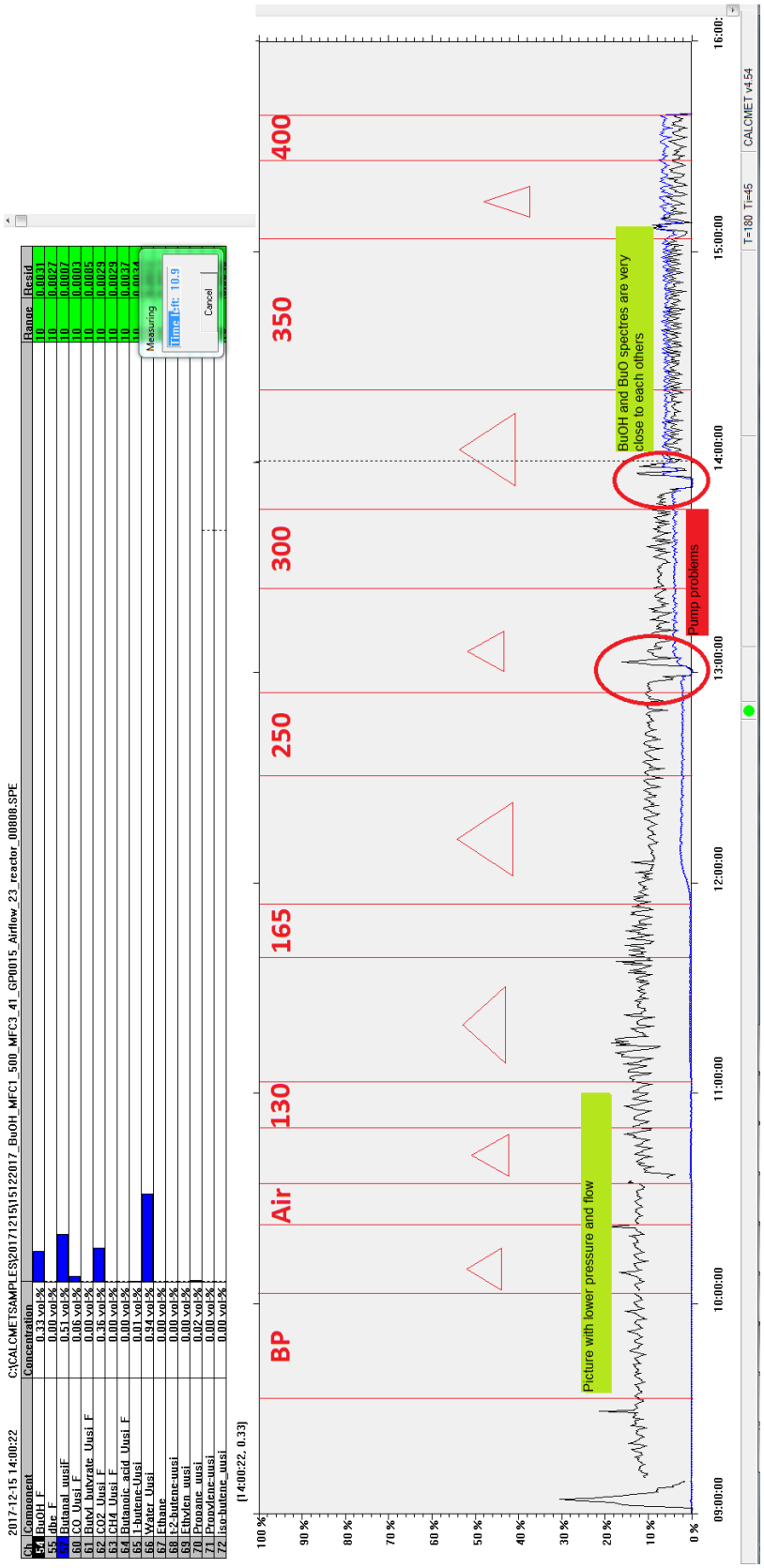

Figure 2. Picture with partial pressure of 13.5 kPa and pump flow 0.015 ml/min of 1-butanol (l)

Appendix B Larger TEM images

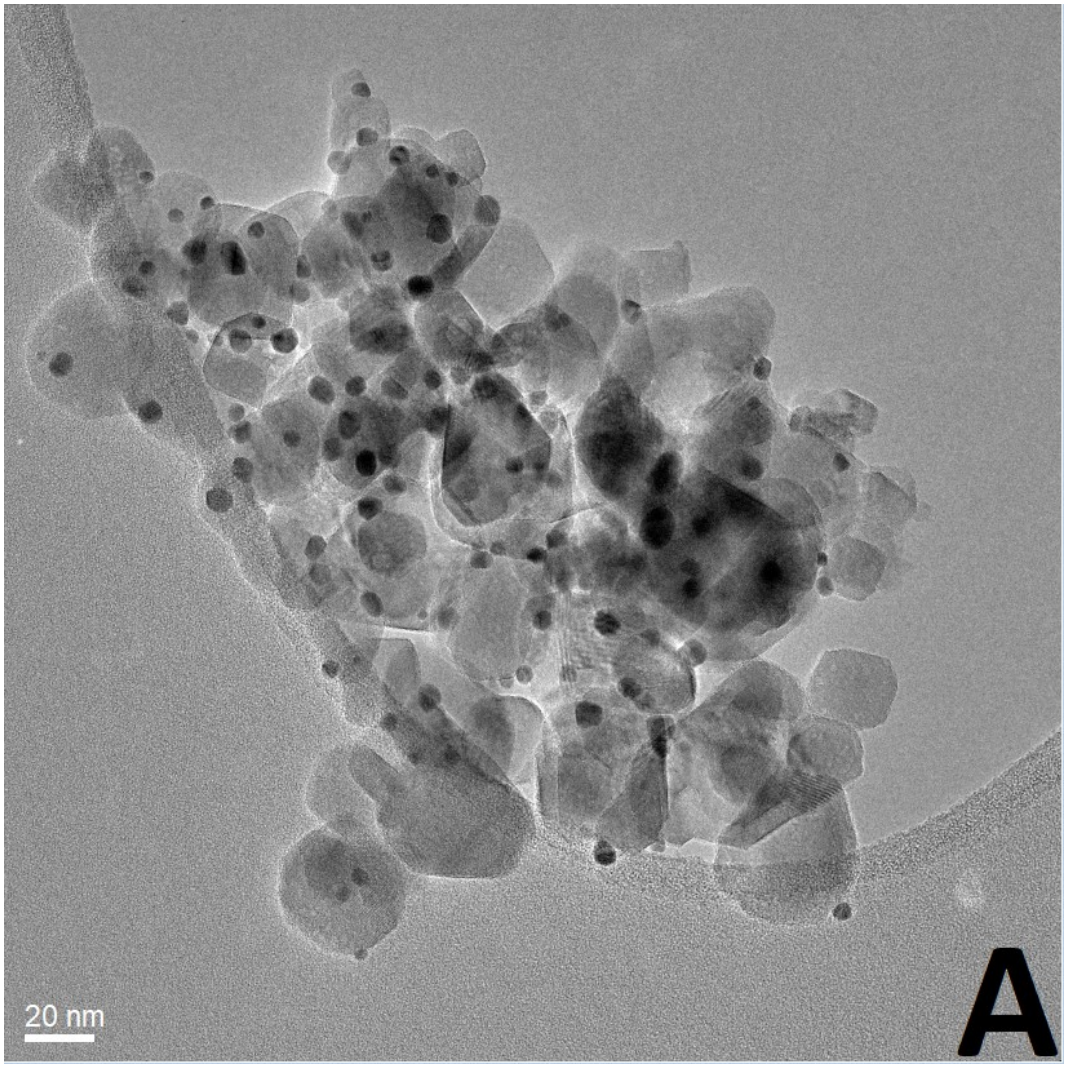

Figure 1. A) Catalyst A picture “b1”, 150k, 20 nm.

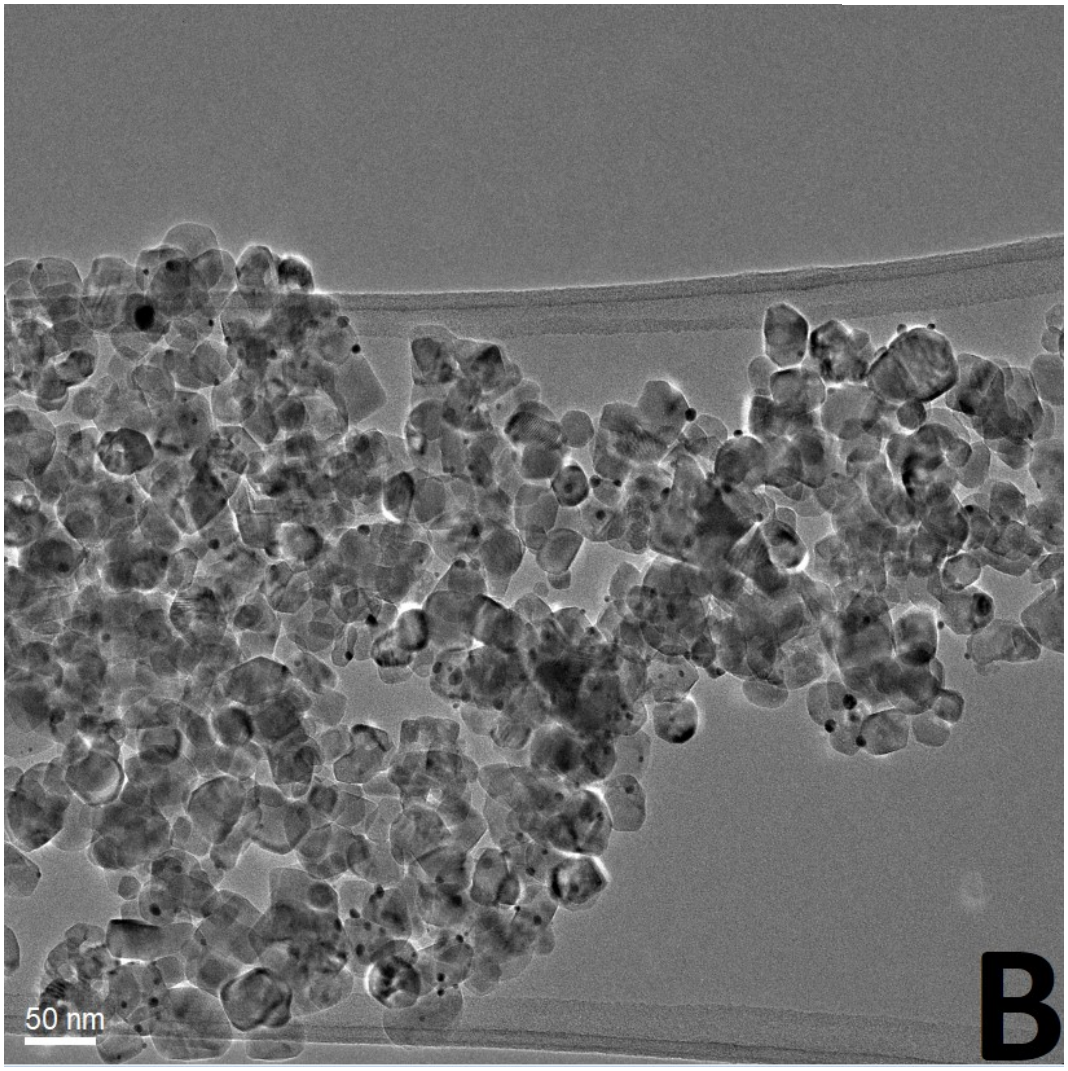

Figure 2. Catalyst B picture “c1”, 60k, 50 nm.

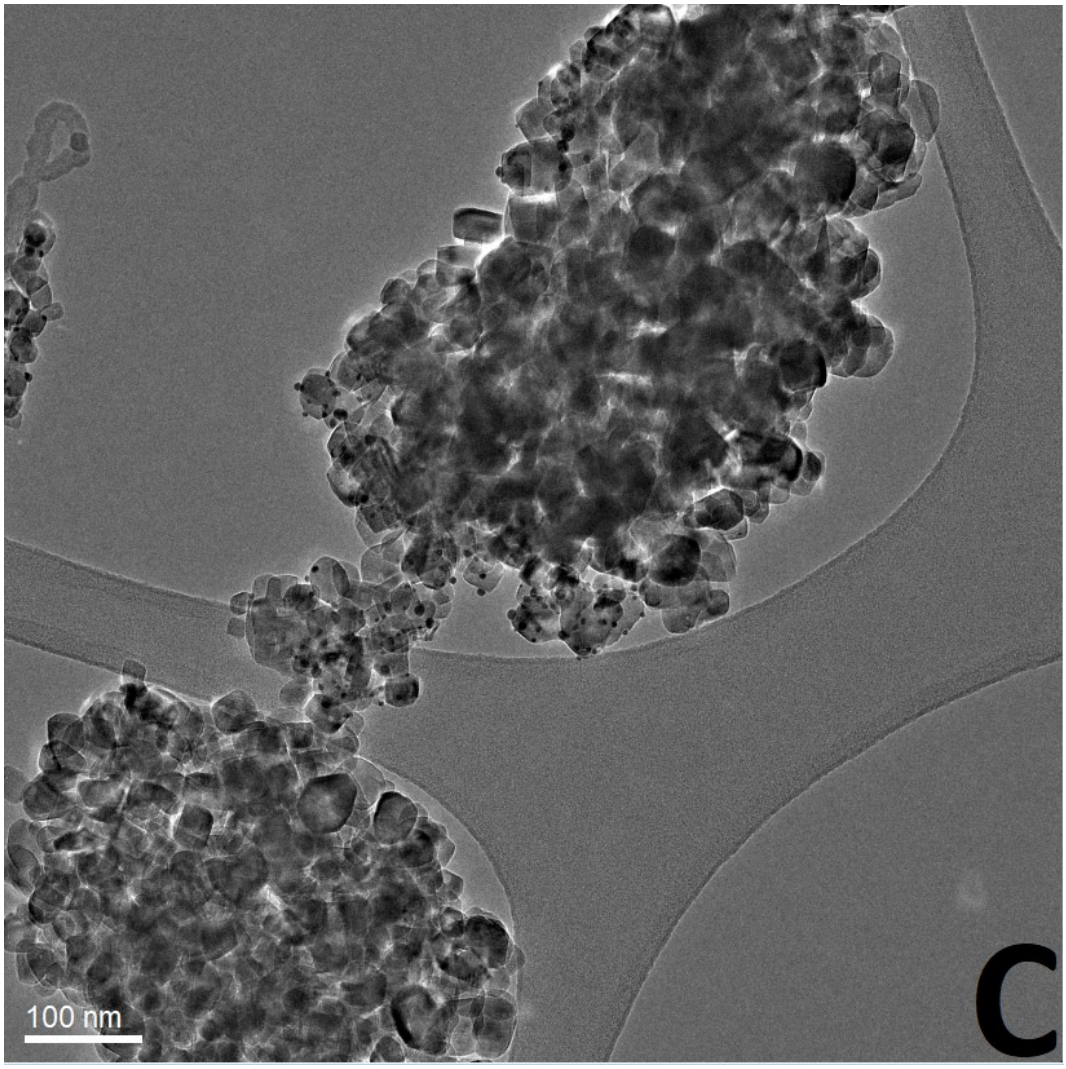

Figure 3. Catalyst C picture “b1”, 50k, 100 nm.

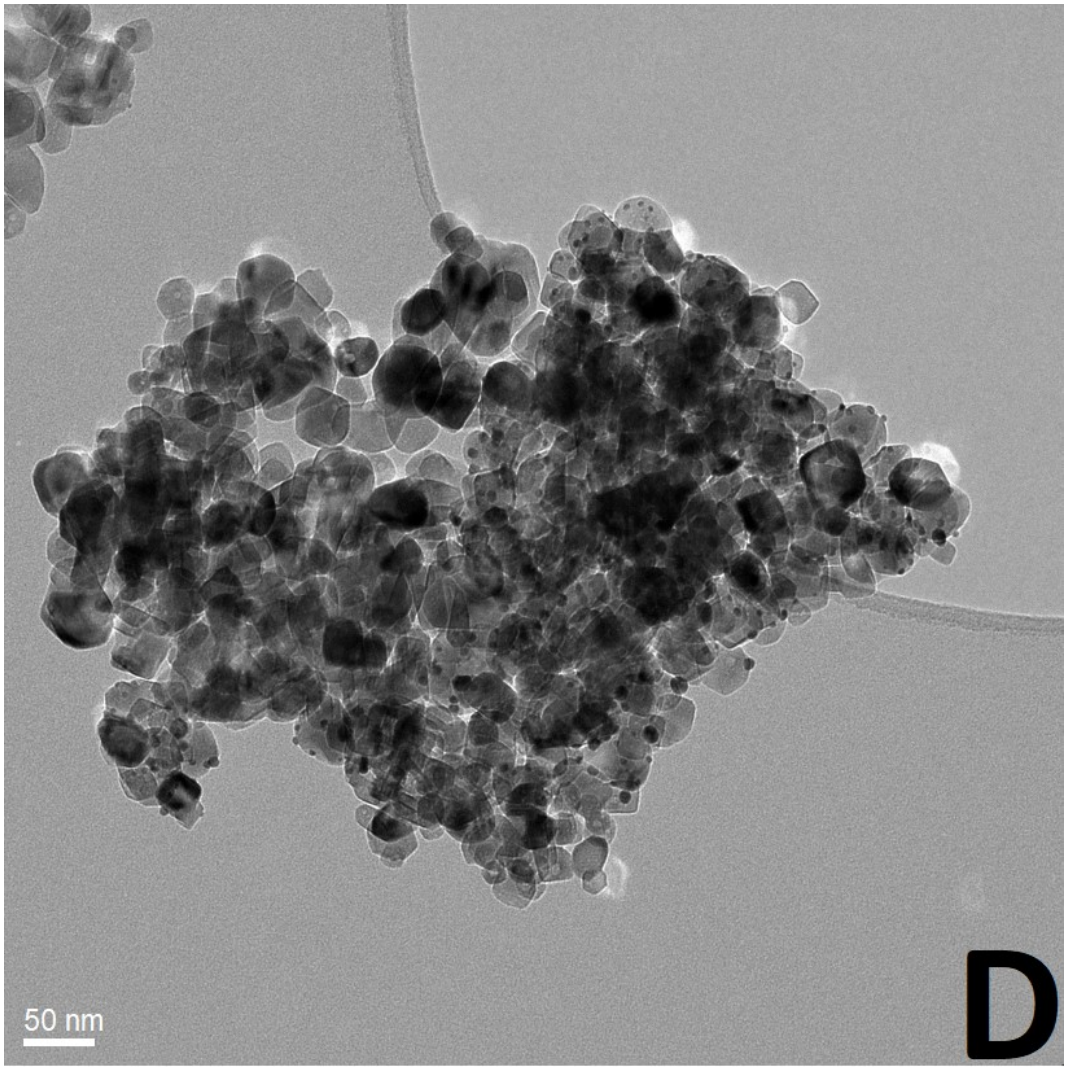

Figure 4. Catalyst D picture “a1”, 160k, 50 nm.

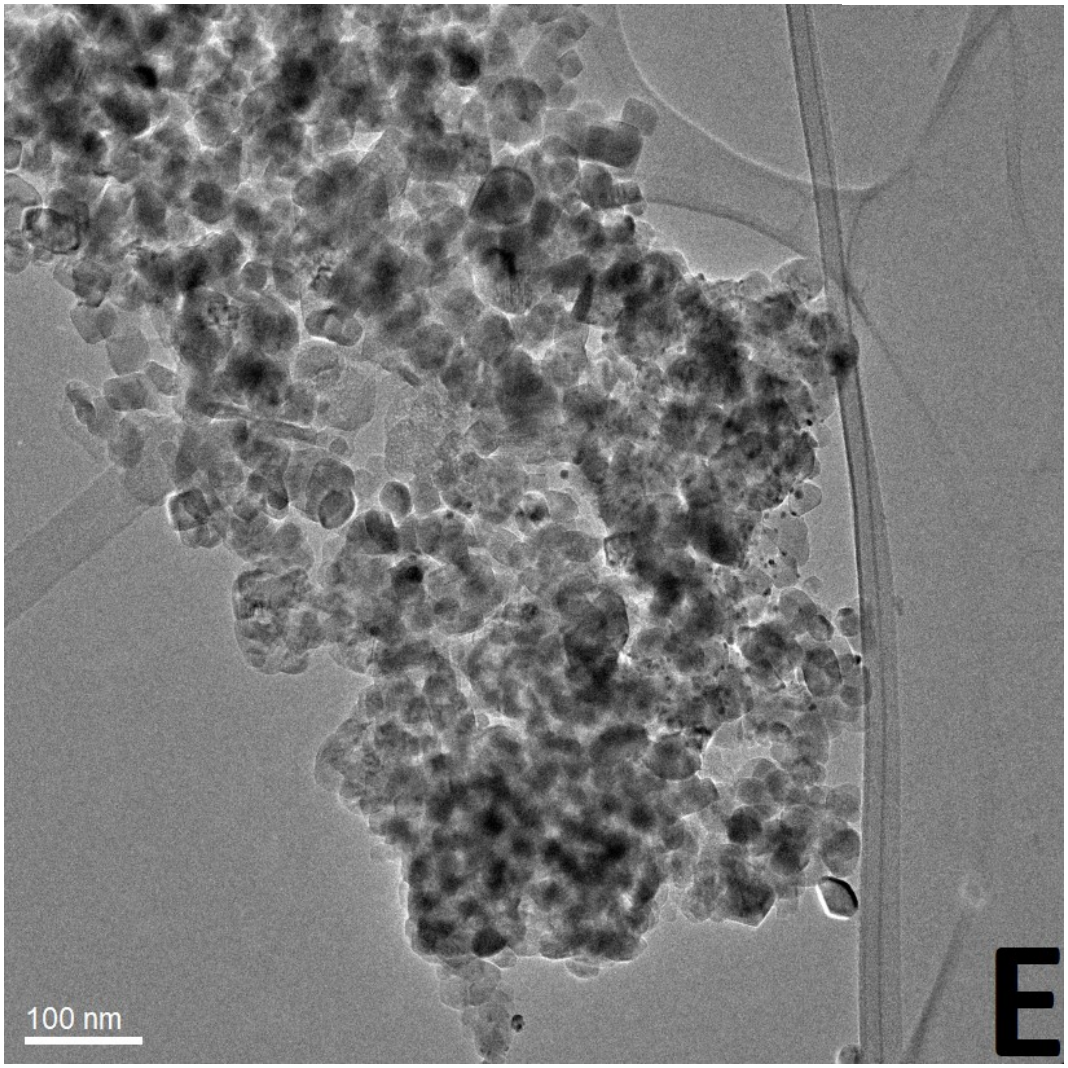

Figure 5. Catalyst E picture “f1”, 600k, 100 nm.

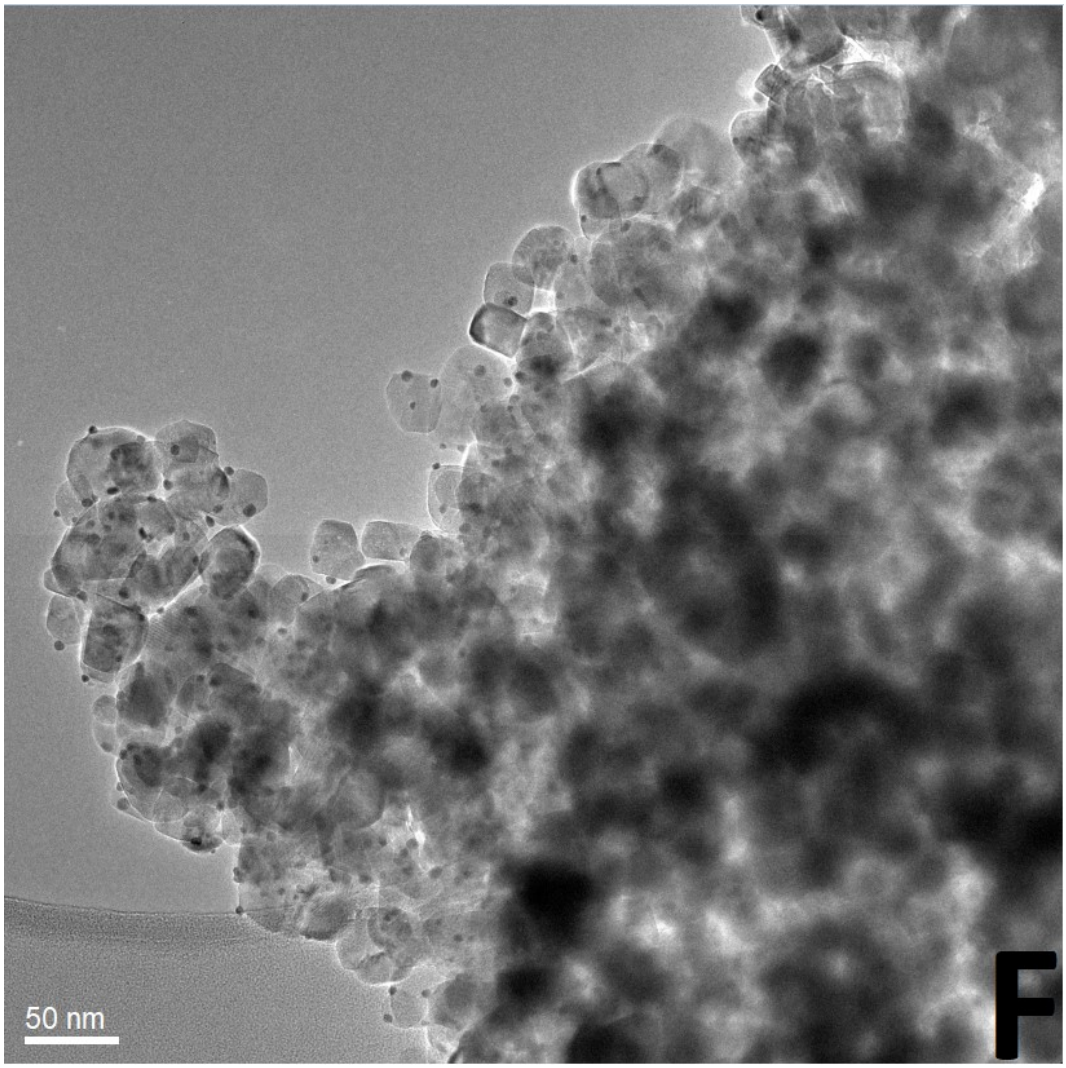

Figure 6. Catalyst O picture “g1”, 80k, 50 nm.

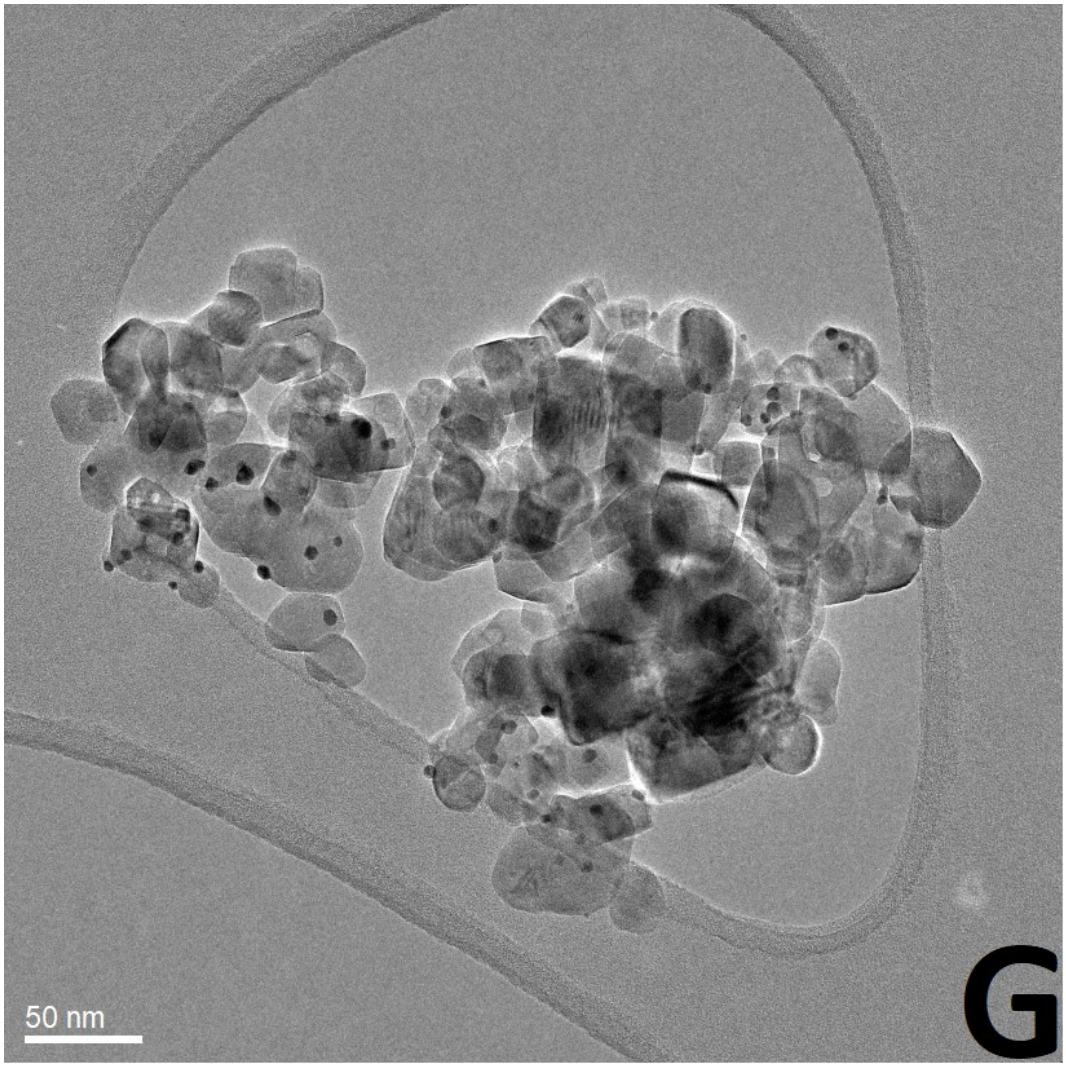

Figure 7. Catalyst A picture 2 “c1”, 100k, 50 nm.

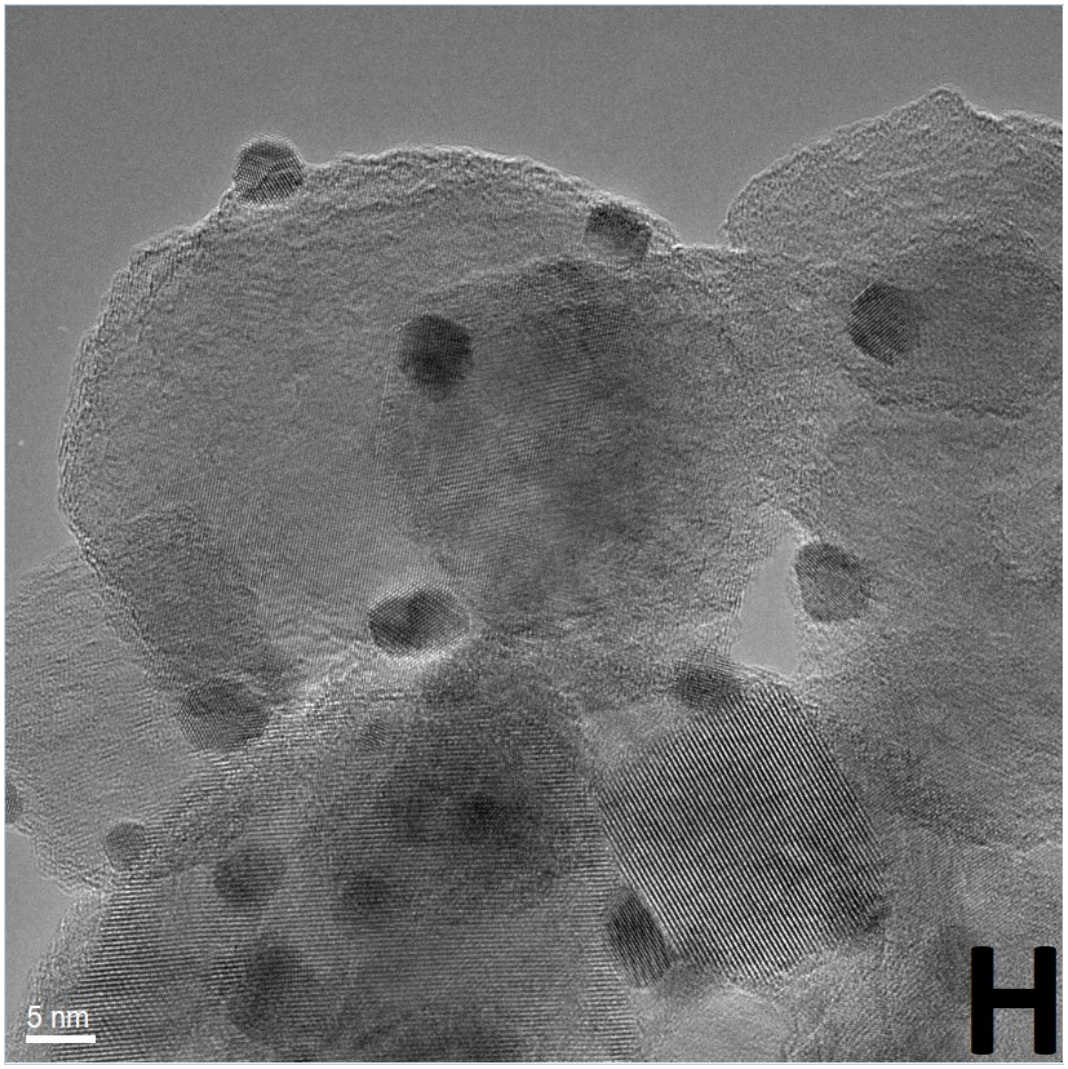

Figure 8. Catalyst O zoomed picture “g4” zoomed to particles, 600k, 5 nm.

Appendix C EDS pictures B-D

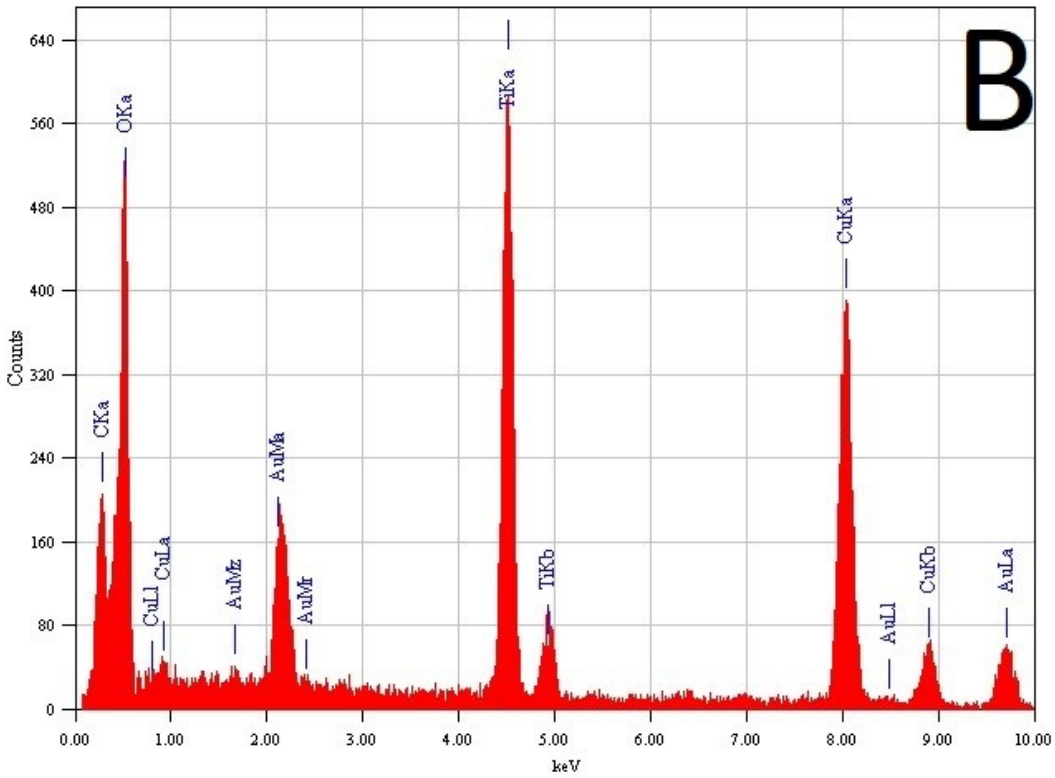

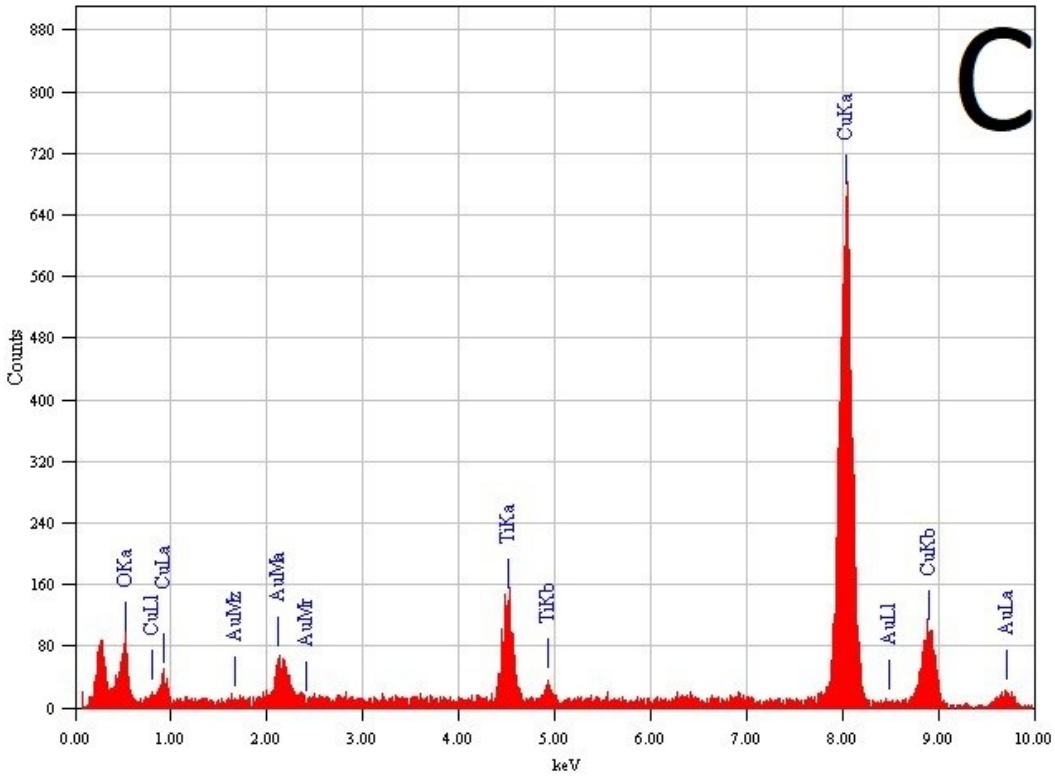

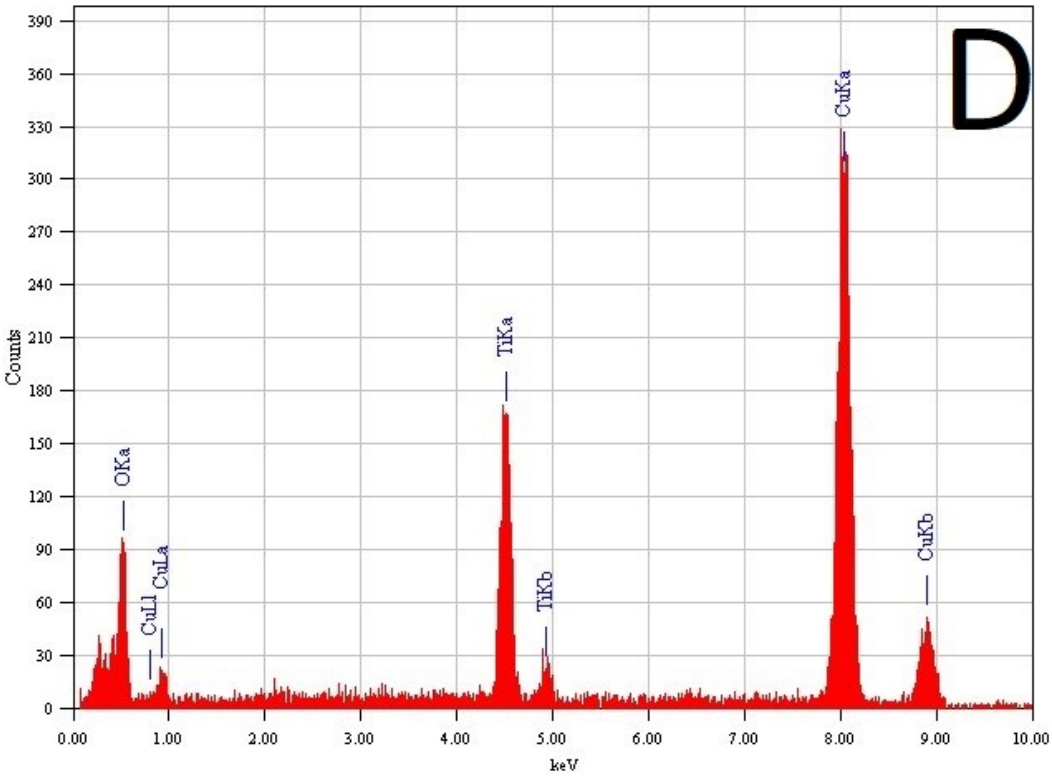

Figure 1. B) Catalyst B, EDS from gold particle. C) Catalyst O, EDS from gold particle. D) Catalyst O, EDS from TiO_2.

Appendix D XPS all measurements.

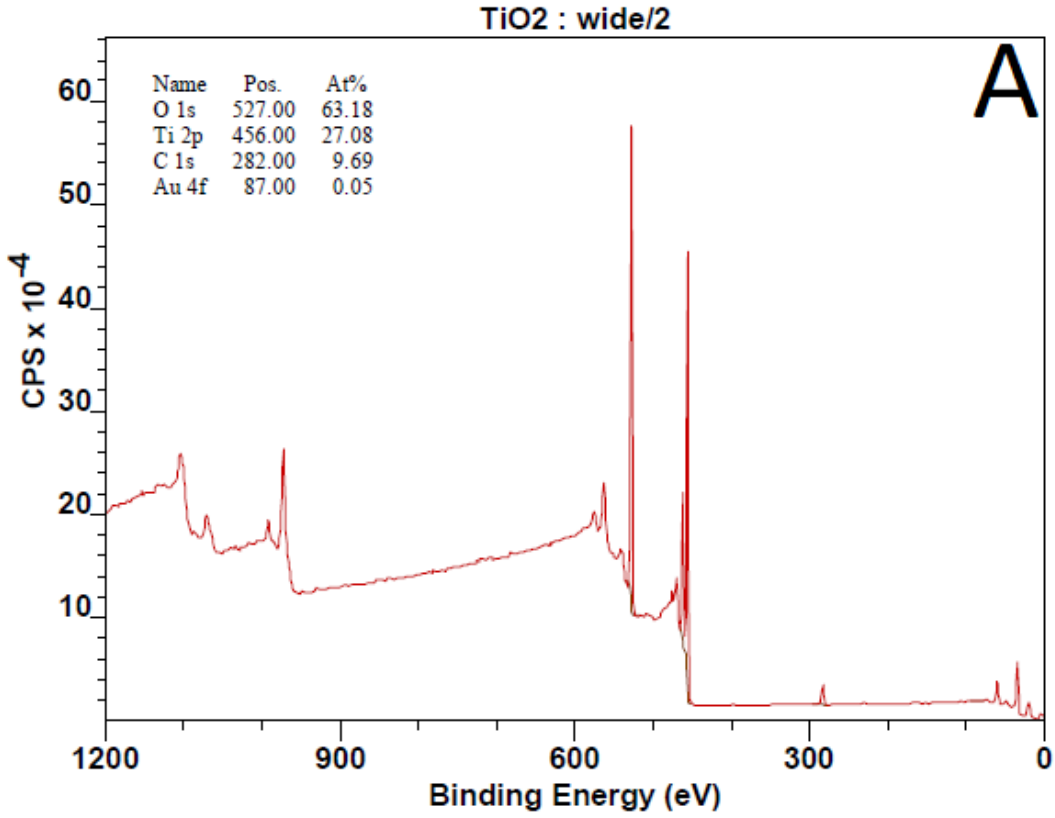

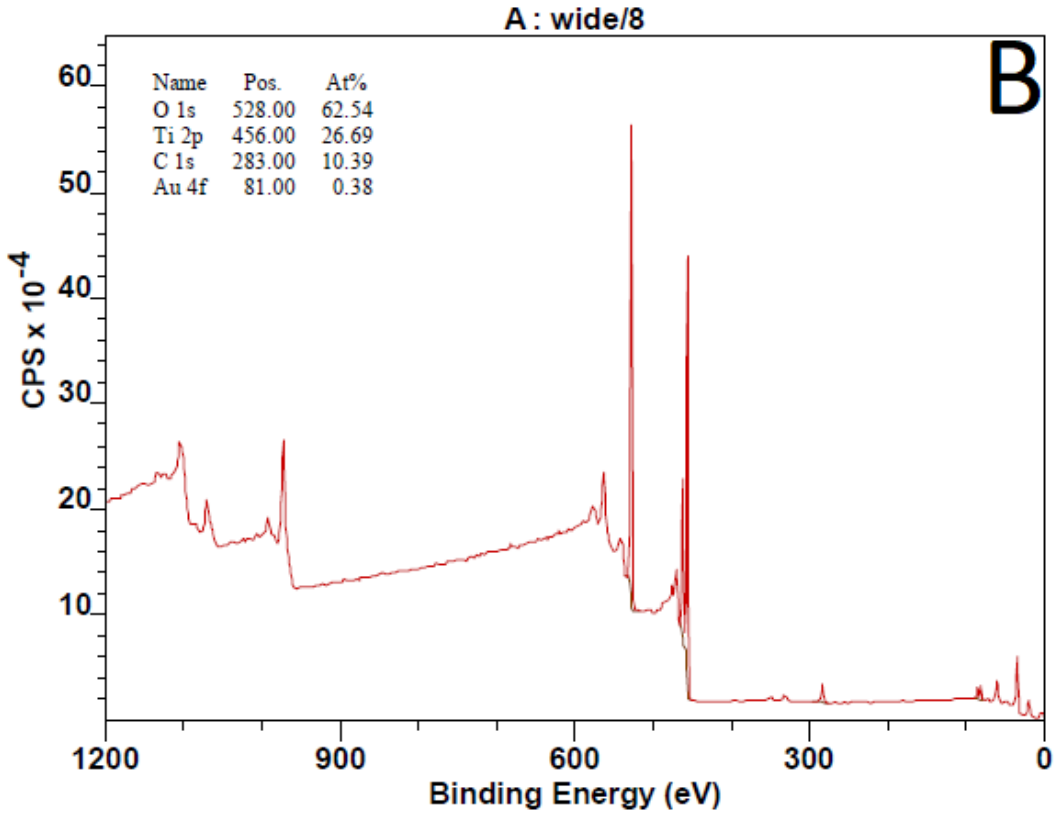

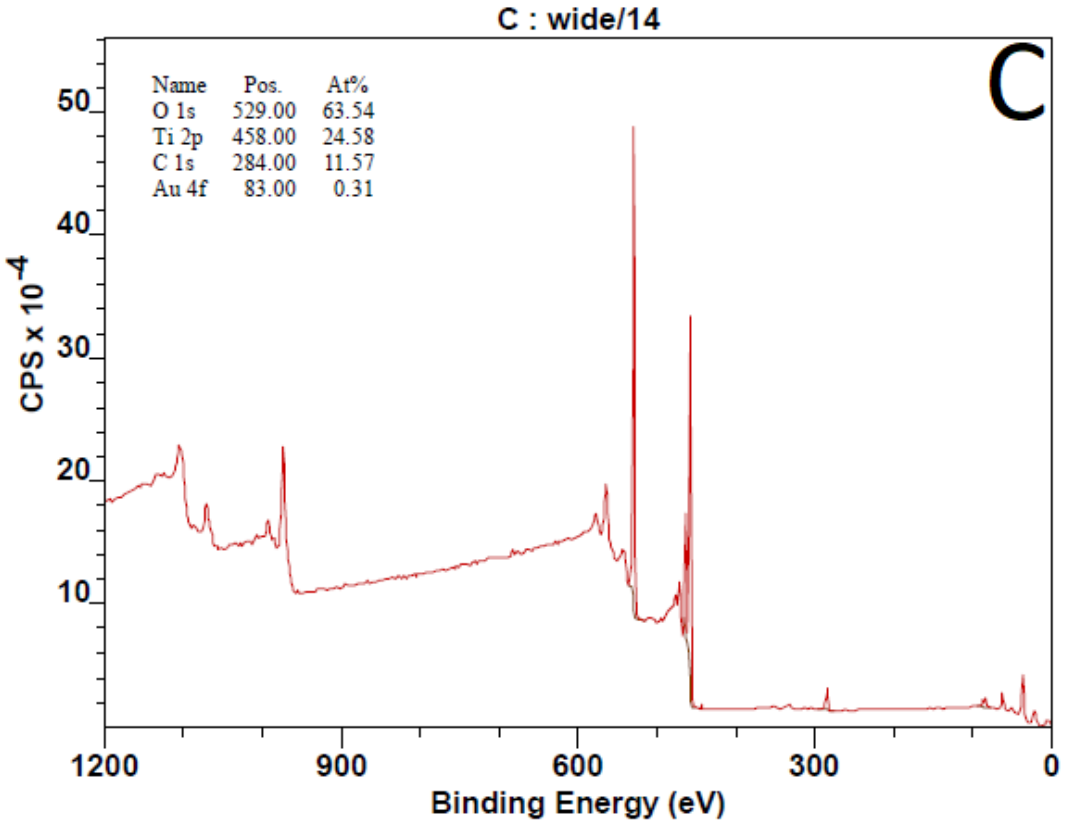
C : wide/14
C
Name Pos. At%
O 1s 529.00 63.54
Ti 2p 458.00 24.58
C 1s 284.00 11.57
Au 4f 83.00 0.31
CPS x 10-4
50
40
30
20
10
1200
900
600
300
0
Binding Energy (eV)

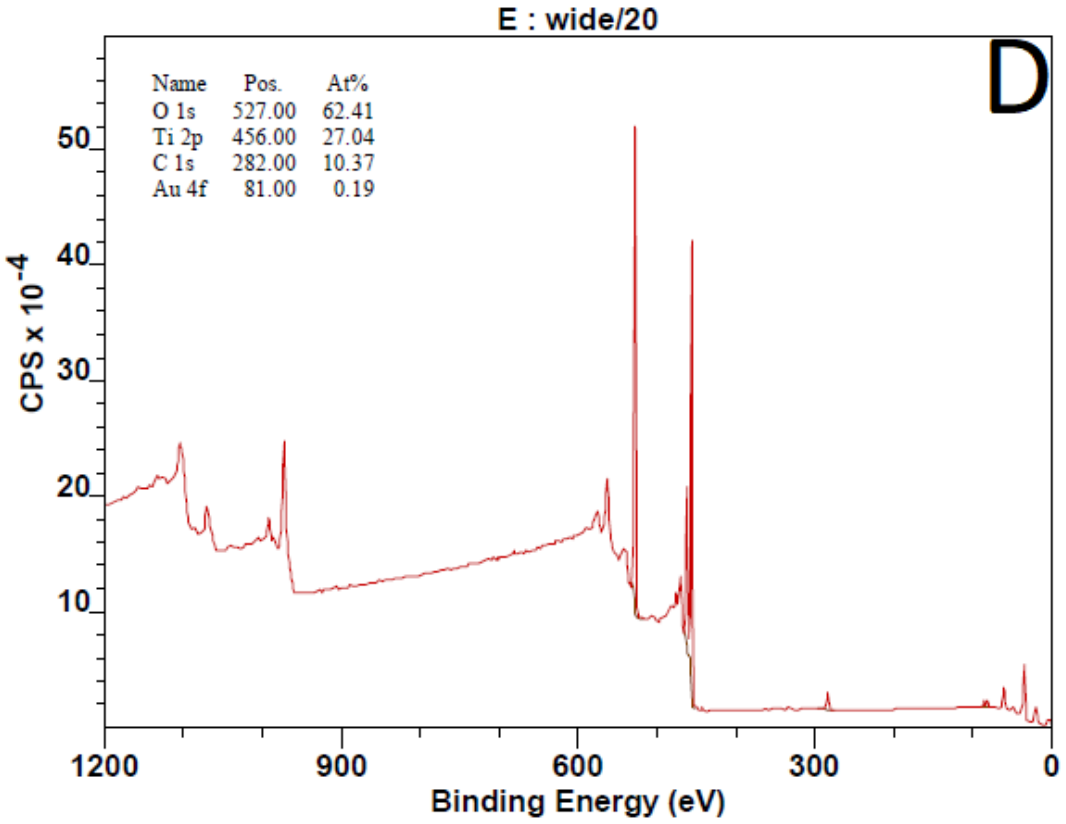
E : wide/20
D
Name Pos. At%
O 1s 527.00 62.41
Ti 2p 456.00 27.04
C 1s 282.00 10.37
Au 4f 81.00 0.19
CPS x 10-4
50
40
30
20
10
1200
900
600
300
0
Binding Energy (eV)

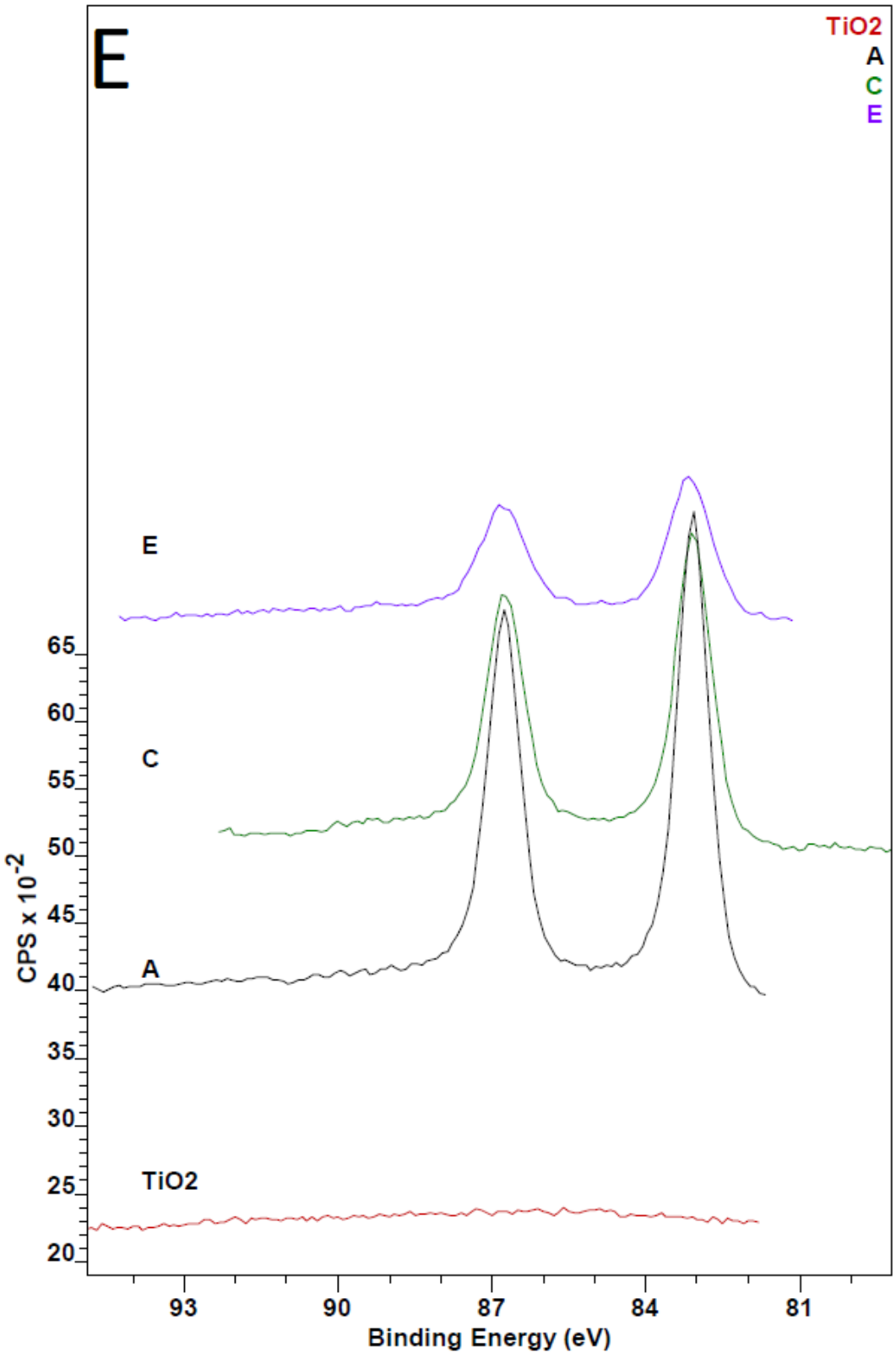
E
TiO2
A
C
E
E
C
A
TiO2
65
60
55
50
45
40
35
30
25
20
CPS x 10-2
93
90
87
84
81
Binding Energy (eV)

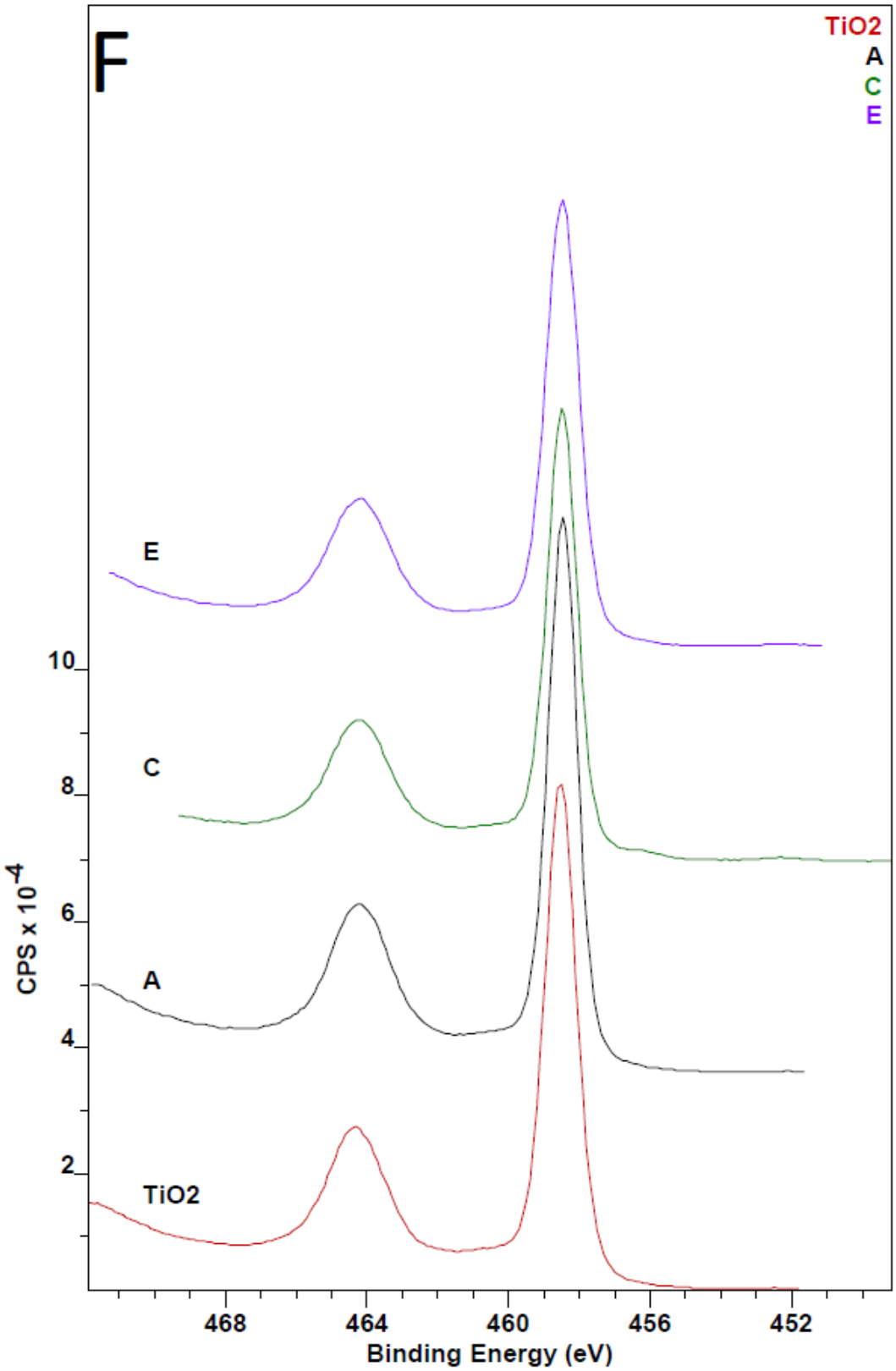
F
TiO2
A
C
E
E
C
A
TiO2
10
8
6
4
2
CPS x 10^-4
468
464
460
456
452
Binding Energy (eV)

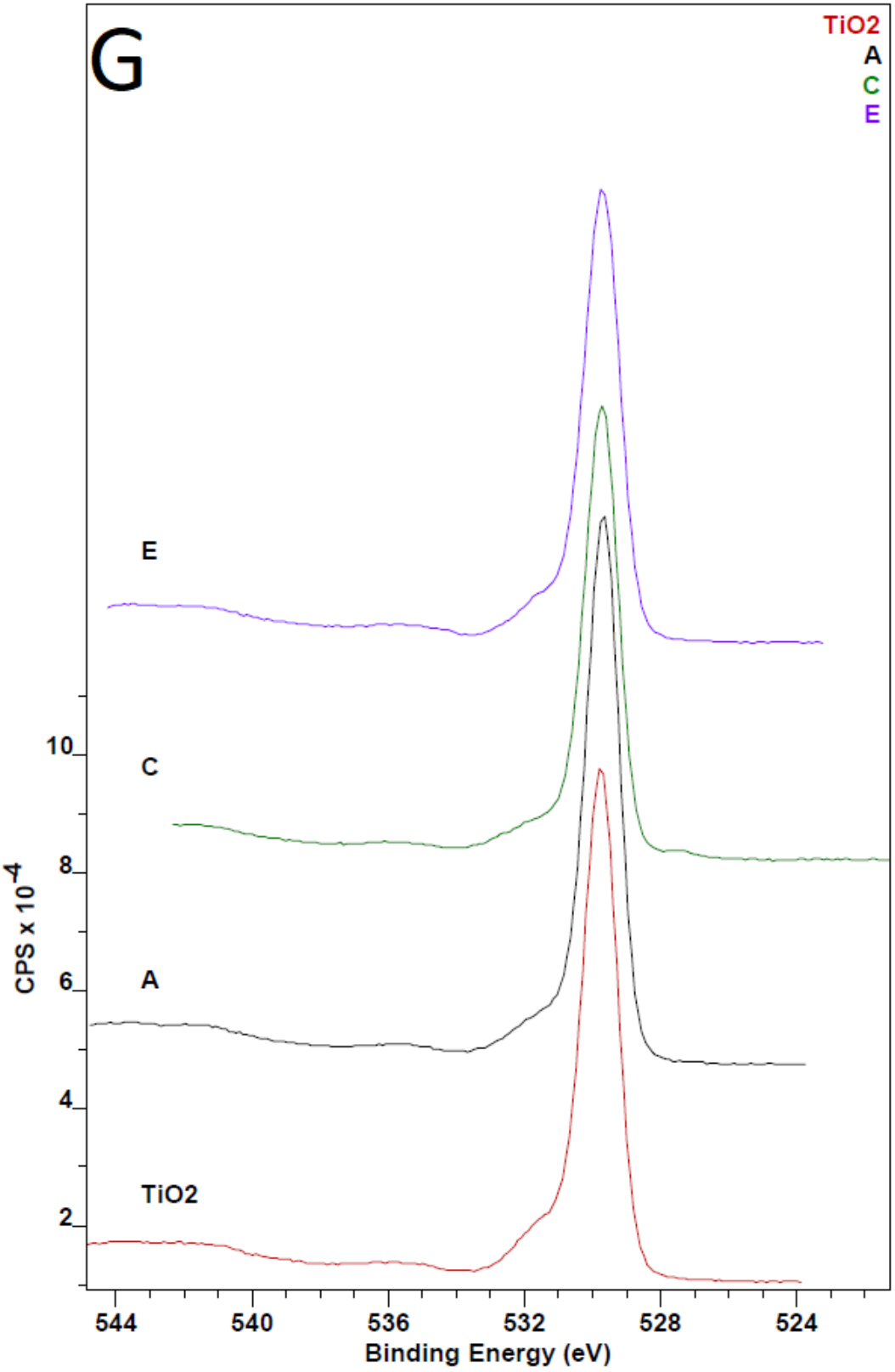
G
TiO2
A
C
E
E
C
A
TiO2
10
8
6
4
2
CPS x 10^-4
544
540
536
532
528
524
Binding Energy (eV)

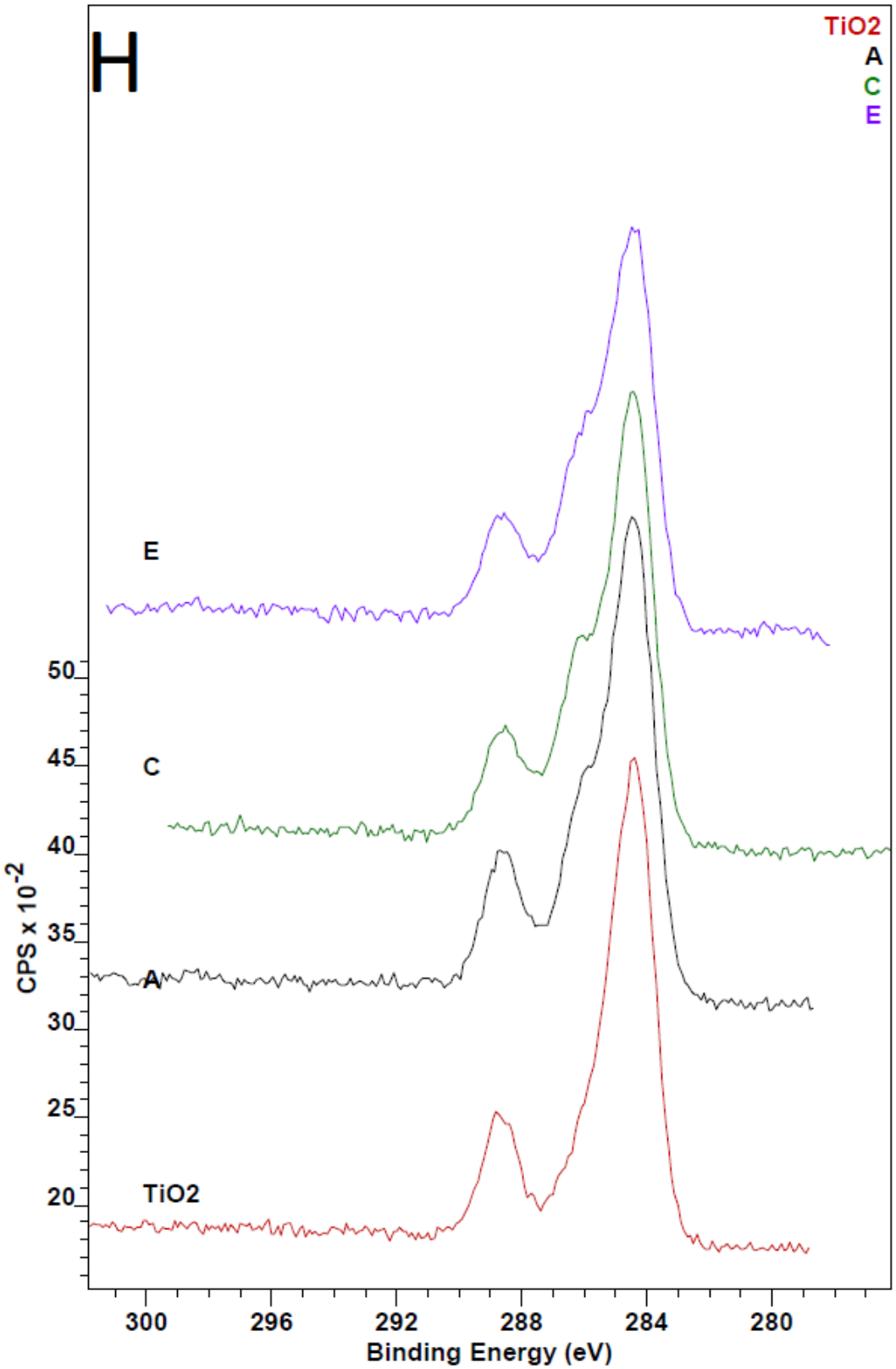

Figure 1. XPS results from catalysts A, C, E and calcined TiO_2. Gold. A) TiO_2 Wide. B) Catalyst A wide. C) Catalyst C wide. D) Catalyst E wide. E) Gold. F) Titanium. G) Oxygen. H) Carbon.

Appendix E Numerical average data from the microreactor results from catalysts A-E and O

Selectivity of Butyraldehyde

Temperature °C	Catalyst A %	Catalyst B %	Catalyst C %	Catalyst D %	Catalyst E %	Catalyst O %
130	7.23	8.89	5.76	4.95	4.37	23.47
165	4.14	11.23	10.21	11.02	8.67	39.03
250	13.38	34.98	44.76	27.27	36.91	63.37
300	27.05	55.88	54.88	35.02	42.53	70.48
350	34.97	53.2	50.95	40.42	43.08	64.19
400	24.46	41.96	46.2	31.31	39.52	73.72

Conversion of 1-butanol

Temperature °C	Catalyst A %	Catalyst B %	Catalyst C %	Catalyst D %	Catalyst E %	Catalyst O %
130	20.3	9.7	13.7	16.8	20.5	3.3
165	19.9	11.4	16.3	20.7	22.9	5.4
250	23.2	15.3	23.9	19.2	39.1	24.1
300	31.0	22.1	39.2	29.8	61.4	38.0
350	45.4	40.8	66.6	51.4	75.0	62.3
400	68.9	56.2	80.9	66.5	85.6	74.0

Average yield of Byturaldehyde

Temperature °C	Catalyst A %	Catalyst B %	Catalyst C %	Catalyst D %	Catalyst E %	Catalyst O %
130	0.4	0.9	0.8	0.8	0.9	0.77
165	0.6	1.3	1.7	2.3	2.0	2.12
250	2.5	5.4	10.7	5.2	14.4	15.26
300	6.8	12.4	21.5	10.4	26.1	26.75
350	15.9	21.7	33.9	20.8	32.3	39.99
400	19.1	23.6	37.4	20.8	33.8	54.52

Average yield of CO

Temperature °C	Catalyst A %	Catalyst B %	Catalyst C %	Catalyst D %	Catalyst E %	Catalyst O %
130	0.0	0.05	0.08	0.02	0.02	0.09
165	0.0	0.05	0.09	0.17	0.03	0.17
250	0.0	0.06	0.11	0.07	1.11	0.17
300	0.2	0.18	0.43	0.19	3.95	1.02
350	1.0	1.04	2.35	0.99	7.98	3.37
400	3.6	3.92	5.76	4.71	10.93	4.37

Average yield of CO_2

Temperature °C	Catalyst A %	Catalyst B %	Catalyst C %	Catalyst D %	Catalyst E %	Catalyst O %
130	0.0	0.00	0.04	0.00	0.01	0.00
165	0.0	0.01	0.07	0.36	0.05	0.01
250	0.1	0.03	0.35	0.05	1.61	0.63
300	0.6	0.61	1.33	0.63	4.23	4.95
350	1.9	2.11	8.00	2.24	14.27	20.30
400	7.6	9.08	21.24	10.60	22.89	21.71

Average yield of 1-butene

Temperature °C	Catalyst A %	Catalyst B %	Catalyst C %	Catalyst D %	Catalyst E %	Catalyst O %
130	-0.1	0.06	0.00	0.08	0.00	0.03
165	-0.3	0.00	0.00	0.15	0.00	0.02
250	0.0	0.06	0.02	0.02	0.06	0.34
300	-0.2	0.37	0.15	0.29	0.85	0.40
350	2.0	2.44	1.08	2.61	1.20	0.05
400	4.2	5.39	0.81	4.89	0.88	0.17

Average yield of t-2-butene

Temperature °C	Catalyst A %	Catalyst B %	Catalyst C %	Catalyst D %	Catalyst E %	Catalyst O %
130	-0.1	0.16	0.15	0.06	0.14	0.01
165	-0.9	0.17	0.25	0.37	0.13	0.07
250	0.3	0.08	0.17	0.06	0.02	0.03
300	-0.5	0.28	0.28	0.22	-0.03	0.99
350	3.8	3.39	2.64	3.14	0.36	2.67
400	9.5	9.71	5.95	8.40	1.81	1.54

Average yield of isobutene

Temperature °C	Catalyst A %	Catalyst B %	Catalyst C %	Catalyst D %	Catalyst E %	Catalyst O %
130	0.1	0.02	0.20	0.00	0.00	0.03
165	0.2	0.05	0.50	0.00	0.00	0.00
250	0.2	0.00	0.08	0.00	0.00	0.03
300	0.1	0.00	0.00	0.00	0.00	0.00
350	0.0	0.00	0.03	0.00	0.00	0.00
400	0.0	0.00	0.19	0.00	0.00	0.00

Average yield of Propene

Temperature °C	Catalyst A %	Catalyst B %	Catalyst C %	Catalyst D %	Catalyst E %	Catalyst O %
130	0.0	0.00	0.00	0.00	0.00	0.00
165	0.0	0.00	0.00	0.00	0.00	0.00
250	0.0	0.00	0.00	0.00	0.25	0.00
300	0.0	0.00	0.00	0.00	0.56	0.00
350	0.1	0.07	0.03	0.01	2.33	0.00
400	0.2	0.10	0.29	0.20	3.95	0.02

Average yield of 2-butene

Temperature °C	Catalyst A %	Catalyst B %	Catalyst C %	Catalyst D %	Catalyst E %	Catalyst O %
130	0.00	0.00	0.00	0.05	0.00	0.00
165	0.00	0.23	0.00	0.00	0.10	0.24
250	0.00	0.24	0.00	0.29	0.17	0.55
300	0.00	0.39	0.00	0.29	0.74	0.22
350	0.00	0.00	0.09	0.22	0.14	0.00
400	0.00	0.00	0.00	0.00	0.00	0.80

Average yield of ButylBut

Temperature °C	Catalyst A %	Catalyst B %	Catalyst C %	Catalyst D %	Catalyst E %	Catalyst O %
130	0.35	0.02	0.03	0.02	0.04	0.01
165	0.21	0.02	0.02	0.01	0.12	0.01
250	0.01	0.00	0.01	0.00	0.42	0.00
300	0.01	0.00	0.00	0.00	0.42	0.00
350	0.00	0.00	0.00	0.00	0.06	0.00
400	0.01	0.01	0.00	0.03	0.01	0.05

Average yield of CH4

Temperature °C	Catalyst A %	Catalyst B %	Catalyst C %	Catalyst D %	Catalyst E %	Catalyst O %
130	0.29	0.27	0.20	0.12	0.16	0.10
165	0.21	0.27	0.24	0.13	0.14	0.10
250	0.17	0.09	0.02	0.05	0.02	0.01
300	0.04	0.02	0.00	0.01	0.00	0.00
350	0.00	0.04	0.00	0.01	0.00	0.00
400	0.00	0.02	0.00	0.00	0.00	0.00

Average yield of But.Acid

Temperature °C	Catalyst A %	Catalyst B %	Catalyst C %	Catalyst D %	Catalyst E %	Catalyst O %
130	0.18	0.11	0.35	0.32	0.16	0.12
165	0.00	0.10	0.29	0.15	0.14	0.16
250	0.64	0.20	0.59	0.50	1.11	0.07
300	0.52	0.31	0.89	0.61	1.77	0.13
350	0.00	0.03	0.07	0.21	0.32	0.00
400	0.00	0.00	0.01	0.06	0.05	0.04

Appendix F Numerical average data from the microreactor results from partial pressure 13.5 kPa experiments

PP 13 average selectivity

Temperature °C	1 (%)	2 (%)	3 (%)	4 (%)	5 (%)	6 (%)
130	36.4	16.5	23.5	19.7	17.9	18.2
165	78.3	19.9	39.0	41.1	65.3	22.4
250	76.5	64.0	63.4	77.7	58.0	56.2
300	73.4	62.5	70.5	74.4	66.7	58.3
350	69.3	62.5	64.2	83.4	83.5	90.5
400	68.6	64.5	73.7	85.7	94.5	98.1

PP 13 average Conversion

Temperature °C	1 (%)	2 (%)	3 (%)	4 (%)	5 (%)	6 (%)
130	4.17	3.5	3.3	4.0	4.0	3.9
165	4.14	7.6	5.4	5.5	3.3	5.6
250	22.47	21.8	24.1	17.5	19.3	17.5
300	43.49	47.5	38.0	30.7	28.7	29.4
350	68.51	65.4	62.3	58.7	55.2	54.6
400	74.00	74.5	74.0	68.4	66.9	65.8

PP 13 average yield of BuO

Temperature °C	1 (%)	2 (%)	3 (%)	4 (%)	5 (%)	6 (%)
130	1.5	0.6	0.8	0.8	0.8	0.7
165	3.2	1.5	2.1	2.3	1.4	1.3
250	17.2	13.9	15.3	13.6	15.0	9.8
300	31.9	29.7	26.8	22.8	21.3	17.1
350	47.5	40.9	40.0	48.9	46.0	49.5
400	50.7	48.0	54.5	58.6	57.3	64.5

PP 13 average yield of CO

Temperature °C	1 (%)	2 (%)	3 (%)	4 (%)	5 (%)	6 (%)
130	0.0	0.0	0.1	0.1	0.1	0.1
165	0.1	0.0	0.2	0.1	0.1	0.1
250	0.4	0.3	0.2	0.1	0.2	0.1
300	2.7	2.3	1.0	0.9	0.9	0.6
350	5.1	4.2	3.4	3.3	3.1	2.8
400	5.9	4.7	4.4	4.1	4.0	3.5

PP 13 average yield of CO2

Temperature °C	1 (%)	2 (%)	3 (%)	4 (%)	5 (%)	6 (%)
130	0.0	0.005	0.0	0.1	0.1	0.0
165	0.0	0.000	0.0	0.5	0.3	0.0
250	1.1	1.429	0.6	0.2	0.3	0.2
300	10.2	13.500	5.0	3.7	3.5	2.4
350	29.2	28.195	20.3	19.5	18.3	14.4
400	29.2	26.615	21.7	19.4	19.0	16.3

PP 13 average yield of 1-butene

Temperature °C	1 (%)	2 (%)	3 (%)	4 (%)	5 (%)	6 (%)
130	-0.1	-0.1	0.0	0.0	0.0	0.0
165	0.1	-0.1	0.0	0.0	0.0	0.0
250	0.5	0.1	0.3	0.1	0.1	0.1
300	1.4	0.4	0.4	0.1	0.1	0.0
350	1.0	0.4	0.1	0.1	0.1	0.0
400	1.7	0.7	0.2	0.0	0.0	0.1

PP 13 average yield of 2-butene

Temperature °C	1 (%)	2 (%)	3 (%)	4 (%)	5 (%)	6 (%)
130	0.2	0.2	0.0	0.0	0.0	0.0
165	0.2	0.2	0.1	0.0	0.0	0.0
250	0.2	0.1	0.0	0.1	0.1	0.3
300	0.2	0.6	1.0	0.4	0.4	1.7
350	0.8	2.0	2.7	0.4	0.4	7.0
400	2.1	2.2	1.5	0.7	0.7	5.5

PP 13 average yield of iso butene

Temperature °C	1 (%)	2 (%)	3 (%)	4 (%)	5 (%)	6 (%)
130	0.0	0.0	0.0	0.0	0.0	0.0
165	0.0	0.0	0.0	0.0	0.0	0.0
250	0.0	0.0	0.0	0.0	0.0	0.0
300	0.0	0.0	0.0	0.0	0.0	0.0
350	0.0	0.0	0.0	0.0	0.0	0.0
400	0.1	0.0	0.0	0.0	0.0	0.0

PP 13 average yield of C3H6

Temperature °C	1 (%)	2 (%)	3 (%)	4 (%)	5 (%)	6 (%)
130	0.0	0.0	0.0	0.0	0.0	0.0
165	0.0	0.0	0.0	0.0	0.0	0.0
250	0.0	0.0	0.0	0.0	0.0	0.0
300	0.0	0.0	0.0	0.0	0.0	0.0
350	0.0	0.0	0.0	0.1	0.1	0.0
400	0.0	0.0	0.0	0.0	0.0	0.2

PP 13 average yield of 2-butene

Temperature °C	1 (%)	2 (%)	3 (%)	4 (%)	5 (%)	6 (%)
130	0.0	0.0	0.0	0.3	0.3	0.0
165	0.8	0.0	0.2	0.4	0.2	0.0
250	1.3	0.0	0.5	0.3	0.3	0.0
300	1.4	0.0	0.2	0.2	0.1	-0.9
350	0.3	0.0	0.0	0.3	0.3	0.0
400	0.2	0.0	0.8	0.1	0.0	-0.6

PP 13 average yield of ButylBut

Temperature °C	1 (%)	2 (%)	3 (%)	4 (%)	5 (%)	6 (%)
130	0.0	0.1	0.0	0.0	0.0	0.0
165	0.0	0.0	0.0	0.0	0.0	0.0
250	0.0	0.0	0.0	0.0	0.0	0.0
300	0.0	0.0	0.0	0.0	0.0	0.0
350	0.0	0.0	0.0	0.1	0.1	0.0
400	0.1	0.0	0.0	0.1	0.1	0.0

PP 13 average yield of CH4

Temperature °C	1 (%)	2 (%)	3 (%)	4 (%)	5 (%)	6 (%)
130	0.3	0.0	0.1	0.1	0.1	0.0
165	0.4	0.0	0.1	0.0	0.0	0.0
250	0.1	0.0	0.0	0.0	0.0	0.0
300	0.0	0.0	0.0	0.0	0.0	0.0
350	0.0	0.0	0.0	0.0	0.0	0.0
400	0.0	0.0	0.0	0.0	0.0	0.0

PP 13 average yield of f But.Acid

Temperature °C	1 (%)	2 (%)	3 (%)	4 (%)	5 (%)	6 (%)
130	0.32	0.22	0.12	0.13	0.13	0.25
165	0.26	0.00	0.16	0.07	0.04	0.15
250	0.11	0.00	0.07	0.08	0.09	0.00
300	0.03	0.00	0.13	0.01	0.01	0.00
350	0.02	0.00	0.00	0.00	0.00	0.00
400	0.27	0.00	0.04	0.00	0.00	0.03

Appendix G Numerical average data from the microreactor results from partial pressure 18.0 kPa experiments

PP 18 average selectivity of BuO

Temperature °C	7 (%)	8 (%)	9 (%)	10 (%)	11 (%)	12 (%)
130	20.7	20.8	11.0	21.0	13.4	17.5
165	24.8	38.4	23.5	34.7	24.5	21.4
250	73.6	70.7	45.3	57.0	66.6	62.4
300	77.4	72.6	56.2	57.4	66.0	76.6
350	60.5	60.0	66.7	84.4	89.4	85.5
400	63.4	72.8	76.7	94.9	96.9	93.3

PP 18 average Conversion

Temperature °C	7 (%)	8 (%)	9 (%)	10 (%)	11 (%)	12 (%)
130	3.0	2.5	9.9	2.5	5.39	3.95
165	7.0	3.0	11.4	4.3	5.78	5.53
250	20.2	18.5	25.5	19.2	16.14	16.02
300	39.9	39.4	38.4	34.7	28.91	27.80
350	65.3	65.8	58.8	56.1	55.95	56.78
400	73.1	73.0	67.7	61.2	61.91	64.44

PP 18 average yield of BuO

Temperature °C	7 (%)	8 (%)	9 (%)	10 (%)	11 (%)	12 (%)
130	0.61	0.52	1.08	0.53	0.72	0.69
165	1.73	1.16	2.68	1.50	1.42	1.18
250	14.88	13.10	11.55	10.93	10.74	10.00
300	30.88	28.62	21.58	19.93	19.09	21.30
350	39.47	39.48	39.19	47.40	50.00	48.57
400	46.33	53.17	51.97	58.10	59.97	60.15

PP 18 average yield of CO

Temperature °C	7 (%)	8 (%)	9 (%)	10 (%)	11 (%)	12 (%)
130	0.03	0.03	0.26	0.04	0.06	0.02
165	0.08	0.04	0.23	0.04	0.05	0.03
250	0.46	0.21	0.34	0.18	0.16	0.09
300	2.74	2.16	1.48	1.11	0.92	0.71
350	4.49	4.48	2.83	3.15	3.36	3.17
400	4.87	5.04	3.21	3.82	3.99	3.86

PP 18 average yield of CO2

Temperature °C	7 (%)	8 (%)	9 (%)	10 (%)	11 (%)	12 (%)
130	0.00	0.00	0.10	0.00	0.00	0.00
165	0.00	0.00	0.30	0.01	0.00	0.00
250	1.94	1.54	0.86	0.50	0.41	0.32
300	12.30	9.99	6.47	4.15	2.95	2.50
350	26.45	27.63	16.85	16.64	16.94	15.95
400	26.19	25.26	15.72	16.35	17.07	16.63

PP 18 average yield of 1-butene

Temperature °C	7 (%)	8 (%)	9 (%)	10 (%)	11 (%)	12 (%)
130	0.0	-0.1	0.0	0.00	0.0	0.0
165	0.2	0.0	0.0	0.00	0.0	0.0
250	0.0	0.1	0.0	0.00	0.0	0.0
300	0.2	0.3	0.1	0.00	0.0	0.0
350	-0.1	0.1	0.1	0.00	0.0	0.0
400	0.0	0.4	0.3	0.00	0.0	0.0

PP 18 average yield of 2-butene

Temperature °C	7 (%)	8 (%)	9 (%)	10 (%)	11 (%)	12 (%)
130	0.0	0.0	0.3	0.02	0.0	0.0
165	0.1	0.0	0.1	0.01	0.0	0.0
250	0.1	0.1	0.0	0.00	0.0	0.0
300	0.3	0.6	1.3	0.65	0.2	0.2
350	1.4	2.7	1.5	1.33	4.3	4.6
400	1.4	1.2	1.5	4.18	2.7	2.3

PP 18 average yield of iso butene

Temperature °C	7 (%)	8 (%)	9 (%)	10 (%)	11 (%)	12 (%)
130	0.0	0.0	0.1	0.00	0.0	0.0
165	0.0	0.0	0.2	0.00	0.00	0.00
250	0.0	0.0	0.0	0.00	0.00	0.00
300	0.0	0.0	0.0	0.00	0.00	0.00
350	0.0	0.0	0.0	0.00	0.00	0.00
400	0.0	0.0	0.0	0.00	0.00	0.00

PP 18 average yield of C3H6

Temperature °C	7 (%)	8 (%)	9 (%)	10 (%)	11 (%)	12 (%)
130	0.01	0.00	0.01	0.00	0.00	0.00
165	0.01	0.00	0.01	0.00	0.00	0.00
250	-0.01	0.00	0.00	0.00	0.00	0.00
300	-0.01	0.00	0.00	0.00	0.00	0.00
350	-0.01	0.00	0.05	0.06	0.01	0.06
400	0.04	0.02	0.03	0.00	0.34	0.37

PP 18 average yield of 2-butene

Temperature °C	7 (%)	8 (%)	9 (%)	10 (%)	11 (%)	12 (%)
130	0.1	0.2	0.0	0.0	0.0	0.0
165	0.1	0.1	0.3	0.2	0.2	0.2
250	0.2	0.5	0.1	0.8	0.8	0.4
300	0.0	0.0	0.0	0.0	0.0	0.0
350	0.0	0.0	0.0	0.0	0.0	0.0
400	0.5	0.5	0.0	0.0	0.0	0.0

PP 18 average yield of ButylBut

Temperature °C	7 (%)	8 (%)	9 (%)	10 (%)	11 (%)	12 (%)
130	0.0	0.0	0.0	0.0	0.0	0.0
165	0.0	0.0	0.0	0.0	0.0	0.0
250	0.0	0.0	0.0	0.0	0.0	0.0
300	0.0	0.0	0.0	0.0	0.0	0.0
350	0.0	0.2	0.0	0.0	0.0	0.0
400	0.0	0.1	0.0	0.0	0.0	0.0

PP 18 average yield of CH4

Temperature °C	7 (%)	8 (%)	9 (%)	10 (%)	11 (%)	12 (%)
130	0.2	0.0	0.2	0.1	0.0	0.0
165	0.5	0.1	0.1	0.1	0.0	0.0
250	0.0	0.0	0.0	0.0	0.0	0.0
300	0.0	0.0	0.0	0.0	0.0	0.0
350	0.0	0.0	0.0	0.0	0.0	0.0
400	0.0	0.0	0.0	0.0	0.0	0.0

PP 18 average yield of f But.Acid

Temperature °C	7 (%)	8 (%)	9 (%)	10 (%)	11 (%)	12 (%)
130	0.16	0.08	0.48	0.04	0.03	0.00
165	0.52	0.03	0.26	0.07	0.02	0.01
250	0.02	0.03	0.06	0.01	0.01	0.01
300	0.00	0.00	0.01	0.00	0.00	0.01
350	0.00	0.01	0.01	0.00	0.00	0.00
400	0.00	0.09	0.43	0.00	0.04	0.02